Departamento de Biología Molecular
Facultad de Ciencias
Universidad Autónoma de Madrid

EXPLORING THE ROLES OF MAJOR SIGNALING PATHWAYS IN EPITHELIAL MORPHOGENESIS

EXPLORACIÓN DEL PAPEL DE RUTAS PRINCIPALES DE SEÑALIZACIÓN EN LA MORFOGÉNESIS EPITELIAL

MADRID, 2019

María Delgado Barea

Memoria presentada por María Delgado Barea, graduada en Bioquímica, con Máster en Biología Molecular y Celular, para optar al título de doctora en Biociencias Moleculares

Director de la tesis:

Dr. Fernando Martín Belmonte

Esta tesis ha sido realizada en el Centro de Biología Molecular Severo Ochoa (CSIC-UAM) bajo la supervisión del Dr. Fernando Martín Belmonte, Investigador Científico del CSIC

La realización de esta tesis ha sido posible gracias al programa de becas de doctorado FPI concedida a María Delgado Barea por el Ministerio de Economía y Competitividad. Este trabajo ha estado financiado por subvenciones del MINECO (BFU2014-57831; BFU2015-71244) y la Fundación Ramón Areces

A Cristina

A mis padres

ACKNOWLEDGEMENTS

A mí me gusta comparar esta tesis con la cerámica de Talavera, que - parafraseando a un gran cómico español - “no es cosa menor, o dicho de otra manera, es cosa mayor”. Puede que esto sea una exageración (todo el mundo sabe que la cerámica de Talavera es insuperable) y esta tesis no sea cosa mayor a grandes rasgos, pero desde luego no ha sido cosa menor en mi pequeño mundo. Yo tenía muy claro que quería estudiar Medicina pero a los 17 añitos se me cruzaron los cables y, en vez de acabar en el Virgen del Rocío, terminé en un campus perdido entre Madrid y Alcobendas siguiendo un larguísimo camino que ahora se vuelve a bifurcar. Suelo tirar hacia la izquierda, pero sea cual sea la dirección que tome lo único que tengo claro es que aunque cometa mil errores tendré el apoyo de muchas personas sin las cuales yo no habría llegado hasta aquí. A ellos y a ellas les dedico esta tesis.

A mi familia. A mis padres, a mis hermanos, a mis abuelos… Por azar me ha tocado la mejor familia que se puede tener, no tengo palabras para expresar toda mi gratitud hacia vosotros y lo afortunada que me siento de teneros conmigo.

A mis amigos de toda la vida y a los que he hecho por el camino. Qué bonito es poder elegir una segunda familia y qué suerte tengo de haberme encontrado con cada uno de vosotros. Especialmente me quedo con todas las carcajadas que hemos compartido porque a qué viene una al mundo si no es a reírse.

A mis mentores y mis compañeros, a quien me ha enseñado, me ha inspirado, me ha apoyado, me ha ayudado y me ha acompañado durante estos años. Esta lista es infinita… algunos leerán esto y se sentirán identificados, otros no lo llegarán a leer… pero todos han sido piezas clave en esta historia.

A ella. ¿Que desde que te conozco veo el mundo de otra manera? Pues sí. ¿Que toda palabra que pueda dedicarte en esta tesis es poca? Deberías saberlo.

Y por último quisiera dar las gracias a los que ya no están pero aún así siguen a mi lado. Y a quien seguirá a mi lado hasta que yo no esté.

Ha sido un viaje que habéis hecho único y especial. A todos, gracias.

SUMMARY

One of the central interrogations in developmental biology is how organs acquire their final size and shape. Two main types of cell communication control organ development: biophysical interactions and cell-cell communication through morphogens. Mechanical cues guide different processes, including cell motility, growth and differentiation, and morphogen gradients have critical roles in patterning and organ growth. To which extent are these two different types of communication necessary and what are the concrete molecular players that ensure proper organogenesis are factors that change depending on the organ and the stage of development. In the present thesis, we investigate the potential role of several signaling pathways and mechanical cues from mesenchymal cells during tubulogenesis of different epithelial organs, including the mammary gland and the zebrafish intestine.

We use the *Drosophila* wing imaginal disc to understand the mechanism by which *Sfrp3* could be modulating the Wnt signaling pathway in mammary gland development, which leads us to the conclusion that SFRP3 is not acting as a negative regulator of Wnt activity, but rather as a diffusor of the Wnt ligands.

Using Next Generation Sequencing (NGS) techniques, we also report that zebrafish carrying a mutation in the Hedgehog pathway transducer *smoothened (smo)*, which show a previously described defect in single lumen formation in the intestine, also display different gene transcriptional profiles in their intestinal epithelial cells when compared to control fish.

In addition, we show that the inhibition of TGF-β pathway generates a defect in lumen resolution in the intestine of developing zebrafish embryos as well. Using different zebrafish lines, we try to understand the causes of this phenotype and its possible link with the phenotype observed in the guts of *smo* mutants. We also detect that mesenchymal cell migration around the epithelial intestinal tube is affected upon TGF-β inhibition, being the lack of physical constraints a potential explanation for the phenotype observed in the case of TGF-β signaling blockade.

Finally, we also demonstrate that the inhibition of TGF-β alters the epithelial morphogenesis of MDCK spheroids *in vitro*, and that TGF-β could be regulating the spindle orientation by affecting the machinery that controls this cellular process.

Una de las cuestiones centrales en biología del desarrollo es cómo los órganos adquieren su forma y tamaño final. Hay dos tipos de comunicación principales que controlan el desarrollo de los órganos: las interacciones biofísicas y la comunicación célula-célula a través de morfógenos. Las señales mecánicas guían diferentes procesos, incluyendo motilidad, crecimiento y diferenciación celular, y los gradientes de morfógenos tienen un papel crítico en el modelado y el crecimiento del órgano. Hasta qué punto son los dos tipos de comunicación necesarios y cuáles son los componentes moleculares específicos que aseguran una adecuada organogénesis son factores que cambian dependiendo del órgano y el estadío de desarrollo. En esta tesis investigamos el papel potencial de varias rutas y de la señalización mecánica de las células mesenquimales durante la tubulogénesis de diferentes órganos epiteliales, como la glándula mamaria y el intestino de pez cebra.

Usamos el disco imaginal de ala de *Drosophila* para entender el mecanismo por el cual *Sfrp3* podría estar modulando la ruta de señalización Wnt durante el desarrollo de la glándula mamaria, lo que nos llevó a la conclusión de que SFRP3 no está actuando como regulador negativo de la actividad Wnt sino como difusor de los ligandos Wnt.

Empleando técnicas de secuenciación de nueva generación, identificamos que los peces cebra que portan una mutación en el transductor de la ruta Hedgehog *smoothened (smo),* los cuales presentan defectos previamente descritos en la formación de un único lumen en el intestino, muestran diferentes perfiles transcripcionales en sus células epiteliales intestinales comparados con los peces control .

Además, también mostramos que la inhibición de la ruta TGF-β genera un defecto en la resolución de lúmenes en el intestino de embriones de pez cebra en desarrollo. Usando diferentes líneas de pez cebra, intentamos entender las causas de este fenotipo y su posible relación con el fenotipo observado en los mutantes *smo.* A su vez mostramos cómo la migración de las células mesenquimales alrededor del tubo epitelial está afectada por la inhibición de TGF-β, siendo la falta de restricciones físicas una posible explicación para el fenotipo observado en el caso de la falta de señalización TGF-β.

Finalmente, también demostramos que la inhibición de TGF-β altera la morfogénesis epitelial de esferoides MDCK *in vitro*, y que TGF-β podría estar regulando la orientación del huso mitótico afectando a la maquinaria que controla este proceso.

INDEX

GLOSSARY

2D: two-dimensional

3D: three-dimensional

AJC: Apical junctional complex

AJs: Adherens junctions

AMIS: Apical membrane initiation site

BMP: Bone morphogenetic protein

CaCo2: Caucasian Colon Adenocarcinoma cell line 2

CFTR: Cystic Fibrosis Transmembrane Conductance Regulator

Dll: Distal-less

ECM: Extracellular Matrix

EMT: Epithelial-to-Mesenchymal Transition

EPP: Epithelial Polarity Programme

ER: Estrogen Receptor / Endoplasmic reticulum

ERM: Ezrin-Radixin-Moesin

ESCRT: Endosomal sorting complex required for transport

F-actin: Filamentous actin

FAs: Focal Adhesions

FACS: Fluorescence-activated cell sorting

FAK: Focal adhesion kinase

FBS: Fetal Bovine Serum

FGF: Fibrobalst growth factor

GFP: Green Fluorescent Protein

GI: Gastrointestinal

Gp135: Podocalyxin

Hh: Hedgehog

Hpf: Hours Post Fertilization

IECs: Intestinal epithelial cells

IF: Immunofluorescence

Ihh: Indian hedgehog

iSMC: Intestinal smooth muscle cells

JAMs: Junction adhesion molecules

KD: Knock-Down

LPM: Lateral plate mesoderm

MDCK: Madin-Darby Canine Kidney cell line

MEC: Mammary epithelial cells

MEM: Minimum Essential Medium

MET: Mesenchymal-to-Epithelial Transition

MG: Matrigel

MRCK: Myotonic dystrophy kinase-related CDC42-binding kinase

MTOC: Microtubule-organizing center

NGS: Next Generation Sequencing

NMII: Non-muscular Myosin class II protein

Nub: Nubbin

NWASP: Neural Wiskott-Aldrich syndrome protein

p-MLC: Phosphorylated NMII Regulatory Light Chain

PAP: Pre-Apical Patch

PC: Primary cilium

PCP: Planar cell polarity

PIP2: Phosphatidylinositol (4,5)-biphosphate

PIP3: Phosphatidylinositol (3,4,5)-triphosphate

Ptch: Patched

PTEN: Phosphatidylinositol 3,4,5-triphosphate 3-phosphatase

ROCK: Rho-associated protein kinase

RT-qPCR: Real time quantitative PCR

Sens: Senseless

Sfrp: Secreted frizzled-related protein

Shh: Sonic hedgehog

siRNA: small interfering RNA molecules

Smo: Smoothened

TGF-β: Transforming Growth Factor β

TGN: Trans-Golgi network

TJs: Tight junctions

Wg: Wingless

ZO: Zonula Occludens

PRESENTACIÓN

Resumen

La formación de un único lumen durante el proceso de tubulogénesis es crucial para el desarrollo y la función de muchos órganos, entre los que se encuentra el intestino o las glándulas mamarias. Durante la morfogénesis del intestino en pez cebra hay múltiples lúmenes que se abren y ensanchan para finalmente fusionarse y formar una única superficie apical continua en un proceso denominado resolución de lúmenes. En este proceso de resolución es necesaria una remodelación de los contactos basolaterales entre células así como un crecimiento de la membrana apical, mecanismos que parecen estar afectados en peces mutantes de *smoothened*, co-receptor y regulador esencial de la vía de Hedgehog. En cuanto a las glándulas mamarias, se ha observado que ratones knock-out para el gen *Sfrp3* presentan importantes defectos durante el desarrollo de los túbulos epiteliales en mama, desconociéndose el papel concreto de SFRP3 en el proceso. El objetivo principal de este proyecto es dilucidar los mecanismos a través de los cuales podrían estar regulándose los procesos de resolución de lúmenes en el intestino de pez cebra así como el papel concreto de *Sfrp3* en el contexto del desarrollo de la glándula mamaria.

Antecedentes del proyecto

Introducción

Muchos órganos pasan durante el desarrollo por un proceso de tubulogénesis en el que adquieren la forma que facilitará su función a través de la formación de un túbulo, o una red de túbulos, que presentan un lumen central abierto. Aunque gracias a los modelos celulares en 3D se han identificado mecanismos moleculares que controlan la formación del lumen *in vitro*, aún no se conoce con exactitud su función durante la organogénesis *in vivo*. Durante el desarrollo del intestino en pez cebra hay múltiples lúmenes que se abren y ensanchan para generar una estructura intermediaria, consistente en lúmenes adyacentes no fusionados separados por contactos basolaterales. Estos se forman independientemente a lo largo del intestino y no comparten una superficie apical continua. La resolución de este intermediario en un único lumen continuo requiere de la remodelación de los contactos existentes entre lúmenes adyacentes, con su sucesiva fusión. Recientemente se ha descubierto que la resolución de los lúmenes del intestino, aunque no su apertura, está afectada en mutantes de la vía Hedgehog, los cuales presentan además perturbaciones en la vía de tráfico de Rab11, demostrando que dicha vía es necesaria para la formación de un único lumen. Uno de los objetivos principales de este proyecto

es entender a través de qué mecanismos la vía de Hedgehog está regulando el proceso de tubulogénesis epitelial en el intestino de los vertebrados.

Por otra parte, hemos identificado que ratones knock-out para *Sfrp3* presentan importantes defectos durante el desarrollo de la glándula mamaria que afectan a la estructura y función de los túbulos epiteliales. Poco se conoce acerca de SFRP3, una proteína que forma parte de la familia de las SFRPs (Secreted Frizzled-Related Proteins), tradicionalmente asociadas a la regulación negativa de la ruta Wnt. Por tanto, el segundo objetivo principal de este proyecto se trataría de averiguar de qué forma estaría SFPR3 implicada en la modulación de la ruta Wnt durante el desarrollo de la mama en vertebrados.

Tubulogénesis: desarrollo del intestino y glándulas mamarias

Los tubos epiteliales se generan durante el desarrollo a través de diversos mecanismos, que se pueden agrupar en dos clases dependiendo del grado de polaridad de las células de origen (Hogan & Kolodziej, 2002; Lubarsky & Krasnow, 2003; Sigurbjornsdottir et al., 2014). Aquellos tubos que se forman a partir de un epitelio polarizado típicamente sufren procesos dirigidos principalmente por cambios en la forma celular. En contraste, los tubos que se originan a partir de células no polarizadas lo hacen a través de un proceso que requiere el establecimiento de polaridad celular y la formación de un lumen *de novo* entre las células (Lubarsky & Krasnow, 2003; Martín-Belmonte & Mostov, 2008). La formación del lumen *de novo* ocurre a través de la coordinación de varios procesos celulares, incluyendo la orientación de las células a través de interacciones celulares (mayormente las existentes entre célula-célula y célula-matriz), el desarrollo de polaridad apico-basal, cambios en la forma y movimientos celulares, la formación y expansión del dominio apical y, finalmente, la fusión de los lúmenes para formar una única cavidad. En estudios llevados a cabo mayormente en modelos celulares se ha descrito que para iniciar la formación del lumen es necesario que proteínas de membrana apical acumuladas en vesículas, como la podocalixina, lleguen a la membrana plasmática donde se fusionan generar una superficie apical (Bryant et al., 2010, Galvez-Santisteban et al., 2012). Aunque estos estudios resaltan la importancia del tráfico de membrana en la formación del lumen, estos sistemas *in vitro* no pueden reproducir completamente la complejidad de los procesos implicados en la formación del lumen en un tubo tridimensional. Por ello, los mecanismos celulares que controlan la formación del lumen en grandes tubos epiteliales como el intestino, particularmente en vertebrados, aún no se comprenden con claridad.

La formación del intestino en pez cebra comienza con una serie de células endodérmicas que se diferencian en epiteliales y atraviesan un proceso de formación de un tubo sin apoptosis (Ng et al., 2005). La formación del lumen se inicia con el desarrollo de múltiples focos ricos en actina entre células seguida por la localización de proteínas de uniones en múltiples puntos a lo largo del intestino (Horne-Badovinac et al., 2001). En dichos puntos, se generan pequeños lúmenes que se expanden a través del transporte paracelular de iones que causa la acumulación de fluido y un aumento de la presión hidrostática luminar (Bagnat et al., 2007). La expansión es seguida por un estado intermediario caracterizado por lúmenes adyacentes sin fusionar que finalmente se unen en dirección anteroposterior gracias a un crecimiento de la membrana apical y una remodelación de las uniones en los puntos de fusión (Navis & Bagnat, 2015). Este proceso de resolución de lúmenes parece estar regulado por la señalización Hedgehog (Hh), ya que peces mutantes para *smoothened* (*smo*) son incapaces de llevarlo a cabo, resultando en intestinos que no desarrollan un único lumen continuo (Alvers et al., 2014). Aún se desconoce cómo este proceso de resolución de lúmenes ocurre exactamente y si otros tipos celulares al margen de las células epiteliales intervienen directa o indirectamente en el proceso, por lo que el objetivo principal del proyecto es averiguar los mecanismos por los que este se lleva a cabo, así como las rutas de señalización y tipos celulares que intervienen y de qué forma están implicados.

En cuanto a la glándula mamaria (GM), se trata de uno de los órganos que lleva a cabo la mayor parte de su desarrollo de forma postnatal. Durante la pubertad, los ductos comienzan a invadir el tejido adiposo en un proceso dirigido por las estructuras terminales denominadas *terminal end buds* (TEBs) y también a través de un proceso de ramificación secundaria. Una vez los ductos alcanzan los límites del tejido adiposo, el árbol ductal permanece quiescente hasta el embarazo. En ese momento, se lleva a cabo un proceso de ramificación terciario masivo que resulta en las estructuras que posteriormente darán lugar a los alveolos, donde se produce la leche materna durante la lactancia. Una vez se produce el destete, las GMs vuelven al estado anterior al embarazo. Durante cada uno de estas fases en el desarrollo de la GM ocurren importantes cambios en la proliferación celular, apoptosis y diferenciación, lo que permite la remodelación de la estructura de la glándula. La GM se compone de dos compartimentos, los ductos epiteliales y el tejido de soporte o estroma en el que se encuentran los ductos. El desarrollo postnatal de la GM se controla de forma global a través de hormonas sistémicas y localmente a través de comunicación bidireccional entre los compartimentos (Sternlicht et al., 2006). Muchos estudios muestran que el estroma dirige la diferenciación y ramificación de las células epiteliales

de la mama a través de señales paracrinas, que se basan en factores secretados como los ligandos Wnt (Howard & Lu, 2014; Hynes & Watson, 2010; Jarde & Dale, 2012).

Sfrp3 ha sido una proteína previamente identificada como inhibidora de la señalización Wnt (Leyns et al., 1997; Wang et al., 1997), con un papel esencial en el desarrollo de otras estructuras pero con un papel hasta ahora desconocido en la morfogénesis de la glándula mamaria.

Hipótesis y principales objetivos

El tracto intestinal desempeña un papel crucial en el desarrollo, regeneración y nutrición animal. Se han encontrado diversos factores que parecen ser importantes para la adquisición de la arquitectura y morfología intestinal durante el desarrollo, incluyendo vías de señalización que determinan el destino celular, reordenamientos celulares morfogenéticos, factores microambientales y determinantes mecánicos externos. A pesar de su relevancia, muchos aspectos importantes del desarrollo y la función intestinal permanecen aún sin explorar. Por ejemplo, aún se desconocen los detalles de cómo las células son capaces de transducir la información transcripcional y señales biomecánicas en dinámicas epiteliales y adquisición de un destino celular. En este proyecto, nos planteamos comprender los mecanismos moleculares asociados con la formación tubular y la adquisición de un patrón en la morfogénesis intestinal. En particular, el principal objetivo es dilucidar los mecanismos de la formación y resolución de lúmenes en el intestino de los vertebrados. Para ello, nos serviremos de una combinación de estudios *in vivo* en el tracto gastrointestinal del pez cebra, donde la señalización de Hedgehog parece tener un papel crucial, e *in vitro* en sistemas 3D de esferoides MDCK que facilitarán la comprensión de los mecanismos celulares por los que esto sucede.

Por otra parte, conocíamos que la pérdida de SFRP3, normalmente secretada por el estroma, causaba una elongación y una ramificación terciaria de las glándulas mamarias en ratones en estadío de pubertad. Este desarrollo prematuro está además acompañado por defectos estructurales en los ductos epiteliales, con un epitelio con una proliferación incrementada, pérdida de polaridad y diferenciación anormal en células secretoras de leche (Bernascone et al., 2019). Basándonos en antecedentes publicados para la proteína SFRP1 (Esteve et al., 2011) nos planteamos el uso de un modelo diferente a la mama de ratón, el disco imaginal de ala de *Drosophila*, para averiguar a través de qué mecanismos podría *Sfrp3* estar interviniendo en la

modulación de la ruta de Wg y que podrían ser extrapolables a la ruta Wnt en vertebrados en el contexto del desarrollo de la glándula mamaria.

INTRODUCTION

1. Epithelial & mesenchymal tissues: origin and links

Animal tissues can be grouped in four main types: epithelial, connective, muscle and nervous tissues. Epithelial cells can organize in monolayers (or simple epithelium, like in tubular organs) or in multilayers (or stratified epithelium, like the skin) to form tissues, which can derive from all of the embryological germ layers: ectoderm (as the epidermis of the skin), mesoderm (as cells coating the blood vessels) and endoderm (as the cells lining the gastrointestinal tract). Epithelial tissues generally serve as a barrier against pathogens and physical or chemical hazards, and separate different physiological environments, sometimes presenting specialized structures that control selective transport of molecules past their membranes. The mesenchyme belongs to the group of connective tissues and is normally found at developing stages of the embryo, when it acts as precursor for other connective tissue cells. The connective tissues (a group that also includes bones, cartilage or fat) mostly derive from the mesoderm layer and their main function is ensuring organ and body integrity by providing cohesion and internal support (Figure I1).

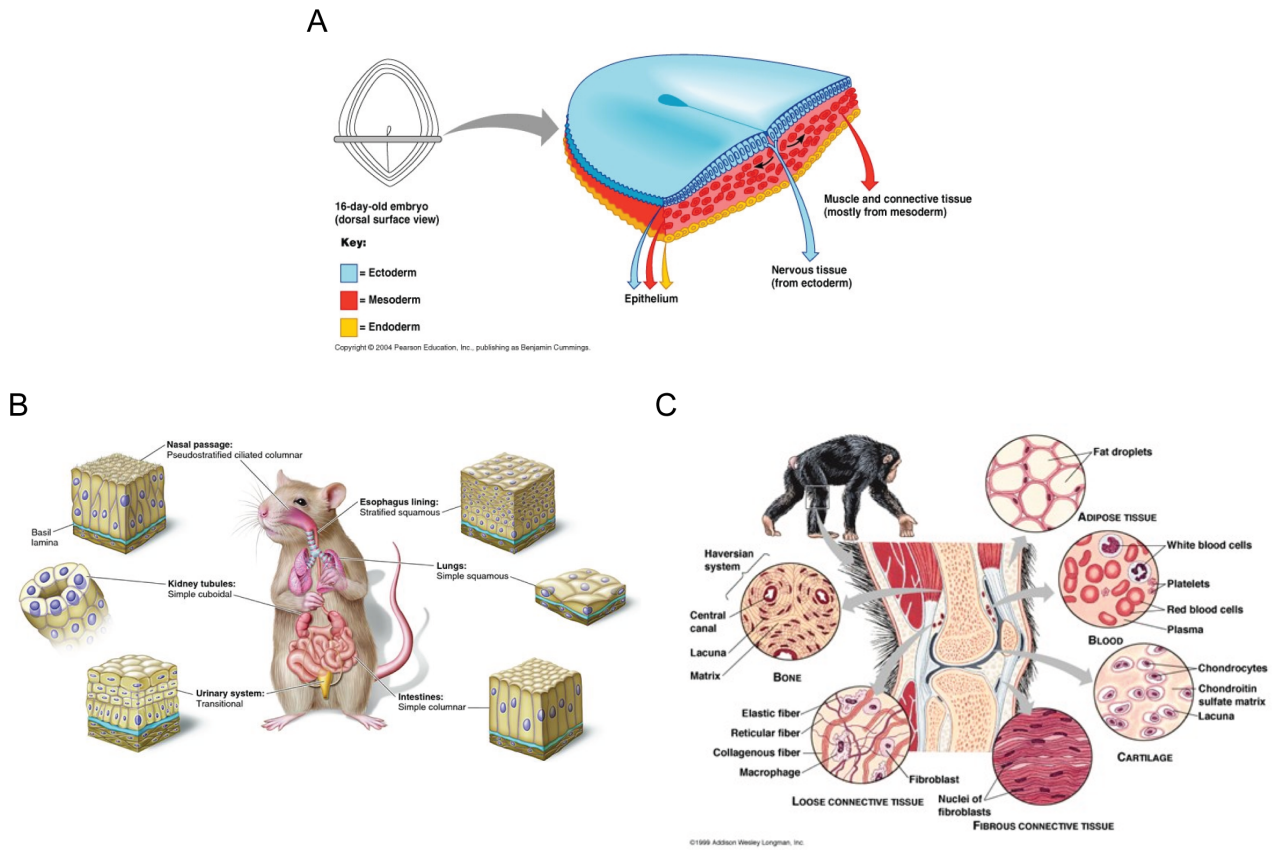

Figure I1. Embryonic origin and types of epithelial and connective tissues. A) Epithelial tissues arise from all three embryonic layers while connective tissues mainly originate from the mesodermal layer. **B-C)** Epithelial and connective tissue cells develop specific characteristics depending on the function they are specialized in.

During development, many cells can transition from epithelial to mesenchymal type and vice versa, two processes called epithelial-to-mesenchymal transition (EMT) or mesenchymal-to-epithelial transition (MET). Epithelial cells can undergo morphology changes, intercalate in processes of convergent extension and move to close injuries during wound healing. However, these behaviors are restricted by their conformation in a two-dimensional (2D) layer. This is the reason why EMT/MET processes are crucial during development for epithelial cells to acquire full migratory capacity, which confers them the ability to organize progenitor cells and allow new inductive interactions, ensuring appropriate development and organogenesis (Nakaya & Sheng, 2013). In addition, epithelial and mesenchymal interactions are key for the morphogenesis of many different organs (Arias, 2001; Ribatti & Santoiemma, 2014). These and every other process that is genetically coordinated, and by which epithelia dynamically contribute to organogenesis and body shape, are together referred to as epithelial morphogenesis. We can distinguish four key types of epithelial morphogenetic mechanisms, all driven by signal transduction molecules and transcription factors activity: (1) cell morphology changes, (2) cell intercalation, ingression, egression and fusion, (3) cell migration and (4) cell division and death (Schöck & Perrimon, 2002). Many studies have focused on different aspects trying to solve the question of how epithelial cells can coordinate and communicate between them and other kind of cells to achieve all these changes that give rise to the wide variability of morphologies and organs. To be able to break down this complex issue we need to comprehend the basic molecular features of epithelial cells and tissues.

2. The process of tubulogenesis

Several main body organ systems, such as the vascular system, the digestive tract, the lungs or the kidneys, are formed by an interconnected network of tubes, which are shaped in a process called tubulogenesis. This process involves the assembly of a polarized sheet of cells in a tubule-like structure with a central lumen that is confronted by the apical cell side, while the basal surfaces face to the inner body (Hogan & Kolodziej, 2002). Epithelial tubular organs can develop following different strategies even when sharing the same basic structure, which generates a wide diversity of tube morphologies in terms of tube size or shape (Iruela-Arispe & Beitel, 2013). Several mechanisms have been described for tube formation (Figure I2): If tubes arise from a polarized epithelium, it can be achieved either by **wrapping** or **budding**. During wrapping, an area of the cell sheet bends and invaginates until the edges fuse, whereas in budding a portion of cells

protrudes from the pre-existing tube or sheet while generating a new tube. Examples of these processes taking place in a living organism are primary neurulation in vertebrates by wrapping and the development of *Drosophila* salivary gland and trachea by budding (Colas & Schoenwolf, 2001; Metzger & Krasnow, 1999).

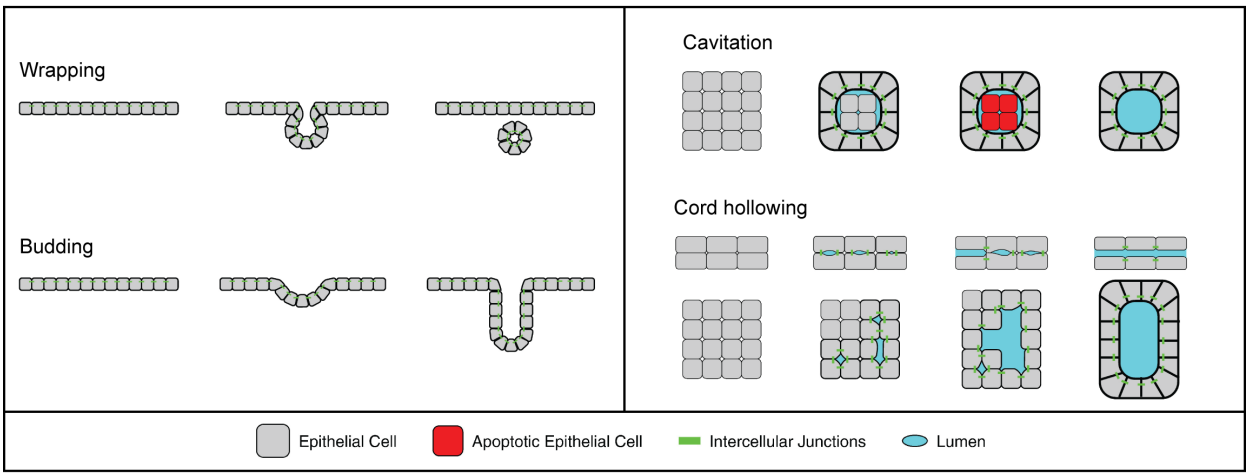

Figure I2. Epithelial tubulogenesis. Epithelial tubes can develop through different mechanisms depending on whether they arise from polarized sheets of cells (wrapping and budding) or from unpolarized cells (cavitation and cord hollowing). In the end, all structures enclose a central cavity or lumen surrounded by a monolayer of epithelial cells. Adapted from Andrew & Ewald, 2010.

On the contrary, tubes can arise as well from clusters or individual cells that are not epithelial but polarize and/or establish junctions as tubes develop. This can be done by **cavitation,** if a central group of cells of a cylindrical mass undergo apoptosis forming the luminal space**,** or **cord hollowing,** if lumens arise between cells in an initially unpolarized cord without apoptotic processes taking place. The vertebrate salivary gland develops by cavitation (Melnick & Jaskoll, 2000), while the *Danio rerio* intestine form by cord hollowing (Ng et al., 2005; Pollack et al., 1998).

A major event during epithelial morphogenesis that constitutes one of the distinctive characteristics of epithelial tubes is the acquisition of apico-basal polarity. Disturbances in the processes that take part in the establishment and maintenance of cell apico-basal polarity can lead to damages in specific organs and systemic diseases, like cancer and tumor expansion and metastasis, cystic fibrosis or polycystic kidney disease, or intestinal diseases like microvillus inclusion disease (Schneeberger et al., 2018; Stein et al., 2002). Consequently, understanding and deciphering the molecular mechanisms involved in the acquisition of epithelial cell polarity and

tubulogenesis is key to develop new tools and ways of diagnosis and treatment for polarity-related diseases.

3. Models to study epithelial morphogenesis

3.1. *In vivo models*

Different animal models can be used for the study of epithelial morphogenesis, including *Drosophila melanogaster, C. elegans*, zebrafish or mice. As every one of them present peculiarities and offer singular advantages, the studies carried out in distinct models are often complementary.

Drosophila melanogaster has been widely used to study developmental processes and diseases, as many essential molecular pathways and mechanisms have been conserved through evolution. The use of *Drosophila* presents several assets: a very complete genetic toolkit and techniques, cheap storage and simple handling, short breeding time, easy genetic manipulation and tracking of mutations and small genetic redundancy. *Drosophila* larvae go through three larval stages during four days at 25ºC, in which the precursory structures of the adult cuticular organs (called imaginal discs) are grown. During the pupal stage, the imaginal discs differentiate and give rise to the adult structures (Figure I3). Imaginal discs, which are formed by pseudostratified epithelial cells that organize in a monolayer, can be used to study epithelial dynamics.

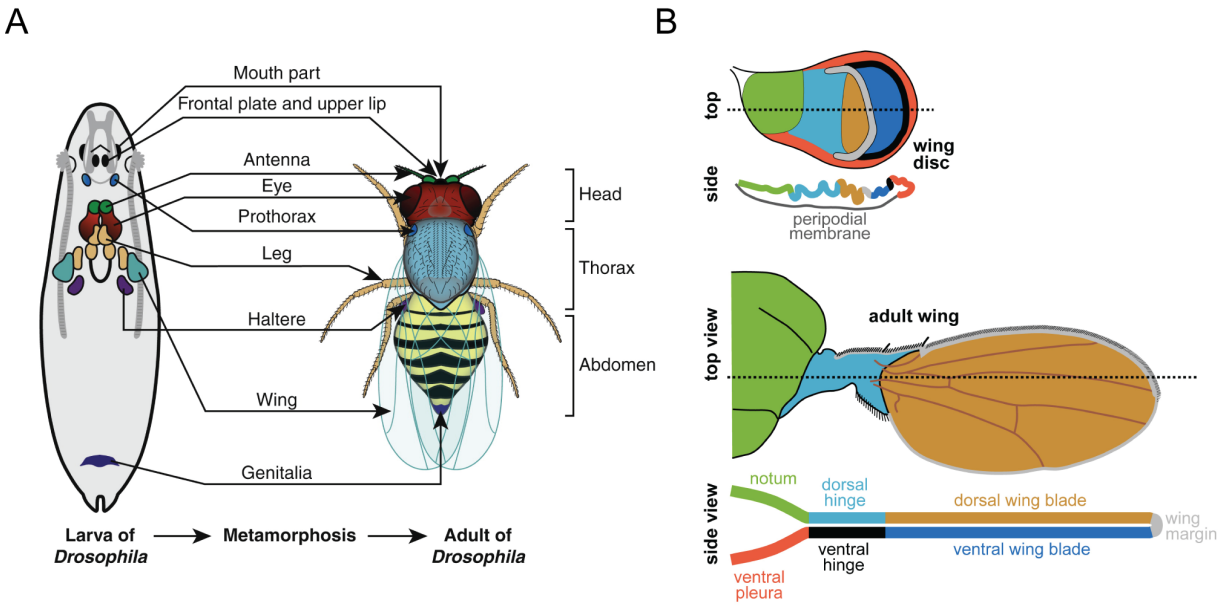

Figure I3. Larvae imaginal discs develop into adult cuticular organs. A) Each imaginal disc develops under a specific genetic program to generate particular adult fly body structures. Adapted from Aldaz & Escudero, 2010. **B)** Marked areas of the wing imaginal disc develop into concrete wing structures driven by a series of morphogenetic events. Image by A. Prokop.

The patterns of expression and roles of many different genes involved in wing imaginal disc development have been extensively studied, which makes this model particularly appropriate to test the impact and functions of ectopic expression or suppression of genes of interests.

Regarding vertebrate animals, *Danio rerio* or zebrafish results in a very suitable model for the study of early developmental processes since embryo development takes place outside the mother's body once the eggs have been fertilized. In addition, embryos are nearly transparent, which facilitates internal structure visualization. This animal offers as well a very powerful genetic toolkit, and they are easier to manipulate and cheaper to maintain than other vertebrate models. Zebrafish has been broadly used for the study of tubulogenesis processes in several organs like the pronephros (kidney precursors), the vascular system or the intestine. Luminogenesis of the zebrafish intestine occurs through *de novo* formation of the apical membrane and the luminal space. Intestinal progenitors cells derive from the endoderm and form a strip at the midline by 26 hours post-fertilization (hpf). A bilayer is subsequently formed, just before the cells acquire apico-basal polarity and small luminal spaces start arising separated by basolateral contacts. These lumens expand and undergo a process of lumen resolution in an anterior to posterior manner to develop a single open lumen (Figure I4).

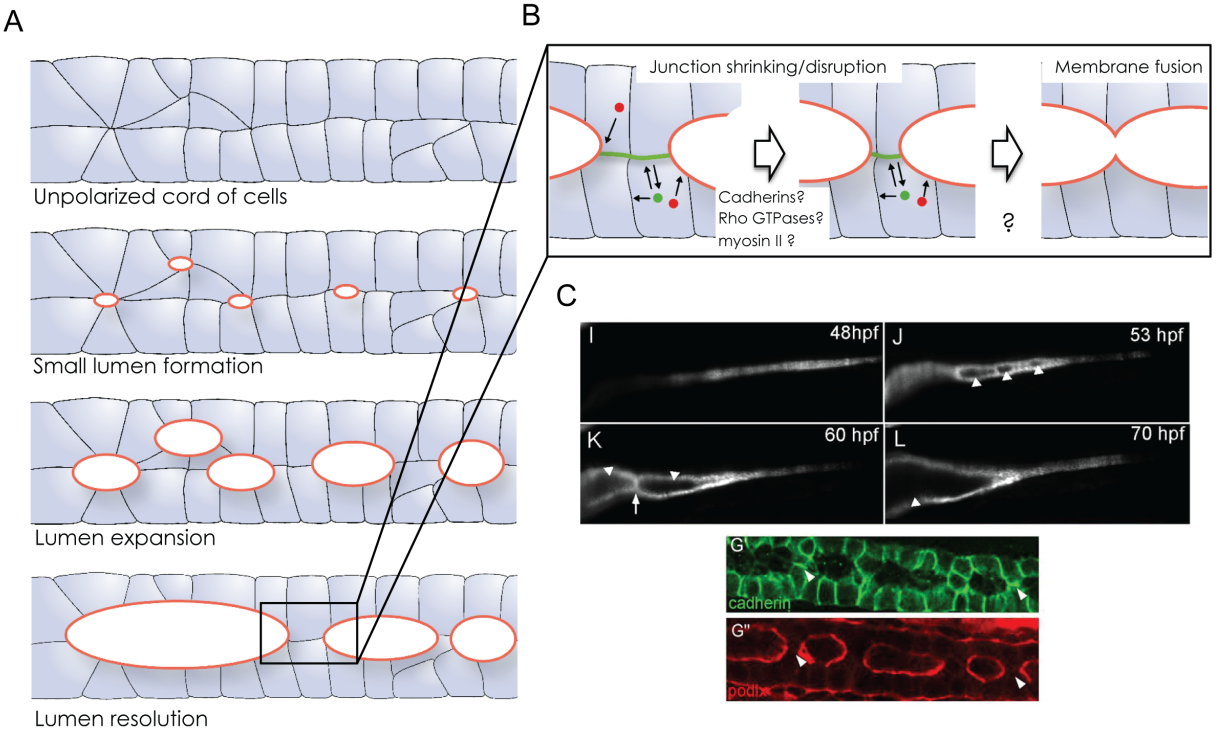

Figure I4. A model for tubulogenesis in the zebrafish intestine. A) The formation of the zebrafish gut occurs through a cord hollowing process. **B)** Lumen resolution requires a step of junction remodeling through junctional shrinking and apical membrane fusion. **C)** Images of tubulogenesis in a zebrafish intestine in which apical membranes (podocalyxin, red) are separated by basolateral contacts (cadherin, green) and fuse in an anterior to posterior manner. Adapted from Alvers et al., 2014.

Lumen coalescence is achieved by mechanisms of apical membrane expansion and junction remodeling dependent on actomyosin contractility and Rab11a-mediated recycling processes (Alvers et al., 2014). By 126 hpf, the cells are already differentiated and the organ is ready to perform its biological functions (Ng et al., 2005). Interestingly, lumen resolution in the zebrafish gut relies on Hedgehog (Hh) signaling activated in mesenchymal cells by ligands, such as Sonic hedgehog a (Shha) or Indian hedgehog a (Ihha), secreted by epithelial cells (Alvers et al., 2014; Winata et al., 2009). In addition, the crosstalk between epithelia and surrounding intestinal smooth muscle cells is key for the organ integrity (Alvers et al., 2014; Seiler et al., 2012).

This working model suggests that mesenchymal cells would respond to this Hh stimulus by signaling back to the epithelium through physical and/or chemical stimuli, generating a response that ensures proper tubulogenesis of the intestine. In the present thesis, we investigated two different issues associated with this hypothesis:

A. How epithelial cells are transducing and responding to signals from mesenchyme to ensure correct morphogenesis of the organ.
B. Through which mechanisms mesenchymal cells interact with intestinal epithelium.

3.2. In vitro models

Different cell types have been used to study the processes underlying epithelial morphogenesis. Since two-dimensional (2D) cultures do not fully recapitulate the mechanisms that take place *in vivo*, three-dimensional (3D) cultures offer a more reliable *in vitro* model to investigate epithelial organogenesis. Among all the 3D systems available, the 3D-MDCK model is one of the most widely used. The Madin-Darby canine kidney (MDCK) cells display properties of the distal tubule and collecting duct, and when embedded in a matrix of ECM proteins, they develop in the form of 3D spherical structures called spheroids (Bryant et al., 2010). Spheroids are formed by a monolayer of epithelial polarized cells enclosing a central fluid-filled lumen (Montesano et al., 1991), which is a simpler but analogous structure to that of the kidney or the intestine in a living organism. In addition, MDCK spheroids have the advantage of growing a fully formed structure in a very short period of time (72h) when cultured within a laminin-rich matrix like Matrigel. Other organotypic cell cultures used for the study of epithelial morphogenesis are CaCo2 cells from human colon carcinoma, primary luminal mammary epithelial cells (MECs) and other cell lines derived from mammary glands (like non-tumorigenic MCF10A line) and micropatterned cell

cultures that facilitate the study of biomechanics in morphogenetic processes (Bosch-Fortea et al., 2019; Rodríguez-Fraticelli et al., 2012; Théry, 2010).

Another system currently being developed and used for the study or developmental and disease-related processes is the organoid culture system. Organoids can form using isolated stem cells or a combination of stem cells with animal explants or cell lines. As a result of culturing under specific conditions, cells form an organ-like structure preserving many similarities with the organ of origin (Eiraku et al., 2011; Nguyen-Ngoc et al., 2015; Pasca, 2019; Sato et al., 2009; Takasato & Little, 2016).

4. The basics of the epithelial polarity program

The mechanisms underlying epithelial cell polarity are orchestrated and encompassed within the concept of epithelial polarity program (EPP).

Apico-basal epithelial polarity main feature is the division of the cell membrane into structurally and functionally different domains: an apical membrane domain that faces the exterior (in the case of the epidermis) or the luminal space (in the case of internal epithelia) and a basolateral domain. Moreover, the basolateral domain can be subdivided into the lateral domain, in contact with neighboring cells and involved in the establishment of cell-cell junctions, and the basal domain, in contact with extracellular matrix (ECM) components. Oriented vesicle trafficking allows the segregation of proteins and lipids into their specific domains, which confers unique functions to the apical and basolateral membrane domains.

The defining events involved in EPP are the cytoskeleton organization, the polarity complexes function and the formation and maintenance of cell-cell junctions.

4.1. The cytoskeleton

Three main structural components conform the network of fibers defined as the cytoskeleton: microfilaments (formed by actin), microtubules (formed by tubulins) and intermediate filaments. In addition to cytoskeleton roles in protein sorting and organelle placing in polarized cells (Bornens, 2008; Ross, 2008) and external mechanical cues transduction (Fletcher & Mullins, 2010), the interactions of the cytoskeleton with polarity proteins and phosphoinositides are key for the establishment of epithelial cell polarity.

4.2. Polarity complexes

Three evolutionary conserved **polarity complexes** that segregate to these domains and are directly related to the acquisition of polarity: Crumbs-Pals1(Stardust)-PATJ, Par3(Bazooka)-Par6-aPKC (often associated with Cdc42 as well) and Scribble-Lgl-Dlg systems (Margolis & Borg, 2005; Nelson, 2003) (Names in parenthesis indicate *Drosophila* nomenclature when it differs from the mammalian name). It is relevant to note that the composition of the complexes may vary as molecular components can interact with each other (Tepass, 2012). **Scribble** is a lateral complex known to antagonize apical Crumbs and PAR complexes (Tanentzapf & Tepass, 2003) and restricts Par3 localization to the apical domain (Rodríguez-Boulan and Macara, 2014). Scribble complex can interact as well with trafficking machinery and small GTPases regulators (Audebert et al., 2004; Musch et al., 2002). **Crumbs** and **Par3** modules are associated with the apical domain regulating its integrity and extension. In the case of mammalian cells, they localize to tight junctions, while in *Drosophila* they can be found in the subapical complex or marginal zone between apical and basolateral domains (Knust & Bossinger, 2002). Phosphorylation of Lgl by aPKC is believed to exclude it from the apical membrane and promote its targeting to the lateral domain. In addition, small GTPases have also a role in cell polarity through interactions with polarity complexes. For instance, Cdc42 can bind to the PAR complex through Par6 and enhance its activity (Macara, 2004).

4.3. Junctional complexes

The formation of **junctional complexes** is tightly linked to the establishment of epithelial polarity and ensures the maintenance of the apicobasal polarity (Martín-Belmonte & Pérez-Moreno, 2012; Wang & Margolis, 2007). Epithelial cells display several junctional complexes that can be classified as tight junctions (TJs), adherens junctions (AJs) or desmosomes. **Desmosomes** are laterally located, crucial for tissue integrity and formed by linkage of integral membrane proteins (desmocollin and desmoglein) via desmoplakins (plakophilin and plakoglobin) to intermediate filaments (Garrod & Chidgey, 2008). Together with other substructures, TJs and AJs belong to the **apical junctional complex (AJC),** which is located at the apex of the lateral membrane of polarized epithelial cells and is involved in cell-cell adhesion, paracellular permeability and cell polarity, delimiting the membrane domains (Wang & Margolis, 2008). In mammals, **TJs** situate

apically to AJs, while in insects, septate junctions (the equivalent of TJs) are positioned under AJs, closer to the basal domain. Claudins are the main transmembrane proteins that conform TJs, along with occludin, junction adhesion molecules (JAMs) and zonula occludens proteins (ZO-1, ZO-2, ZO-3), which act as a nexus between occludin and the actin cytoskeleton through α-actinin (Fanning et al., 1998). **AJs** are involved as well in functions other than cell adhesion, acting as transducer for intracellular signaling and transcriptional regulation (Hartsock & Nelson, 2008). Cadherin proteins are the principal components of AJs, being E-cadherin the most abundant in the case of epithelial cells. Other proteins, such as α-catenin, β-catenin, APC and plakoglobin interact with cadherins on the cytoplasmic side and connect them to the cytoskeleton.

4.4. The link between polarity complexes and cell-cell junctions in epithelial polarity

It is believed that the recruitment of polarity complexes to their membrane domains is prompted by the initiation of cell contacts. Cross-regulation between members of polarity proteins is essential to generate the molecular asymmetry that is exclusive for each membrane domain and coordinate the maturation and preservation of the AJC to strengthen polarization (Figure I5). Indeed, it has been shown that TJ formation is compromised when a member of any polarity complex is disrupted (Bilder & Perrimon, 2000; Joberty et al., 2000, Lemmers et al., 2004; Shin et al., 2005; Suzuki et al., 2001; Yamanaka et al., 2003).

After the first contact between neighboring cells, AJs and TJs proteins are recruited to their place in the membrane. Cell junctions are established by the nectin family of adhesion receptors in the first place. After that, E-cadherin and JAM-A start forming AJs and subsequently, claudins situate apically to AJs to establish TJs (Sakisaka et al., 2007). Regarding the polarity complexes, Par3 is fundamental for AJs and TJs formation, being first recruited to nectin adhesion complexes from where it recruits other proteins (Ooshio et al., 2007) (Figure I5).

Scribble complex proteins Scribble and Dlg are targeted to the basolateral membrane by E-cadherin (Navarro et al., 2005) and prevent Par3 recruitment to the lateral domain (Rodríguez-Boulan & Macara, 2014). Pals1 could as well be stimulating AJs by promoting E-cadherin supply at cell-cell contacts (Wang et al., 2007), while aPKC is involved in maintenance of E-cadherin at the cell surface (Sato et al., 2011).

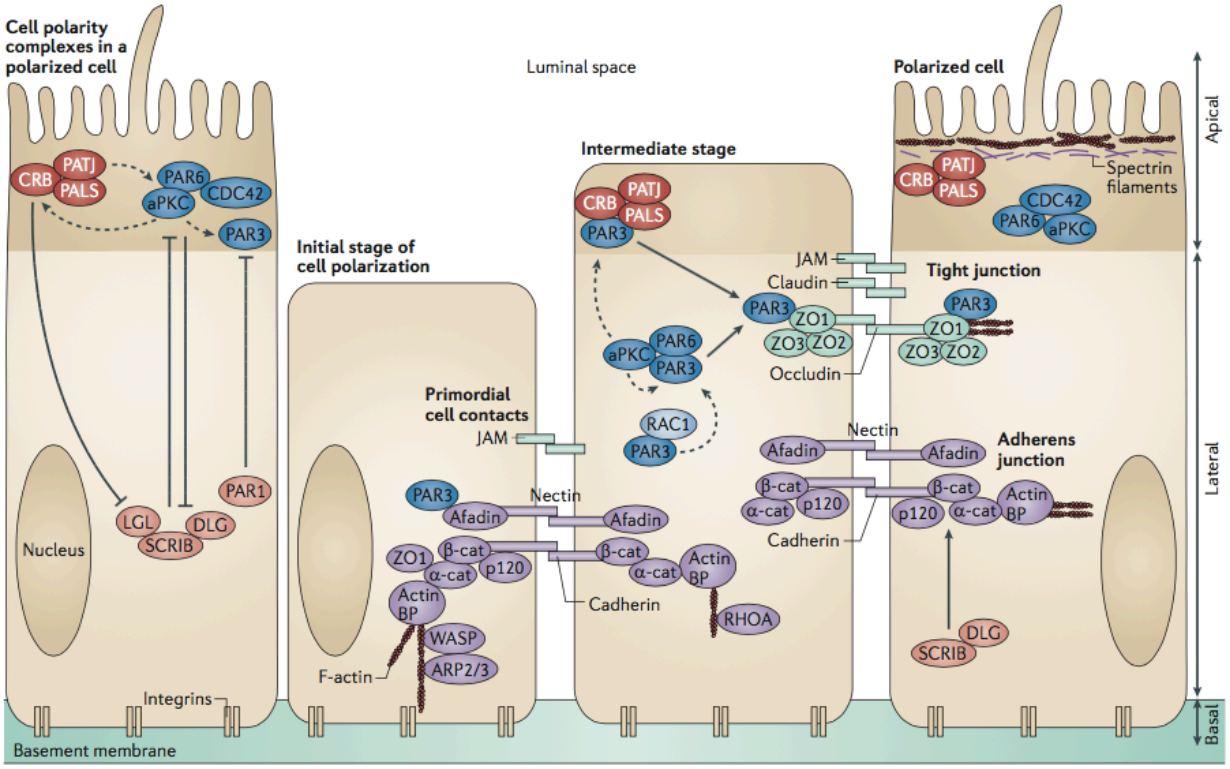

Figure I5 Apico-basal polarization in epithelial cells. Three main polarity complexes participate in the establishment of apico-basal polarity: Crumbs (in red), Par (in blue) and Scribble (in orange) complexes. At initial stages of cell polarization, primordial contacts are established to maturate and give rise to AJs and TJs that localize to the apico-basal membrane border. During intermediate stages, Par3 phosphorylated by aPKC and to exclude it from adhesions and subsequently from PAR and Crumbs complexes to establish the apico-basal border. At the same time, Scribble defines the basolateral domain antagonizing Par and Crumbs complexes and avoiding the expansion of the apical domain. From Martín-Belmonte & Pérez-Moreno, 2011.

5. Cytoskeletal and cell polarity regulators interactions in dynamic processes

Cells participate in dynamic cellular processes driven by the contractile activity of the actomyosin network and sustained by microtubules and intermediate filaments. Migrating cells show a front-rear polarity in which actin polymerization, controlled by Arp2/3, is limited to the leading edge and linked to lamellipodia formation. These cells also show microtubule-organizing center (MTOC), Golgi and nuclei reorientation depending on the direction of migration. Interactions between Cdc42, components of the PAR complex and proteins related to filament activity (such as dynein, MRCK or ROCK) have been shown to play a key role during cell migratory (Cau & Hall, 2005; Crespo et al., 2014; Etienne-Manneville & Hall, 2002; Gomes et al., 2005; Schmoranzer et al., 2009) and non-migratory processes like epithelial polarization (Feldman & Priess, 2012).

Rho GTPases are important participants in cellular dynamic processes. The formation of filopodia and lamellipodia relies on the activity of the small GTPases Cdc42 and Rac1, respectively, while RhoA is critical for stress fibers and focal adhesions to develop (Sit & Manser, 2011) (Figure I6). Moreover, actin protrusion formation is determined by Rac activity (Couto et al., 2017; Georgiou & Baum, 2010). In another context, the assembly of tight junctions in MDCK cells depends on Rac activity suppression mediated by Par3 (Chen & Macara, 2005).

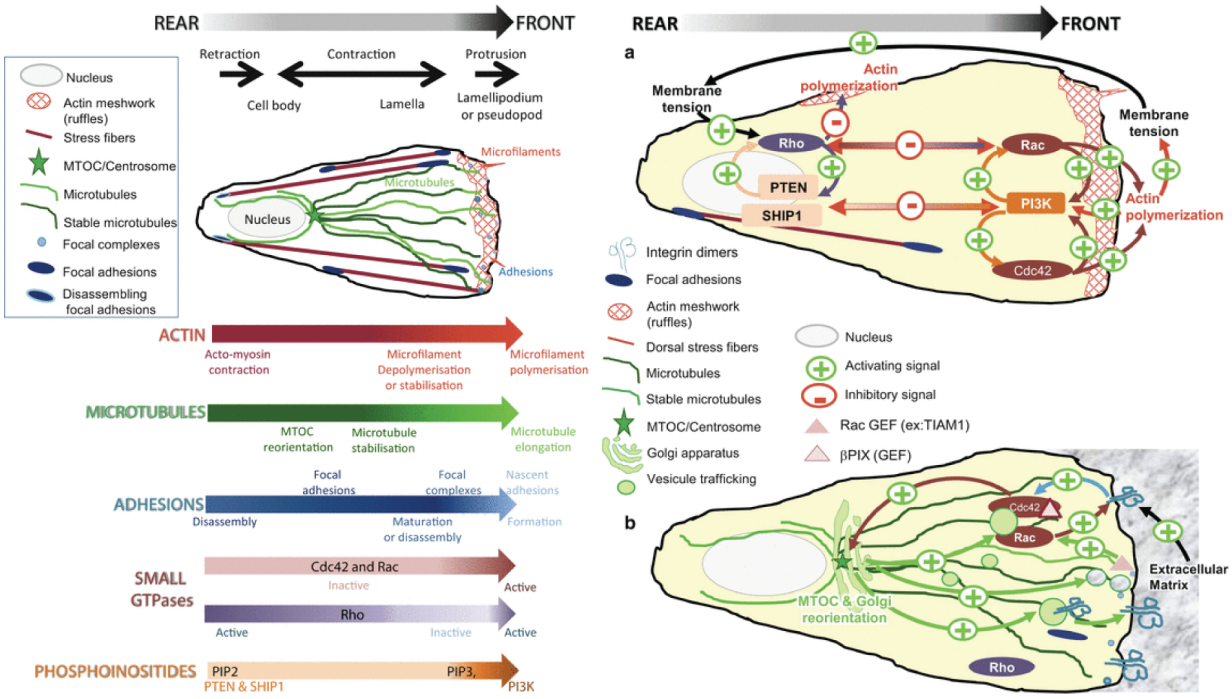

Figure I6. Front-rear polarity in migrating cells. A) The front-to-rear polarity axis extends along the major axis of the cell and is apparent in functional and structural differences between the edges. **B)** Many positive or negative feedback loops act enhancing the polarity axis during cell migration, being Rho GTPases key components of these loops. From Llense & Etienne-Manneville, 2015.

In epithelia, Scribble polarity complex is known to maintain the basolateral domain but its function varies in migrating cells. In the polarized mammary cell line MCF10A, Scribble is required to achieve wound closure and directional migration by regulating lamellipodium formation and recruitment of Cdc42 and Rac1 to the leading edge (Dow et al., 2007). In addition, Lgl interacts with non-muscle myosin II (NMII), an event regulated by aPKC-dependent phosphorylation of Lgl, which prevents that interaction (Dahan et al., 2014). When cells migrate, Lgl presence is increased at the leading edge, where it forms a complex with aPKC and Par6. After phosphorylation by aPKC, Lgl is directed to the lamellipodium where it will be dephosphorylated to allow interaction with NMII. It has

been hypothesize that Lgl could be preventing NMII filament generation by this association, which would enhance F-actin formation at the leading edge. This could explain the absence of Lgl from the rear end, where NMII filaments need to be assembled (Ravid, 2014).

6. *De novo* luminogenesis

During epithelial tubulogenesis, when tubes derive from unpolarized cells, the luminal space has to be generated "*de novo*" while cells acquire apico-basal polarity, as it is the case of cord hollowing processes in which this work is focused on. Different processes of *de novo* lumen formation have been described in a variety of *in vivo* and *in vitro* systems, as zebrafish vasculature and *Drosophila melanogaster* trachea development or 3D organotypic cell cultures, all of them sharing a common series of biological steps: (1) tube initiation and polarity acquisition, (2) luminal and apical membrane enlargement dependent on vectorial membrane trafficking, (3) maturation and termination of the structure. Details for each step are addressed below.

6.1. Polarity initiation and acquisition of membrane identity

Acquisition and maintenance of apico-basal polarity is a key event in any epithelial tissue. It relies on the establishment of cell-cell junctions and the generation of different membrane domains, apical and basolateral, with specific protein and phospholipid composition. For this molecular segregation to be achieved, sorting signals, vectorial trafficking and asymmetric cytoskeletal and subcellular components organization are essential (Mellman & Nelson, 2008). The mechanisms that initiate polarization can differ among cell types. **Extracellular matrix components and neighboring cells** can provide the external cues necessary for the initiation of the process, which are transduced by sensing proteins such as integrins or cadherins (Drubin & Nelson, 1996). This is the case of epithelial and endothelial cell cultures, which require integrin to induce lumen formation through cytoskeletal regulators (Davis & Bayless, 2003; O'Brian et al., 2001). β1-integrin can interact with collagen and this signaling activates Rac1 and the RhoA-ROCK1-myosin II cascade, which in turn regulates the cytoskeletal changes needed to generate the lumen initiation site and reinforce the orientation-signaling pathway (O'Brian et al., 2001; Wu et al., 2009; Zhang et al., 2009).

Phosphoinositides are membrane phospholipids associated with several cell functions, such as signaling, cytoskeleton regulation and cell motility, development and intracellular trafficking (Balla, 2013). The enrichment of different phosphoinositide types contributes to determine membrane identity. In MDCK cells, the apical membrane presents an enrichment in phosphatidylinositol (4,5)-biphosphate (PIP2), while the basolateral membrane displays higher amounts of phosphatidylinositol (3,4,5)-triphosphate (PIP3) (Martín-Belmonte & Mostov, 2007). This distribution contributes to the asymmetric localization of different membrane proteins and polarity complexes, which at the same time drive the apical positioning of PTEN (phosphatidylinositol 3,4,5-triphosphate 3-phosphatase) that enhances PIP2 enrichment at the apical domain and recruits Cdc42 to the cell cortex (Martín-Belmonte et al., 2007).

6.2. Apical membrane initiation and expansion

The formation of the apical membrane initiation site (AMIS) starts with the delivering of podocalyxin by transcytosis to a membrane spot in the contacting surface between two cells, which then matures to become the pre-apical patch (PAP) or the site of assembly for apical polarity determinants (Bryant et al., 2010; Gálvez-Santisteban et al., 2012) (Figure I7).

After the formation of the PAP, several small GTPases, such as Rab8a and Rab11a, collaborate in apical vesicle trafficking of several major polarity complex components and regulators (Par3, aPKC, Crb, Cdc42) (Bryant et al., 2010). These events enable as well the positioning of PTEN to the AMIS to generate the phospholipid asymmetric distribution of the membrane domains, which at the same time enhances recruitment of apical proteins with PIP2-binding domains (Gassama-Diagne et al., 2006; Martín-Belmonte et al., 2007).

To expand the apical membrane, large amounts of membrane material have to be delivered to the apical domain through guidance by **vectorial vesicular transport** and the **cytoskeleton**. The delivery of apical and basolateral components to their specific domains is controlled by intrinsic sorting signals of the cargoes (Folsch, 2008). In addition, there are several trafficking pathways and sorting mechanisms in epithelial cells: biosynthetic, endocytic, recycling and transcytotic pathways. In the biosynthetic route, newly synthesized components are carried through the secretory pathway (endoplasmic reticulum (ER), trans-Golgi network (TGN), carrier vesicles) or directly transferred from the ER and delivered to the targeted membrane domain (Zhang & Schekman, 2013). Proteins at different membrane domains can also be endocytosed

and targeted to degradation in lysosomes or recycled through endosomes to sort them back to the membrane (Eaton & Martín-Belmonte, 2014; Desclozeaux et al., 2008). These proteins can also be carried across the cell to the opposite plasma membrane through transcytosis (Bryant et al., 2010; Madrid et al., 2010).

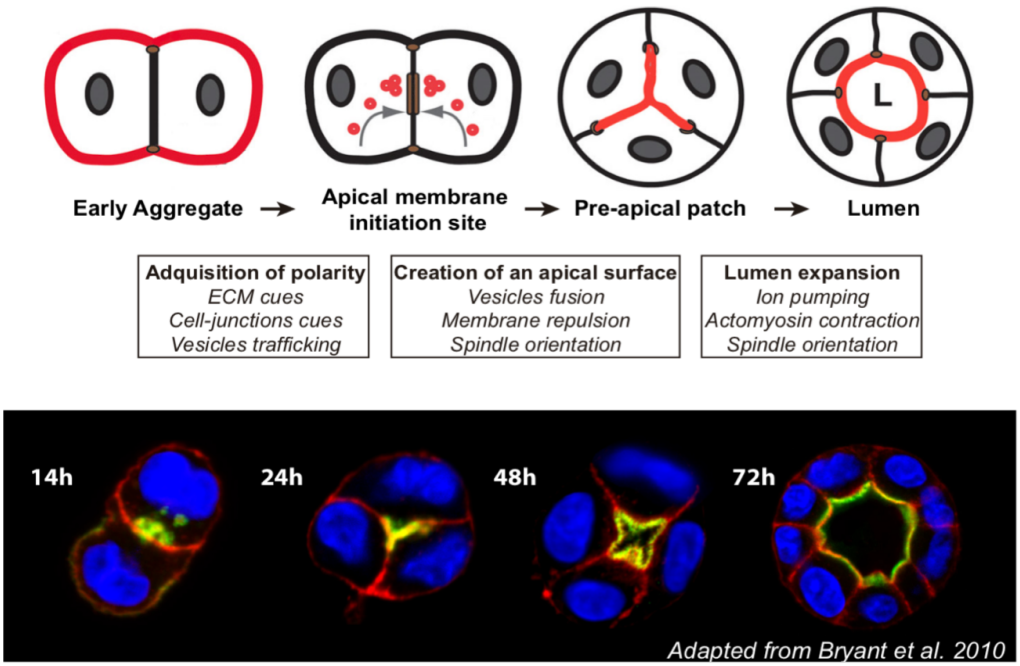

Figure I7. *De novo* lumen formation in *in vitro* epithelial morphogenesis. Several mechanisms contribute to the generation of a new luminal space during epithelial morphogenesis: Firstly, cells acquire apico-basal polarity and a novel apical surface between the contacting membranes of different cells is formed, generating a pre-apical patch. Finally, the single lumen expands and is maintained by proper spindle orientation. Adapted from Bryant et al., 2010.

Specialized proteins with important roles in vesicle trafficking and molecular sorting are involved in the enlargement of the apical domain. In MDCK 3D culture, synaptotagmin-like proteins SLP2A and SLP4A coordinate the spatiotemporal organization of vesicular transport (Gálvez-Santisteban et al., 2012). SLP2A, together with Rab27, directs vesicles to the AMIS and once there, SLP4A, in combination with Rab27-Rab3-Rab8 and syntaxin 3, regulates membrane fusion. Syntaxin 16 is also necessary for the recycling of E-cadherin and avoiding mispositioning of apical membrane components that results in multiluminal cysts (Jung et al., 2013).

Oriented vesicle trafficking and apical expansion also rely on microtubule and actomyosin networks, which allow vesicle transport through motor proteins and are necessary for these processes to take place. There is a cortical network of actin filaments that localizes subapically upon PIP2 enrichment and subsequent Cdc42 activation after initial polarization (Martín-Belmonte

et al., 2007). These filaments might regulate the transport of Rab11a- and Rab8a-positive vesicles to the AMIS at initiation stages (Roland et al., 2011).

6.3. Maturation of the lumen, junctional rearrangements and termination

Another main function of the **cytoskeleton** is providing physical support and organizing the newly delivered apical membrane components into the correct shape. This and other mechanisms allow the tubular organs to acquire and maintain the correct shape and perform their physiological functions.

The expansion of the lumen to reach an appropriate width that stabilizes the structure is accomplished through two mechanisms: (1) deposition of **anti-adhesive components**, such as glycosylates or sialylated proteins like Crumbs, podocalyxin (also called Gp135) and Mucin-1 or polysaccharides like chitin in tracheal cells (Meder et al., 2005; Wang et al., 2006) with highly negatively charged extracellular domains, and (2) the **creation of turgor**. Anti-adhesive factors force membrane detachment by steric hindrance of cell-cell adhesion. The force needed for lumen expansion and stability is generated by the F-actin−ERM−RhoA−myosinII network, which localizes to the subapical region as a consequence of Gp135 presence (Nielsen & McNagny, 2008). Regarding the acquisition of turgor, it can be achieved by boosting the hydrostatic pressure as a result of the activation of apical channels and pumps (like the cystic fibrosis transmembrane conductance regulator (CFTR) in MDCK *in vitro* and zebrafish gut *in vivo*, or the Na-K-ATPase used for lumen expansion) and the role of claudins that regulate TJs permeability (Bagnat et al., 2007; Bagnat et al., 2010; Krupinski et al., 2009). Turgor can also derive from external forces like blood flow in the zebrafish vasculature system (Herwig et al., 2011).

Furthermore, during tubulogenesis **cell-cell junctions** need to be remodeled to achieve multiple lumen resolution and obtain a single open lumen along the tube. Two main processes underlie the dynamics of cell-cell junctions: the shift of AJs components and the equilibrium of adhesion and cortical tension forces at the cell surface. While adhesion favors the contact between adjacent cells, cortical tension tends to reduce it (Lecuit & Lenne, 2007). AJ components turnover is accomplished by the endocytosis and recycling of cadherins, which seems to be mediated by the actomyosin cytoskeleton (Ivanov et al., 2004; Yap et al., 2007) and polarity proteins like Cdc42 and the Par complex (Georgiou et al., 2008). The maintenance of AJs is in turn regulated by Rho

GTPases (Rho, Rac and Cdc42), which control actin network stability through effectors like Neural Wiskott-Aldrich syndrome protein (NWASP) or formins (Kovacs et al., 2011; Otani et al., 2006).

Once a lumen is formed, polarized architecture is reinforced and maintain during tissue expansion by symmetric **oriented cell division**, although the direction of tissue growth can be guided as well by mechanical tension in other systems (Bosveld et al., 2016). In vertebrates, the core components of the cortical machinery are three conserved proteins: NuMA (*Drosophila* Mud, *C. elegans* LIN-5), LGN (*Drosophila* Pins, *C. elegans* GPR1/2) and Gαi (which has the orthologues GOA-1 and GPA-16 in *C-elegans*). Gαi is attached to the plasma membrane and interacts with Pins/LGN through the C-terminal domain. Pins/LGN is at the same time linked to Mud/NuMA, which interacts with dynein, the motor protein that generates the force to pull the microtubules towards the cortex (di Pietro et al., 2016) (Figure I8).

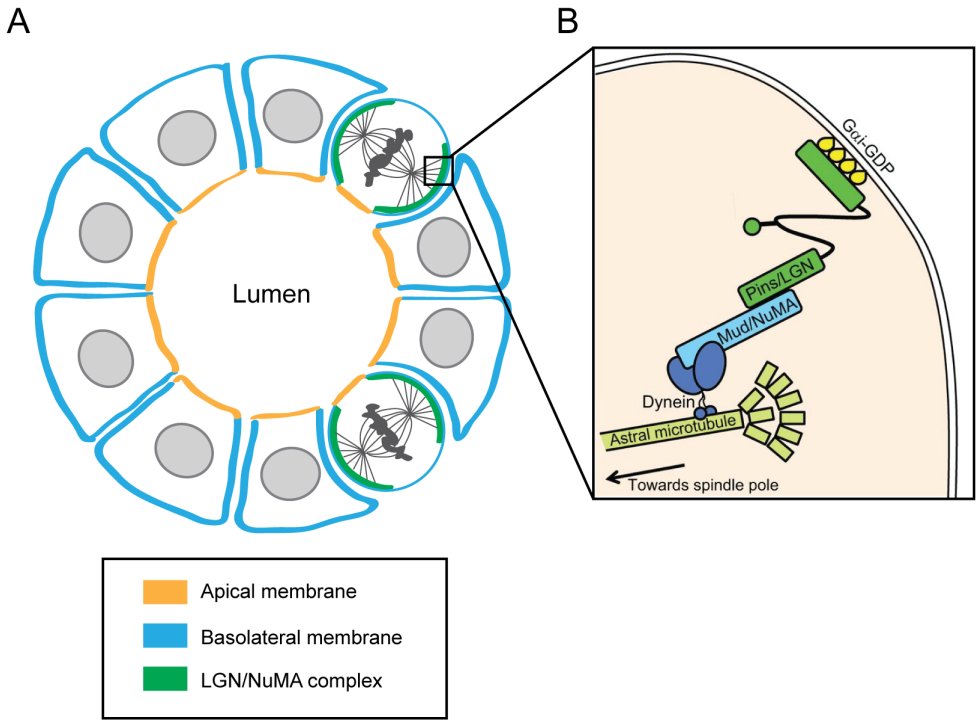

Figure I8. Schematic model for spindle orientation. A) Dividing cells in a 3D polarized epithelial structure position their spindle poles perpendicularly to the apico-basal axis (apical in yellow, basolateral in blue) to maintain a single lumen. LGN/NuMA complex (in green) is excluded from the apical membrane and attaches to the lateral cortex from where they anchor astral microtubules. **B)** The basic cortical machinery that orients cell division is formed by Gαi, which attaches to the membrane and binds to Pins/LGN. Pins/LGN interacts with Mud/NuMA, which can bind to the motor protein dynein, the one interacting with astral microtubules to pull the spindles as the cell divides. Adapted from Bergstralh et al., 2017.

During epithelial morphogenesis, Cdc42 and Par3 play a central role, as their activities and mediated recruitment of aPKC to the apical membrane are required to regulate mitotic spindle

orientation (Hao et al., 2010; Jaffe et al., 2008; Qin et al., 2010; Rodríguez-Fraticelli et al., 2010). The LGN-NuMA complex that directly positions the spindle during cell division is excluded from the apical surface upon aPKC phosphorylation, which causes the cell to divide in the plane of the epithelial monolayer (Hao et al., 2010; Zheng et al., 2010).

7. Major signaling pathways in development

The development of a complex multicellular organism from a single cell is a very intricate process in which a variety of genetically regulated events (including cell proliferation, migration and differentiation) occur in a coordinated manner that leads to the generation of the different tissues and organs of a body. Several main signaling pathways act during development at specific locations and times triggering the cellular responses that ensure proper embryo development. Among the most important developmental pathways we can find Fibroblast Growth Factor (FGF), Wnt, Notch, Bone Morphogenetic Protein (BMP), Hedgehog (Hh) and Transforming Growth Factor Beta (TGF-β) signaling pathways. The components, signals and responses generated by these pathways during development often appear evolutionary conserved, and are also associated with adult homeostasis and regeneration. Therefore, understanding their function and regulation will provide valuable information to better decipher and treat congenital malformations and diseases associated with their malfunction. For the purpose of this thesis, Wnt, Hh and TGF-β signaling pathways will be described below.

7.1. Wnt pathway

The Wnt signaling pathway regulates stem cell renewal, cell proliferation and cell differentiation during embryonic development as well as in adult tissue homeostasis (Logan & Nusse, 2004). The core components of the pathway are evolutionary conserved and were being first discovered in *Drosophila* in relation to a series of embryonic morphogenetic defects (Nusslein-Volhard & Wieschaus, 1980; Sharma & Chopra, 1976).

The canonical pathway is also called Wnt-β-catenin pathway. β-catenin is normally targeted for degradation by a complex formed by Axin, APC CK1 and GSK3 when the pathway is inactive. Secreted Wnt proteins bind to the receptor, which is formed by a heterodimer of a Frizzled receptor and one of the co-receptors LRP5 or LRP6, and activate the pathway. Upon ligand-receptor binding, cytoplasmic protein Dishevelled is recruited along with the Axin-GSK3 complex, which

results in the triple phosphorylation of LRP5/6 by GSK3, Cyclin Y and CK1. As a consequence of recruitment of the Axin complex to the plasma membrane, β-catenin is stabilized in the cell and translocated to the nucleus, where it binds Tcf/Lef DNA-binding proteins to regulate their function by avoiding their binding with Groucho/Tle co-repressors (Figure I9A). De-repressed target genes are different between cell types except for genes related to cell-cycle progression, stem cell function and feedback loops, which have been found to be common in all cases (Nakamura et al., 2016).

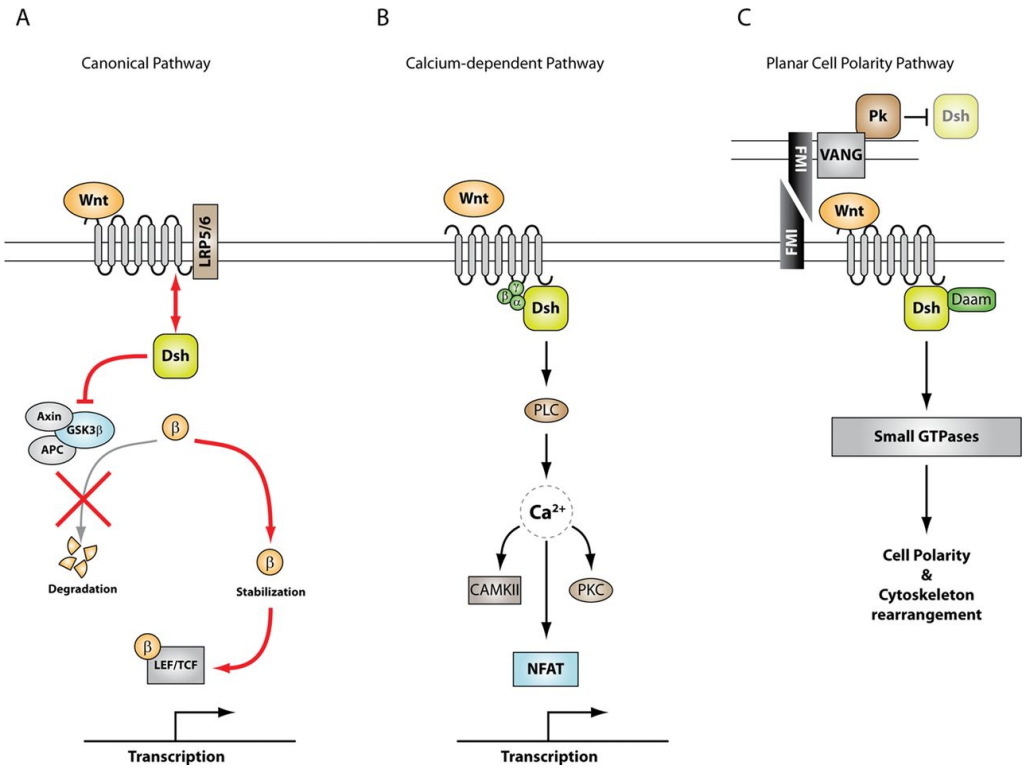

Figure I9. Overview of canonical and non-canonical Wnt signaling A) In the canonical pathway, the activation by Wnt ligand binding to Frizzled receptor blocks GSK3-dependent degradation of β -catenin, which translocates into the nucleus for transcriptional regulation of genes. **B)** In the non-canonical calcium-dependent pathway, the activation of Frizzled receptors causes the release of calcium within the cell. As a consequence, several effectors, like calcium/calmodulin-dependent kinase II (CamKII), protein kinase C (PKC) and NFAT are activated. C) The non-canonical Wnt PCP pathway results in cytoskeletal and polarity changes mediated by Small GTPases. From Mayor & Theveneau, 2013.

Canonical and non-canonical (or β-catenin-independent) Wnt pathways involve different ligands, receptors and transducers. Non-canonical signaling includes the planar cell polarity (PCP) pathway and the Wnt/Ca^{2+} pathway (Figure I9B-C). The PCP pathway seems to be transcription-independent and regulates cell polarity and the actin cytoskeleton to allow asymmetric positioning of the structures (in a planar axis) and directed migration, having a crucial role in convergent extension movements. The Wnt/Ca^{2+} pathway further modulates canonical pathway for dorsal axis

formation and PCP pathway for gastrulation movements and heart formation (Komiya & Habas, 2008).

Wnt pathway also regulates several mechanisms during mammary gland development, being its malfunctioning associated with breast cancer (Yu et al., 2016). SFRP family of proteins has been shown to modulate Wnt pathway in different contexts (Bovolenta et al., 2008). Our laboratory found that stromal SFRP3 secretion is linked to mammary gland development and cancer, as knockout mice for *Sfrp3* show an increase in proliferation of luminal epithelial cells and tertiary branching, cell polarity loss and anomalous differentiation, and is related to cancer susceptibility. Nevertheless, whether *Sfrp3* could have been regulating these processes by modulating the Wnt pathway still remained to be solved.

7.2. Hedgehog pathway

Hedgehog signaling was first described in *Drosophila*, where it mediates the larval epidermis and adult appendages patterning through crosstalk with other signaling pathways, regulating cell proliferation and identity (Hartl & Scott, 2014; Ingham & Placzek, 2006). A similar function in limb development was identified in vertebrates, in which it has been found to associated with the development of many other organs and structures (neural tube, eye, gastrointestinal tract, kidney, pancreas, or muscles, among others) and in adult tissue homeostasis and regeneration (bladder, heart or fin) (McMahon et al., 2003; Wang et al., 2015; Wehner & Weidinger, 2015).

Vertebrates have between three to five Hh morphogen genes (*Desert*, *Indian* and *Sonic*, with duplicated *Indian* and *Sonic* genes in fish), while *Drosophila* genome only encodes one gene. Several factors have been proposed to be involved in their release, including Dispatched, Scube2 and ADAM proteases, as well as endosomal sorting complex required for transport (ESCRT) proteins (Briscoe & Thérond, 2013; Matusek et al., 2014). In vertebrates, two genes codify for Patched receptors (*Ptch1* and *Ptch2*) whose activity is inhibited when bound to Hh proteins. Three co-receptors are necessary for the activation of the pathway: Cdo, Boc (Ihog and Boi in *Drosophila*) and Gas1. The mechanism of transduction occurs by receptor inactivation when Ptch receptors bind to Hh proteins, which prevents them to continue inhibiting Smoothened (Smo), a G-protein coupled receptor protein. Downstream, transcription factors Gli2 (duplicated in fish) and Gli3 act through activator or repressor domains (PKA turns them from activators into repressors), while Gli1 only functions as an activator (Figure I10). Interestingly, vertebrate Hh signaling is remarkably

different from *Drosophila* in that it depends on the primary cilium (PC), a hair-like structure that acts as biological sensor.

In addition to the canonical pathway described above, other non-canonical Hh signaling have been suggested, as the induction of stress fibre formation in endothelial cells and fibroblasts caused by Smo-dependent stimulation of RhoA and Rac1, not related to Gli factors activity (Brennan et al., 2012).

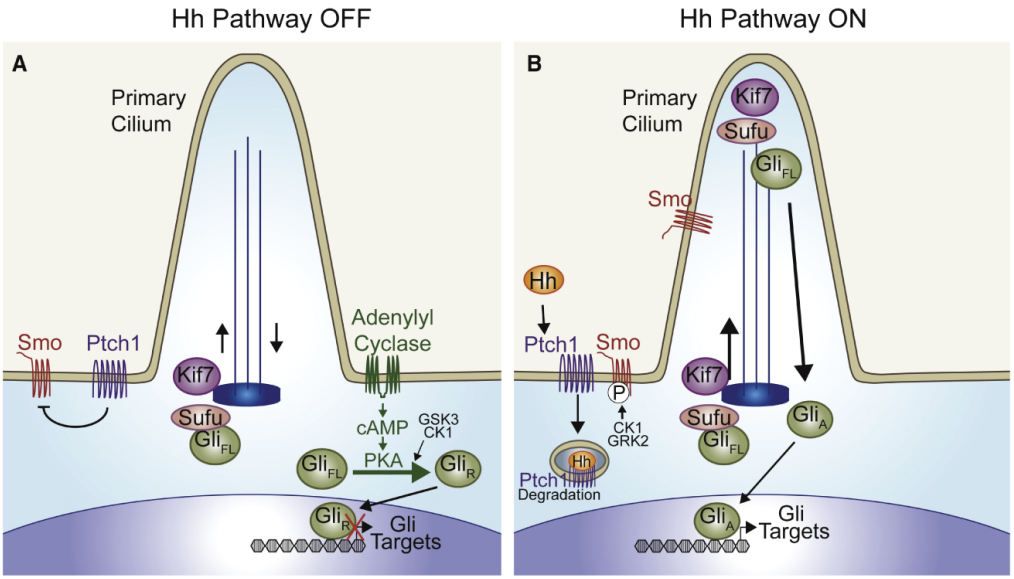

Figure I10. Simplified scheme of vertebrate Hedgehog pathway. A) In the absence of Hh ligand, Ptch receptor suppress Smo activity and ciliary positioning. Low levels of Kif7, Sufu and full-length Gli go into the PC, which enhances GliFL transformation into the repressive form (GliR) after phosphorylation by PKA. **B)** If Hh ligands bind to Ptch, they are both endocytosed and targeted for degradation. Smo is phosphorylated, acquires an active conformation and localizes to the PC, in which Kif7, Sufu and Gli are being accumulated. Smo stimulates Sufu-Gli dissociation and Gli transformation into its active form (GliA). Adapted from Pak & Segal, 2016.

7.3. TGF-β pathway

TGF-β pathway activation has been shown to have different and even opposite consequences depending on the cellular and environmental conditions. Only a few genes are targeted in all cell types that activate this pathway (SMAD7 and SKIL), with the canonical SMAD signaling being shared in all conditions. The differences rely on the cell epigenetic status and transcriptional landscape, as well as the molecular composition of TGF-β transduction system (degree of presence and activity of ligands, receptors and modulators) (Massagué, 2012). TGF-β is implicated in many biological processes, such as embryonic stem cell (ES) renewal and differentiation (Young, 2011), lineage regulation (Mullen et al., 2011), EMT (Thiery et al., 2009),

regulation of immune and inflammatory events (Li & Flavell, 2008) or tumor suppression or progression (Massagué, 2008).

Ligands can be classified in two families: the TGFβ-activin-Nodal and the BMP subfamily. The receptors, which share Ser/Thr protein kinase activity, must form a complex of two type I (signal-propagating) and two type II (activator) modules. After binding to the ligand, type II receptors phosphorylate type I receptors, which spreads the signal by SMAD phosphorylation. There are seven type I receptors and five type II receptors in humans, which display binding-specificity for different ligands. The subsequent activation of SMAD proteins (known as R-SMAD or receptor-regulated SMAD proteins) leads to the transcriptional regulation of target genes and the opening of repressive chromatin. TGFβ-activin-Nodal type I receptors phosphorylate SMAD2 and SMAD3 while BMP type I receptors target SMAD1, SMAD5 and SMAD8. SMAD4 acts as partner in a trimer with two R-SMAD proteins to carry out transcriptional regulating functions (Figure I11A).

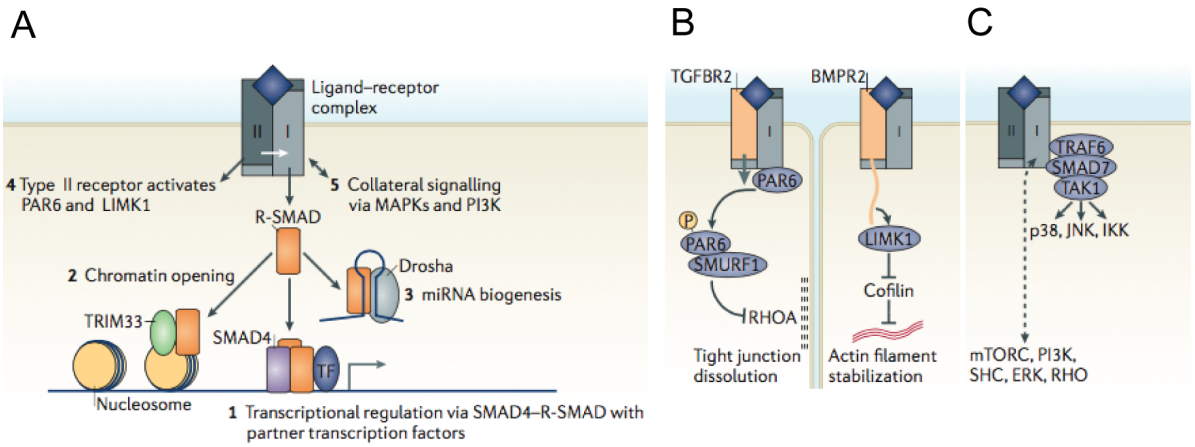

Figure I11. TGF-β pathway components and signals. A) TGF-β family ligands act through a heterotetrameric structure formed by two type I and two type II receptors. A phosphorylation cascade causes the activation of R-SMAD, which can act through canonical signaling by pairing with SMAD4 and transcription factors (option 1) and mediating chromatin opening (option 2). Non-canonical pathways involve options 3 to 5. **B)** Option 4: type II receptors can also generate a response by phosphorylating PAR6 or activating LIMK1. **C)** Option 5: other pathway transducers, such as JNK, mTORC, PI3K, ERK and RHO can also be activated by TGF-β receptors. Adapted from Massagué, 2012.

Moreover, TGF-β can activate SMAD-independent pathways (known as non-canonical) through signaling by type II receptors or activation of other signaling cascades (Figure I11B-C). For instance, type II receptors accelerate EMT by phosphorylation of Par6, which triggers RhoA to be degraded and tight junctions to be removed (Ozdamar et al., 2005). TGF-β can also mediate MAPK and PI3K activation (among others) by mechanisms involving TRAF6 and mTORC (Mu et al., 2012).

OBJECTIVES

The present work has focused on the accomplishment of the following main objectives:

I. Characterization of SFRP3 in Wnt pathway modulation in the context of epithelial morphogenesis.

II. Uncovering the role of the main signaling pathways Hedgehog and TGF-β *in vivo* during zebrafish intestine development.

III. Analysis of possible mechanisms of action of TGF-β in 3D epithelial morphogenesis *in vitro*.

MATERIALS & METHODS

Fly care

Drosophila melanogaster strains were kept in a standard culture medium in incubation chambers with controlled temperatures (17º or 25º, depending on the experimental requirements) and relative humidity (75%).

The Gal4/UAS system

Experiments were performed using the Gal4/UAS system (Brand and Perrimon, 1993), which allows us to control gene expression in temporally and spatially restricted domains. It consists of the cloning of the yeast transcriptional activator Gal4 under the control of a known promoter (called '*driver*' sequence) that will direct its expression in a specific localization at a particular developmental time. When Gal4 is expressed under the activity of the driver, it binds to the UAS (Upstream Activation Sequence) and triggers the transcription of the genes downstream UAS sequence (Figure M1).

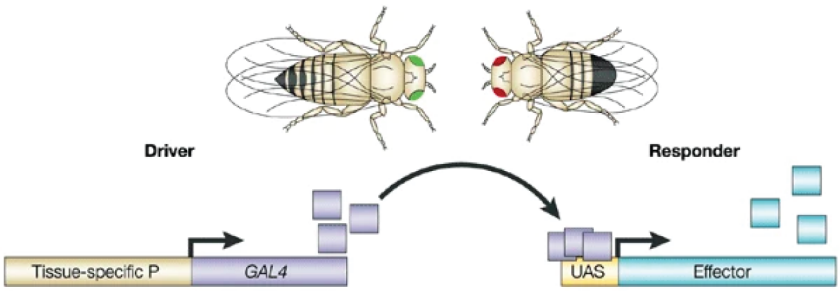

Figure M1. The Gal4/UAS system. Conditioned expression widely used in *Drosophila*. The expression of a *Gal4* transcription factor is spatiotemporally controlled by the tissue-specific promoter ("Tissue-specific P"). Gal4 recognizes the UAS sequences and transcribes the genes associated ("Effector"). Being placed each transgene in different flies avoids unwanted expression of the UAS-Gene. If the flies are crossed, such expression is obtained. Adapted from Wimmer, 2003.

Drosophila strains

Unless stated otherwise, the fly strains used are described in Flybase (http://www.flybase.org) and publicly available at Bloomington Drosophila Stock Center (http://www.bdsc.indiana.edu).

We used the following Gal4 lines to drive gene expression: *hh-Gal4* (Tanimoto et al., 2000), *nub-Gal4* (Calleja et al., 1996). The expression patterns of the Gal4 lines used in this work in a L3 wing imaginal disc are shown in Figure M2 (green).

UAS lines used in this work: UAS-*GFP* was used to visualize Gal4 expression and as a control and UAS-*Sfrp3-myc* was generated by fusing *Sfrp3* cDNA in frame to a C-terminal Myc tag and then cloned into a pUAST vector to obtain transgenic *Drosophila* lines expressing SFRP3 under the UAS promoter. The fly line with NRT-wg background was a gift from G. Morata, previously described in Alexandre et al., 2014.

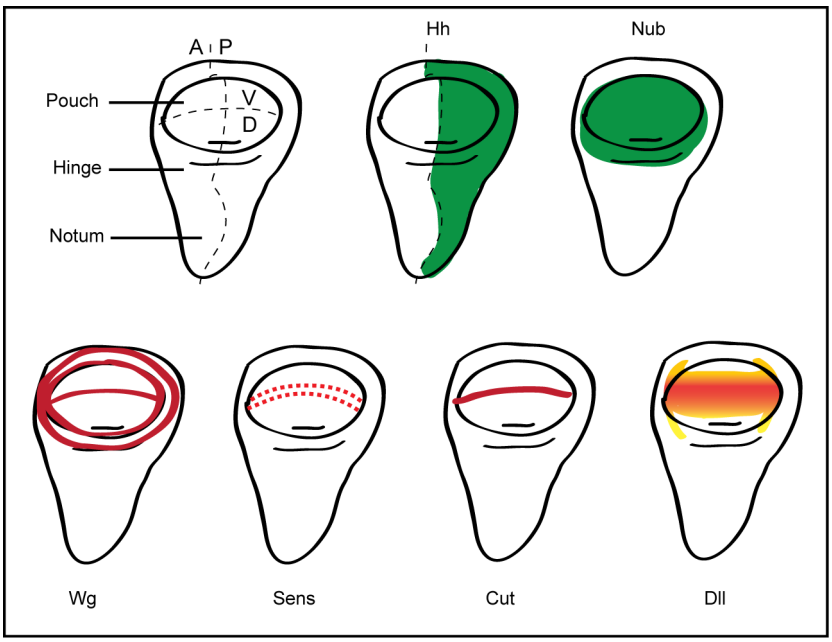

Figure M2. *Drosophila* wing imaginal disc. Simplified scheme of third instar wing discs. Pattern of expression of Gal4 lines used are shown in green. Pattern of expression of genes of interest for this work are shown in red. A, anterior; P, posterior; D, dorsal; V, ventral. Hh, Hedgehog; Nub, Nubbin; Wg, Wingless; Dll, Distal-less.

Cell culture

2D Culture

MDCK II cells were maintained in MEM supplemented with 5% Fetal Bovine Serum (FBS), 2 mM L-glutamine, 100 U/ml penicillin and 100 mg/ml streptomycin at 37ºC in a humidified atmosphere containing 5% CO_2. Cell lines were passaged approximately three times per week and subcultured at a 1:5 or 1:10 ratio. Mycoplasma testing was regularly

performed to avoid contamination. MDCK stable cell line expressing mCherry was maintained using medium with 0.5 mg/ml G418.

3D Culture

To culture MDCK II to form spheroids, cells were trypsinised to a single cell suspension of $2x10^4$ cells/ml and mixed in cold 2% Matrigel (BD Biosciences) in 5% FBS-supplemented MEM. After mixing, cells were plated in 8-well coverglass chambers (250 µl/well) (IBIDI) that had been previously precoated with Matrigel (8-10 µl/well). The medium was changed every 2 days maintaining a 2% Matrigel concentration and spheroids were grown for 1-4 days or until lumens formed in the control sample.

Fish stocks

Zebrafish were maintained at 28ºC and bred according to standard procedures (Westerfield, 2000). Strains used in this work include: wild-type AB, EW and TL lines, mutant *smo*^{s294} (Aanstad et al., 2009) and transgenic *Tg(ptch2::kaede)a4596Tg* (Huang et al., 2012). *TgBAC(cldn15la-GFP)pd1034* and *TgBAC(myadm-GFP)* lines were provided by Dr. Michel Bagnat.

Fish drug treatments

Drug treatments were carried out by incubation of 30-32hpf embryos previously dechorionated in E3 medium with EW-7197 (40-60 µM depending on the experiment, MedChem Express). Controls for the treatments were incubated in E3 medium with an equivalent concentration of DMSO, as EW-7197 stocks were maintained in DMSO. The drug was removed at 4dpf and embryos were either washed and fixed for further analysis or washed and prepared for *in vivo* analysis.

Fish live imaging

Embryos were embedded in low melting point agarose (Sigma) at 1.5% in E3 with 1x tricaine for confocal imaging using different lens and microscopes (see Microscopy section).

Transcriptomic analysis

Embryo dissociation and cell isolation by FACS for RNA sequencing

Embryos were rinsed with calcium-free Ringer's solution for 10 min. After removing Ringer's solution, embryos were incubated in 0.25% trypsin-EDTA (Gibco) and 300 µg/ml collagenase (Sigma) for approximately 60 min at 31ºC with pipetting every 15 min to achieve cell dissociation. Cells were washed with PBS supplemented with 5% fetal bovine serum (FBS) and passed through a 30 um CellTrics filter (Partec). Cell suspensions were stained with propidium iodide (Invitrogen) to filter out dead cells and then sorted on a BD FACS Diva sorter at the Flow Cytometry Shared Resource center (Duke University). Cells were collected in Buffer RLT (Qiagen) and total RNA extraction for each population was performed using RNeasy Plus Micro Kit (Qiagen). The integrity of RNA samples was analyzed and only samples with an RNA integrity number (RIN)>7.0 were selected for RNA sequencing (RNA-seq).

RNA sequencing and bioinformatic analyses

Clontech Ultra low libraries were prepared in triplicate and sequenced using the Illumina HiSeq 4000 50 bp single-end read platform. Raw data were uploaded to the online Galaxy platform (https://usegalaxy.org) for analysis (Afgan et al., 2016). Reads were mapped to the GRCz11 (danRer11) genome using HISAT2, and gene counts were analyzed using htseq-counts (Kim et al., 2015). Htseq-counts were input into DESeq2 to calculate differential expression for each condition (Anders et al., 2015; Love et al., 2014). Genes were considered to be up or downregulated in a condition if their expression presented a 2-fold increase or decrease in comparison with the other condition with adjusted p-value of <0.05. Principal-component analysis was performed using the DESeq2 package. The differentially expressed genes were examined for enrichment of known biological processes using DAVID Bioinformatics Resources (Huang et al., 2009a, 2009b).

Gene expression analysis

For real-time quantitative PCR (RT-qPCR) assays, MDCK II cells were grown in 60-mm dishes to form 2D monolayers or 3D cysts in Matrigel (at 10^5 cells/ml in a final volume of 4

ml). For 3D cultures 60-mm dishes were pre-coated with 100 µl of Matrigel before seeding the cells. Total RNA was isolated at 24h, 48h and 72h after cell seeding and purified using the RNeasy kit (Qiagen). All RNA samples were analyzed by Bioanalyzer (Agilent Technologies) to ensure RNA quality. Typically 1µg of RNA per condition was used to retrotranscribe into cDNA using the High Capacity cDNA Reverse Transcription kit (Applied Biosystems). To perform the PCR, a set of primers was design with the NCBI primer-designing tool (www.ncbi.nih.gov/tools/primer-blast) (Supplementary Table 1, Appendix). All the amplicons were designed to spam an exon-to-exon junction whenever it was possible. Real-time PCR was performed in 386-well plates in an ABI 7900 HT system (Applied Biosystems) using the Master Mix SYBR Green Kit (Agilent, Santa Clara, CA). Conditions of RT-qPCR were as follows: 95ºC for 10min, 40 cycles of 95ºC for 15s and 60ºC for 1min followed by a dissociation stage. Analysis of the melting fluorescence was used to validate a single melting peak, indicating target specificity. Every condition was tested by 3 experimental replicates per gene and assay. Experiments were typically conducted at least 3 times in independent conditions.

Mathematical and statistical analysis

To normalize the RT-qPCR data, the HPRT gene was used as housekeeping gene. Relative quantification analysis was used to determine the relative amount of RNA relative to 2D at 24 h (condition 0). To test gene silencing, the amount of RNA was relative to the control siRNA sample. The Pfaffl model was used to calculate the N number (relative quantity of RNA relative to control) (Pfaffl, 2001),

$$N_{\text{gene A condition 1}} = \frac{E_{\text{gene A}}^{-\Delta CT\,(CT_{\text{condition1}} - CT_{\text{condition0}})}}{E_{\text{Normalizer gene}}^{-\Delta CT\,(CT_{\text{condition1}} - CT_{\text{condition0}})}}$$

E represents the efficiency of the amplification (E ≤ 2) of the PCR. The efficiency was calculated for each gene by creating a standard curve with a gradient of concentrations of

cDNA and calculating the slope of the straight line. CT is the cycle threshold, which is the cycle number at which fluorescence generated within a reaction crosses the fluorescence threshold, a fluorescent signal significantly above the background fluorescence (typically between 1/10th to 1/100th of maximum signal). At the threshold cycle, a detectable amount of amplicon product has been generated during the early exponential phase of the reaction. Δ CT is the difference between the CT of the two conditions examined (Control vs KD). The three experimental replicates were used to calculate the standard error of the experiment. All the data with an SE > 50% was suppressed and repeated.

Silencing by siRNA

RNAi oligo sequences are listed in Table 1. For each gene, 25 nucleotide stealth siRNA duplexes targeting specific mRNA sequences were designed and purchased from Sigma.

Table 1: List of siRNA sequences designed against canine Smad2 and Smad3. Sequences marked with an asterisk (*) were usd to generate the presented data.

siRNA	Target sequence (5'-3')
siSmad2_1*	GAAUCGAGCCACAGAGUAAUU
siSmad2_2	CAGGACGAUUAGAUGAGCUUGAGAA
siSmad2_3	CAGUGGGAUACAACAGGCCUUUACA
siSmad3_1	CGCUUCUGCCUCGGCCUGCU
siSmad3_2	CCUCGCAGAGCAGACUGAUAAGUGU
siSmad3_3*	AGGCUCGGCGCUUAUGCAAUGUAUA
siControl	GCUGGUCCGGAGGCAUUAAUUGUUA

Sequences were submitted to BLAST search to ensure targeting specificity. For siRNA transfection, MDCK cells were transfected by Lipofectamine 2000 with siRNA duplexes or scrambled siRNA. 24h later, cells were transfected with the Amaxa Nucleofector device using a specific nucleofection program. After 24h incubation, cells were resuspended and plated in 12-well plates and/or in coverglass chambers coated with Matrigel to grow into cysts. Total

cell lysates from 2D and 3D cultures were analyzed by immunoblotting or real-time quantitative PCR (RT-qPCR) to confirm siRNA efficiency.

Immunofluorescences

Cell cultures

For immunofluorescence (IF), MDCK II cells in 2D monolayers (over borosilicate coverslips) and spheroids (IBIDI chambers) were fixed with 4% PFA for 20 min and then permeabilised with PBS + 0.2% Triton Tx-100 + 0.2% SDS for 10 min at 4ºC. After that, cells were blocked with PBS + 3% BSA at room temperature (RT) for 30min (monolayers) or 1h (spheroids). Primary antibodies were diluted in PBS + 3% BSA and cells were incubated with them for 1h at RT or overnight (O/N) at 4ºC. After several washes in PBS, secondary antibodies, phalloidin or DAPI were incubated for 30min (monolayers) or 1h (spheroids) in blocking solution in the dark and then washed with PBS. Cells cultured as 2D monolayers were mounted with Fluoromont-G (SouthernBiotech) over glass slides. Cells cultivated as spheroids in chambers did not need mounting medium and were conserved with PBS 0.05% azide at 4ºC for a maximum period of 2 weeks.

Zebrafish

Zebrafish embryos and larvae were fixed with 4% PFA for 2h at RT or O/N at 4ºC. Embryos were stained either in whole mount or sectioned in slices. For sectioning, embryos where embedded in 4% low-melting point agarose, cut with a vibratome into 150 µm and placed in PBS-0.1% Tween 20 (PBST). The embryos or the sections were washed in PBST, and blocked in PBST with 3% BSA for 1h at RT. Primary antibodies and reagents were incubated overnight at 4ºC using the following concentrations: acetylated tubulin, 1/500; TRITC-Phalloidin, 1/1000 (whole-mount) or 1/2000 (slices); 647-Phalloidin, 1/100; DAPI, 1/2000. The embryos were mounted with Fluoromont-G for posterior microscopy analysis.

Drosophila

For *Drosophila* embryos, standard procedures were used to fix and stain larval wing imaginal discs. Larvae were dissected in PBS and fixed with 4% PFA, 0.1% Deoxicholate and 0.1% Triton X-100, in PBS for 25min at RT. They were blocked in PBS, 1% BSA, 0.3% Triton X-100 and 0.03% Azide (Washing Buffer) for 1h and incubated with the primary

antibody O/N at 4ºC. Larvae were then washed four times in Washing Buffer, and incubated with the appropriate fluorescent secondary antibodies for 1.5h at RT in the dark. They were washed again four times in Washing Buffer and mounted in Vectashield medium (Vector Laboratories) for later confocal analysis.

Antibodies

Table 2: Primary antibodies used in the present work.

Protein	Species	Reference	Dilution IF	Dilution WB
Wingless	Mouse	DSHB	1:50	-
c-Myc	Rabbit	Invitrogen – Thermo Fisher	1:500	-
Senseless	Guinea Pig	A gift from Dr. I. Guerrero	1:1000	-
Cut	Mouse	DSHB	1:100	-
Distal-less	Guinea Pig	A gift from Dr. C. Estella	1:2000	-
GFP	Chicken	Invitrogen (A10262)	1:500	-
p-Smad2,3	Rabbit	Sta. Cruz Biotechnology (sc11769-R)	1:500	-
PKCλ	Mouse	BD (610207)	1:500	-
ZO-1	Rat	DSHB (R4076)	1:500	-
Rab11	Rabbit	Life Technologies (715300)	1:500	-
Gp135	Mouse	A gift from Dr. Ojakian	1:500	-
Laminin	Rabbit	Sigma-Aldrich (L9393)	1:500	-
GM130	Mouse	Abcam (EP892Y)	1:300	-
Acetylated α-tubulin	Mouse	Sigma-Aldrich Clone 6-11B-1 (T7451)	1:500	-
NuMA	Rabbit	Abcam (ab97585)	1:500	-
Ki67	Rabbit	ThermoFisher Scientific (RM-9106)	1:500	-
Smad3	Rabbit	Abcam (ab28379)	-	1:1000
GAPDH	Mouse	Santa Cruz Biotechnology (sc-32233)	-	1:1000

Table 3: Secondary antibodies and other fluorescent reagents used in this work.

Antibody	Species/Tracer	Reference	Dilution IF	Dilution WB
Anti-mouse IgG, HRP	Goat	Jackson Immunoresearch	-	1:5000
Anti-rabbit IgG, HRP	Goat	Jackson Immunoresearch	-	1:5000
Alexa-Fluor 488 anti-Mouse	Donkey	Invitrogen (A-21202)	1:1000	-
Alexa-Fluor 488 anti-Rabbit	Donkey	Invitrogen (A-21206)	1:1000	-
Alexa-Fluor 555 anti-Mouse	Donkey	Invitrogen (A-31570)	1:1000	-
Alexa-Fluor 555 anti-Rabbit	Donkey	Invitrogen (A-31572)	1:1000	-
Alexa-Fluor 555 anti-Guinea Pig	Goat	Invitrogen (A-21435)	1:1000	-
Alexa-Fluor 647 anti-Mouse	Donkey	Invitrogen (A-31571)	1:500/1:1000	-
Alexa-Fluor 647 anti-Rabbit	Donkey	Invitrogen (A-31573)	1:500/1:1000	-
Alexa-Fluor 647 anti-Guinea Pig	Goat	Invitrogen (A-21450)	1:500/1:1000	-
Alexa-Fluor 647 anti-Rat	Goat	Invitrogen (A-21247)	1:500/1:1000	-
DAPI	Nuclei	Merck (268298)	1:2000	-
Phalloidin-488	F-actin	Invitrogen (A-12379)	1:1000	-
Phalloidin-555	F-actin	Sigma (P-1951)	1:5000	-

Microscopy

Carl Zeiss laser scanning confocal microscopes LSM510, LSM710, two-photon LSM710, LSM800, and confocal microscopes Olympus Fluoview FV3000 and Nikon AR1+ were used for laser scanning confocal imaging. Objectives used were usually 30x/1.05

silicone oil objective (Olympus), 40x/0.95 oil-Plan Apochromat and 63x/1.4 oil-Plan Apochromat (Zeiss) and 40x/1.3 oil Plan-Fluor and 60x/1.4 oil Plan-Apochromat (Nikon). The analysis and composition of images taken from the microscopy were done with ImageJ (NIH) or Zen (Zeiss) programs. For quantifications, more than three experiments were quantified per condition.

Measurements and quantifications

MDCK spheroids with a single or double actin/Gp135 staining specific at the interior surface were identified as normal “single” lumens. We exclude spheroid experiments that presented lower than 50% normal lumen formation (at 72 h), usually due to poor Matrigel gelification conditions. To randomize spheroid or cell counting, we randomly selected fields using low magnification, and then counted or took images at higher magnification for measurements. Immunofluorescence experiments were performed at least three independent times and images shown are representative from samples that were used for quantification. A significant number of spheroids (approximately 50 cells) and fish were quantified per experiment, a minimum of three experiments per condition. GraphPad Prism version 8.0 for Mac and Microsoft Excel were used to analyze and plot data.

RESULTS

1. Role of *Sfrp3* in the regulation of Wnt pathway during mammary gland development

1.1. *Sfrp3* expression alters localization pattern of extracellular Wg

To test how SFRP3 could be modulating Wnt signaling in mice mammary gland, we decided to explore its role using the *Drosophila melanogaster* wing imaginal disc, which provides several advantages. In this model, Wingless (Wg, the *Drosophila* homologue for vertebrate Wnt-1) pathway has been profoundly described (Chen and Struhl, 1999; Couso et al., 1994; Neumann and Cohen, 1997; Zecca et al., 1996), contributing to the understanding of its role in the regulation of different developmental processes and unveiling conserved mechanisms in the vertebrate Wnt pathway. In addition, this model provides an *Sfrp* null background, due to the fact that the *Drosophila* genome does not present any SFRPs homologues (Bovolenta et al., 2008).

Wg acts as a morphogen in the wing imaginal disc, being normally expressed at the dorsoventral (DV) boundary, from which is known to diffuse towards surrounding cells (Neumann and Cohen, 1997; Zecca et al., 1996). We proceeded to express myc-tagged *Sfrp3* in the posterior compartment of *Drosophila* wing imaginal discs under the influence of the hedgehog (Hh) driver using the UAS-Gal4 system (HhGal4>UAS-Sfrp3-myc).

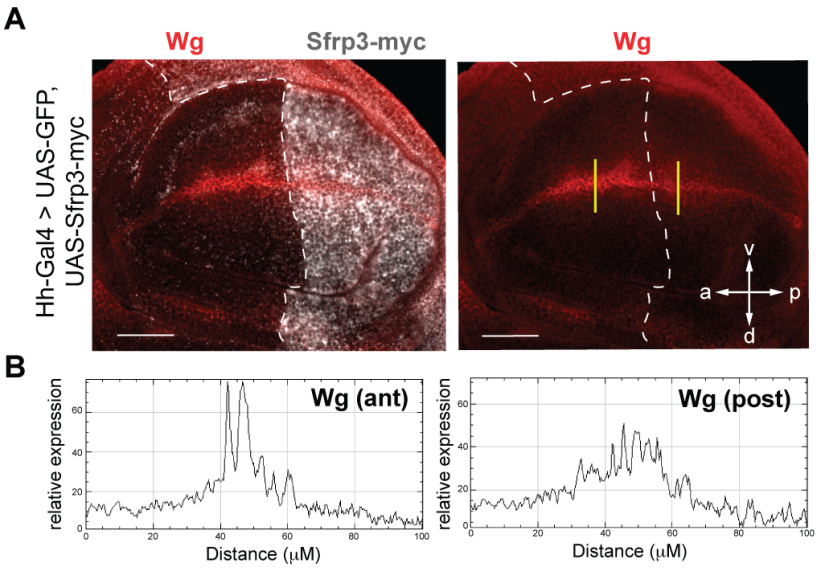

Figure R1. SFRP3 modifies the expression pattern of Wg in Drosophila wing imaginal discs. A) Immunofluorescence of extracellular Wg and SFRP3-myc in wing imaginal discs of Hh-Gal4>UAS-GFP, UAS-Sfrp3-myc flies. **B)** Fluorescent intensity profiles of Wg across the dorsoventral boundary in both anterior and posterior regions of the imaginal disc (yellow bars in A indicate the line of measurement). Scale bars, 50μm. a, anterior; p, posterior; v, ventral; d, dorsal. Dotted line separates anterior and posterior compartments.

We found that, in contrast to what happens in the anterior compartment that serves as a control, extracellular Wg localization is disturbed in the posterior compartment, showing a broader expression pattern with a decreased peak of expression at the center of the DV boundary (Figure R1). This result is consistent with previous data related to another protein of the family, SFRP1, which is known to directly interact with Wg protein (Üren et al., 2000) and negatively modulate its function (Esteve et al., 2011).

1.2. Sfrp3 is specifically modulating Wg pathway

To further analyze the effects of *Sfrp3* in the posterior compartment of the wing imaginal disc, we checked the expression of *senseless* (*sens*), a canonical target of Wg pathway that is activated by high levels of Wg in cells close to the DV boundary (Figure R2).

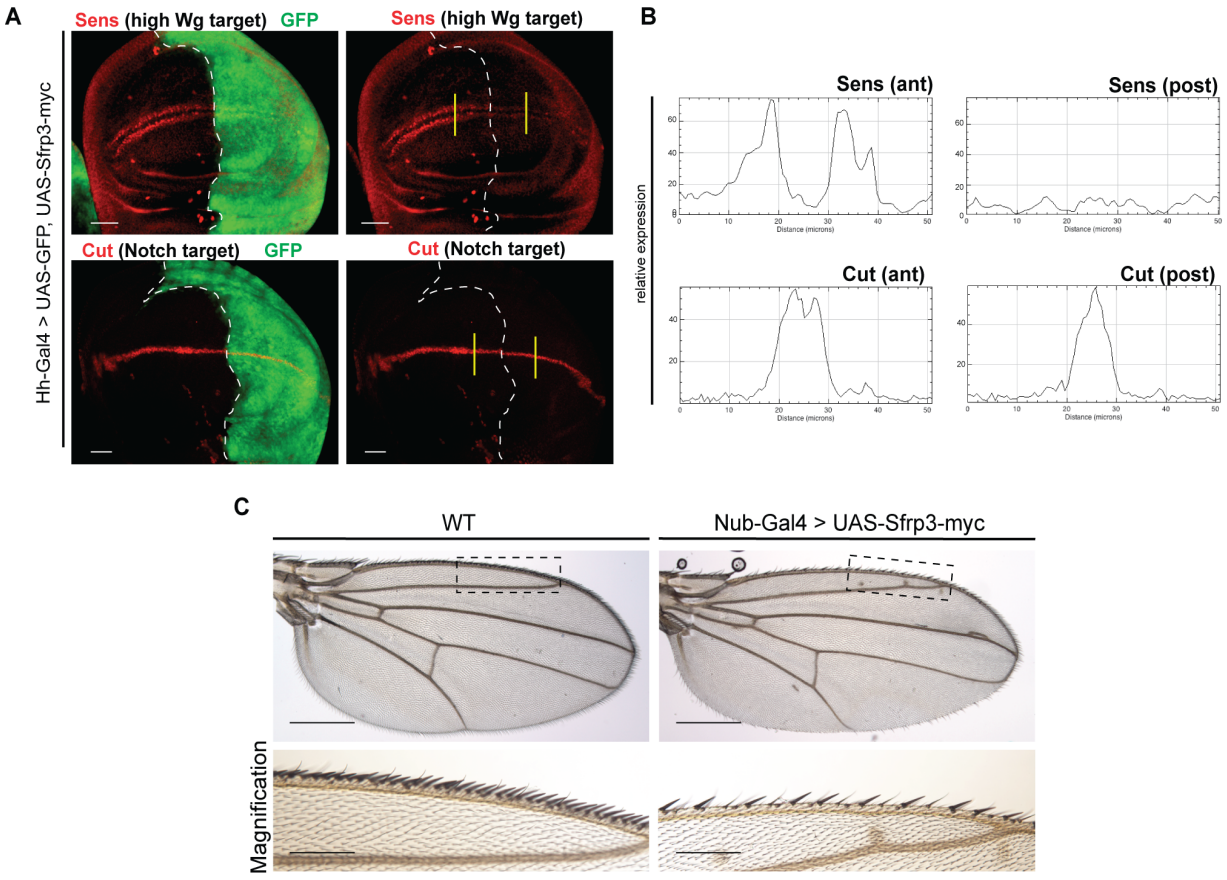

Figure R2. SFRP3 specifically modulates Wg pathway during *Drosophila* wing development. A) Immunolabelling of Wg target Sens and Notch target Cut in wing imaginal discs of Hh-Gal4>UAS-GFP,UAS-Sfrp3-myc flies. **B)** Fluorescence intensity profiles of Sens and Cut across the dorsoventral boundary in both anterior and posterior regions of the imaginal disc. Yellow bars indicate the line traced to perform measurements. Scale bars, 50µm. **C)** Adult wings of both wild type and Nub-Gal4>UAS-Sfrp3-myc flies and magnifications of their margins (dashed line). Scale bars,100µm.

The expression of *sens* is normally seen as a pair of stripes at both sides of the DV boundary. We found that SFRP3 prevented the normal expression of *sens*, which was almost absent in the posterior compartment (Figures R2A & R2B). On the contrary, the expression of *cut*, a direct target of Notch pathway, remains unaffected. These results suggest that SFRP3 functional activity is exclusive for Wg pathway, unlike to what has been published for SFRP1, which also affects Notch pathway in *Drosophila* wing imaginal discs (Esteve et al., 2011).

In addition, the expression of *Sfrp3* in the wing pouch under the Nubbin (Nub) driver results in a lack of sensory organs along the adult wing margin, a phenotype related to the blockade of Sens activity (Nolo et al., 2000) (Figure R2C).

1.3. *Sfrp3* expands Wg territory of action

As these previous results clearly indicate a modulation of Wg pathway by *Sfrp3*, either by inhibition of Wg morphogen activity or by modification of its spatial range of action, we decided to further investigate these options. To that end, we checked the expression of *distal-less (dll),* another Wg target activated by low concentrations of the morphogen. We found that the territory of expression of *dll* was expanded in the posterior compartment of the wing disc, demonstrating that SFRP3 does not block the signaling but disperses the ligand (Figure R3).

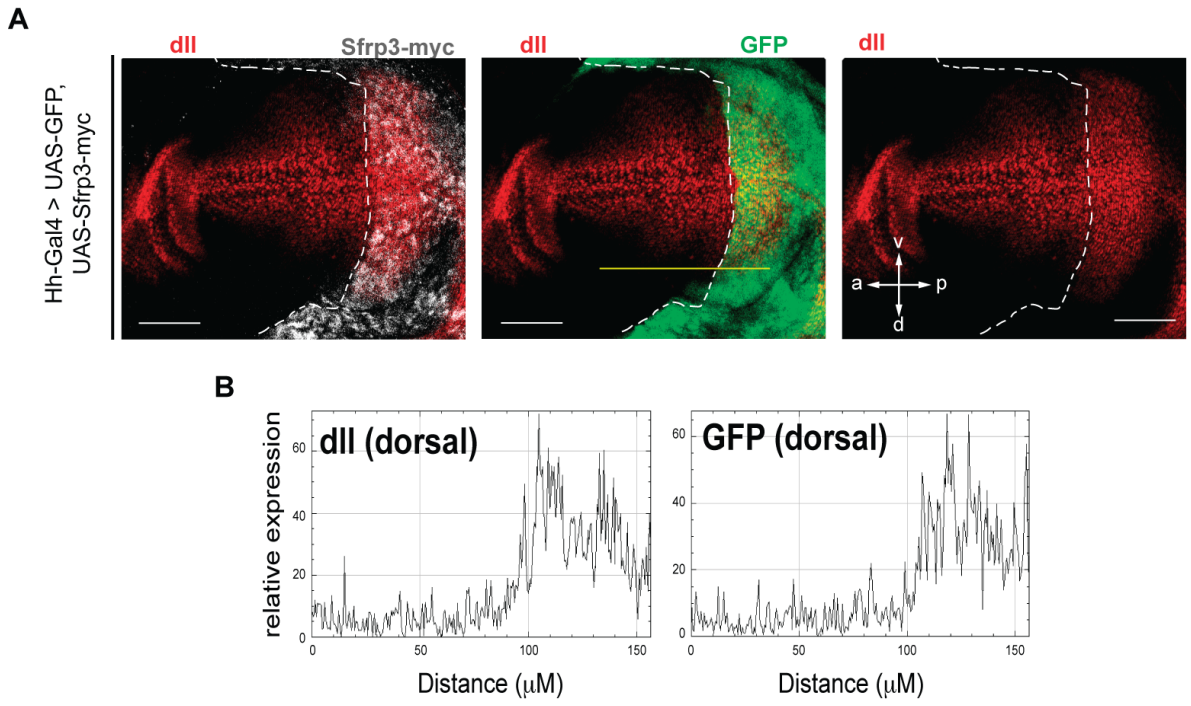

Figure R3. Wg territory of action is expanded when *Sfrp3* is being expressed A) Immunolabelling of Wg target Dll and SFRP3-myc in wing imaginal discs of Hh-Gal4>UAS-GFP, UAS-Sfrp3-myc flies. Scale bar, 50μm. **B)** Fluorescence intensity profiles of Dll and GFP along the dorsal area of the wing pouch. Yellow bar indicates the line traced to perform the measurements.

To verify this result, we used a *Drosophila* line in which endogenous *wg* was replaced by a gene encoding the transmembrane protein Neurotactin fused to Wg (NRT-Wg), a still functional membrane-tethered version of the morphogen that is unable to diffuse (Alexandre et al., 2013). In this case, the expression of *Sfrp3* in the posterior compartment does not alter the expression pattern of *sens* across the DV boundary of the imaginal disc (Figure R4), indicating that the pathway is active in spite of *Sfrp3* expression.

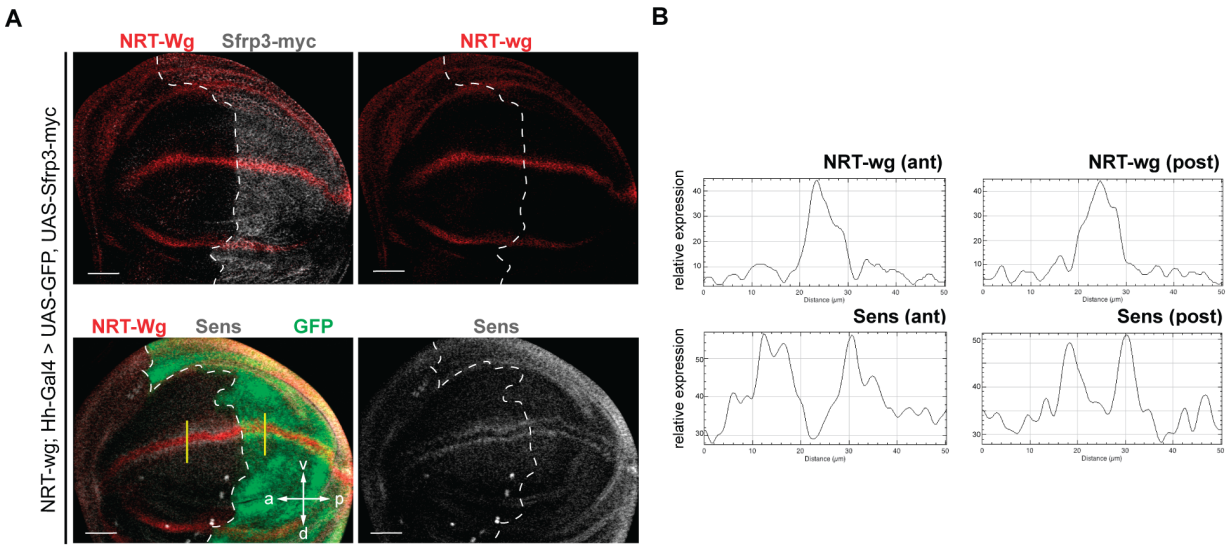

Figure R4. SFRP3 acts as a modulator of morphogen concentration in the intercellular space. A) Immunolabelling of Wg, Sens and SFRP3-myc in wing imaginal discs of Hh-Gal4 > UAS-GFP, UAS-Sfrp3-myc flies. **B)** Fluorescent intensity profiles of NRT-Wg and Sens across the dorsoventral boundary of the wing disc. Yellow bars indicate the line trace followed for measurements. Scale bars, 50µm.

Altogether, these results support the hypothesis that *Sfrp3* positively modulates Wnt pathway by bringing Wnt ligands closer to their receptors. In the mammary gland model, SFRP3 would modulate Wnt signaling by avoiding ligand accumulation at the boundary between tubular epithelial cells and stromal cells, expanding Wnt morphogens range of action. The lack of SFRP3 coming from the stroma of the mammary glands in knockout mice leads to the increase of ligand concentration at the boundary, causing increased ductal invasion and branching, epithelial cells structural defects and abnormal proliferation (Figure R5).

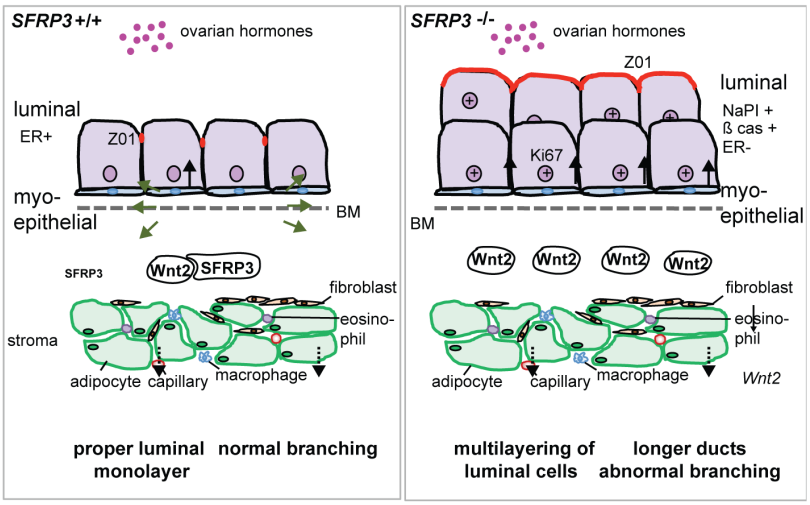

Figure R5. Hypothetical model of action of *Sfrp3* in the mammary gland in both wild-type and knockout mice for *Sfrp3*. After being secreted by stromal cells, SFRP3 works as modulator of Wnt signaling by binding to Wnt morphogens and expanding their range of action. Its absence in knockout mice allows Wnt accumulation in the intercellular space, which affects epithelial cell morphology and behavior.

2. Role of main signaling pathways in zebrafish intestine morphogenesis

2.1. Mesenchymal cells surrounding zebrafish intestinal epithelial cells express the Hedgehog ligand receptor Patched 2

Organogenesis is a complex process in which several kinds of signaling take place, including intracellular autocrine signaling or intercellular juxtacrine and paracrine signaling between different cell types, which are key to ensure the correct development of an organism. The interactions between epithelial cells from the endoderm layer and the mesenchymal cells derived from the mesoderm during morphogenesis of tubular epithelial organs have been widely studied during the past decades (Archambeault et al., 2009; Bernascone & Martín-Belmonte, 2013; Shannon & Hyatt, 2004; Volckaert & De Langhe, 2015). It is well known that this communication occurs through cellular contacts or soluble factors and is also greatly influenced by extracellular matrix (ECM) components, with an increasing importance for mechanical signaling mechanisms in the process (Mammoto and Ingber, 2010; Seiler et al., 2012, Wallace et al., 2005). Hedgehog (Hh) signaling is particularly important for intestinal development in vertebrates (Apelqvist, 1997; Roberts, 1995). During gut development, endodermal epithelium determines the establishment of the different layers that form the organ through the expression of both *Sonic hedgehog (Shh)* and *Indian hedgehog (Ihh),* which regulate radial differentiation and mesenchymal growth, and are crucial for gastrointestinal (GI) tract organogenesis (Mao et al., 2010; Ramalho-Santos et al., 2000; Sukegawa et al., 2000). Interestingly, although it is well-known that zebrafish GI development

differs to that of mammals, Hh signaling seems to be equally important for gut development, as intestinal epithelial cells (IECs) of mutant fish for *smoothened (smo)*, a key signal transducer receptor of Hh pathway, are unable to resolve intestinal lumens (Alvers et al., 2014). We confirmed which cells involved in intestinal tubulogenesis in zebrafish were being directly affected by the *smo* mutation by analyzing the expression of the *ptch2::kaede* reporter (Huang et al., 2012) across different stages of early zebrafish development (Figure R6A).

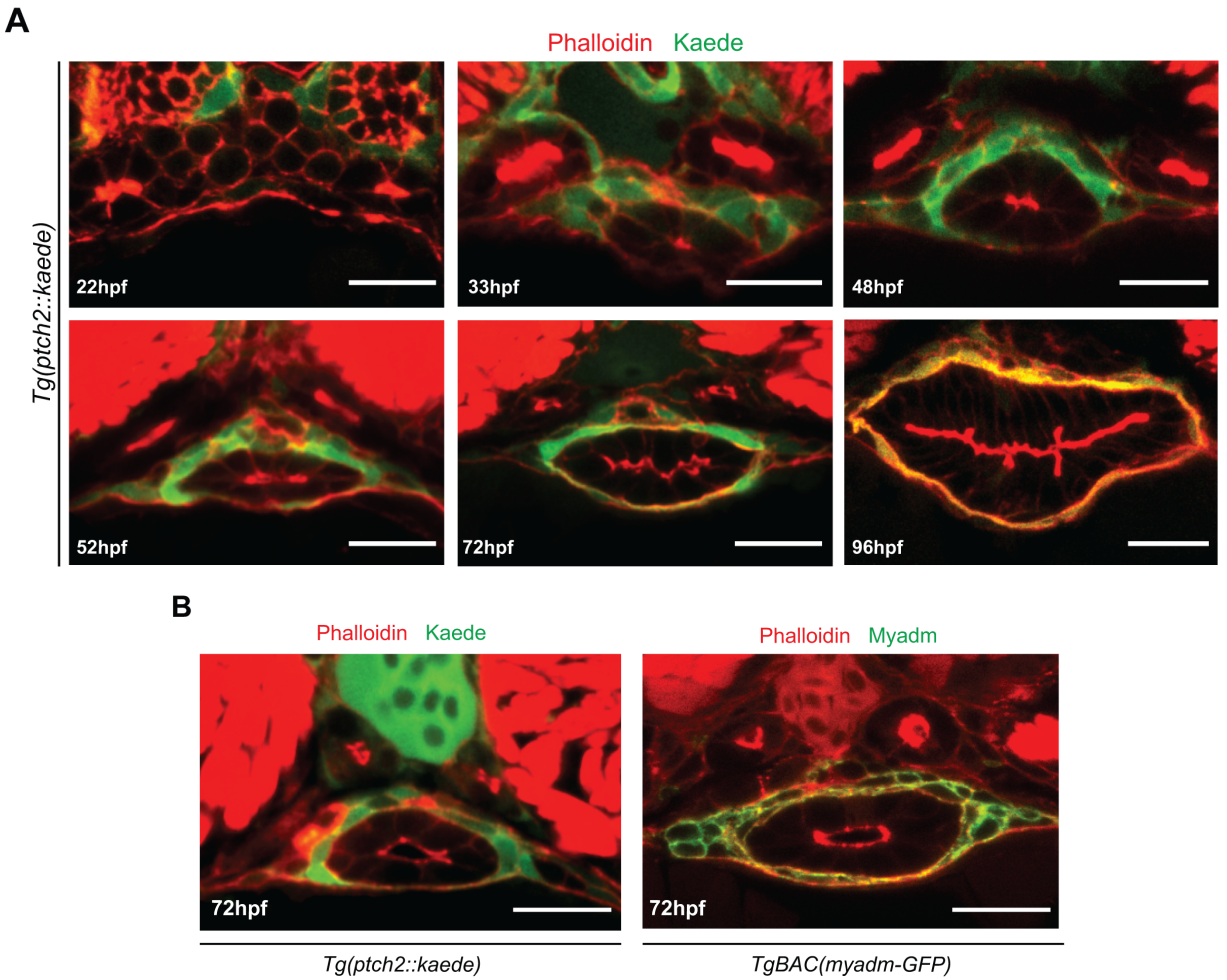

Figure R6. The transgene *ptch2::kaede* is expressed in mesenchymal cells surrounding intestinal epithelial cells in zebrafish. A) Confocal cross sections of *Tg(ptch2::kaede)* zebrafish at different stages during embryo develoment. Phalloidin (red), Kaede (green). **B)** Confocal cross sections of *Tg(ptch2::kaede)* and *TgBAC(myadm-GFP)* fish at 72hpf. Phalloidin (red), Kaede (green), Myadm (green). Scale bars, 20µm.

The dynamics of the *ptch2::kaede*-expressing cells are identical to those of the mesenchymal cells that give rise to intestinal smooth muscle cells (iSMC) during zebrafish development (Gays et al., 2017). This work showed how mesenchymal cells undergo ventral and

dorsal migration around the epithelial tube until it is completely surrounded, and before differentiating into iSMC. We also compared the expression of the transgene *ptch2::kaede* to that of *myadm-GFP*, a marker we use for mesenchymal cells, concluding that the cells responding to hedgehog ligands belong to a group of mesenchymal cells surrounding the epithelial cells that form the intestine (Figure R6B), in a mechanism that recreates intestinal development in mammals (Kolterud et al., 2009; Mao et al., 2010).

We also observed that mesenchymal cells start expressing *ptch2::kaede* at early stages of development, simultaneously to the initiation of the epithelial tube morphogenesis, which suggest that their presence and the activation of Hh pathway may be critical at these initial stages of intestinal development. Furthermore, the expression of *ptch2::kaede* remains active at least until 96 hpf, when the intestine is completely formed, which may indicate that Hh pathway might have additional roles at later stages of fish development and in processes other than lumen resolution, such as in the patterning of intestinal crypts and villi (Madison et al., 2005; Walton et al., 2012).

2.2. RNA-seq of isolated epithelial cells reveals a key role for cell architecture dynamics in intestinal organogenesis

While mechanisms for intestinal lumen opening in zebrafish have been already explored (Bagnat et al., 2007; Ng et al., 2005), the processes that drive lumen coalescence *in vivo* are still widely unknown. As previously mentioned, only Hh pathway has been shown to be critical for multiple lumens in zebrafish intestine to be properly resolved (Alvers et al., 2014). We decided to address this issue by performing fluorescence-activated cell sorting (FACS) to isolate intestinal epithelial cells from developing zebrafish for subsequent transcriptional analysis. We carried out the experiment in 60 hpf larvae, a stage in which lumen resolution is taking place, using fish expressing *TgBAC(cldn15la-GFP)* (Alvers et al., 2014) and comparing them to *TgBAC(cldn15la-GFP)* embryos carrying the *smo*^{s294} mutation as well (Aanstad et al., 2009). We isolated the cells and, after RNA extraction and NGS analysis, proceeded to look at differentially expressed genes (DEGs) to identify transcriptional programs associated with lumen coalescence.

We confirmed that, according to principal-component and differential expression analysis, wild type and *smo*^{s294} IECs had unique enrichment signatures (Figure R7A & R7B). Taking a closer look to the top ten upregulated and the top ten downregulated genes, we found a group of DEGs associated with the regulation *(rnd2, pvalb4, itga2.2, itga2.3)* or the constitution *(myl10)* of the

actomyosin cytoskeleton and microtubules (Figure R7C, black arrowheads). This suggests that changes in cell architecture play a central role in lumen resolution, which is in correlation with previous work showing that rearrangement of cellular contacts together with apical expansion are necessary for zebrafish gut development (Alvers et al., 2014), due to the fact that these lumens must coalesce by mechanisms other than apoptosis (Ng et al., 2005).

On the other hand, we also found two other genes between the ten most downregulated genes in IECs of *smo*^{s294} fish whose main function is related to fin development and regeneration, *actinodin1 (and1)* and *actinodin2 (and2)* (Figure R7C, green arrowheads).

Profiling using Gene Ontology (GO) terms and Kyoto Encyclopedia of Genes and Genomes (KEGG) pathway analysis revealed that DEGs in *smo*^{s294} mutants are mainly involved in cellular interaction with surrounding cells and the environment, sensing mechanisms, as well as in the modification of cell structure and cell motility. However, if we separate in groups of down- and upregulated genes, we can detect that each of these groups associates specifically with particular processes.

Downregulated genes are associated with inner ear development and ion transport, such as genes encoding subunits of Na-K-ATPase transporting channels, which, together with junction proteins (claudins), mediate fluid flow towards the luminal space to facilitate lumen expansion in several organs, and whose mutation or malfunctioning can result in lumen formation defects (Bagnat et al., 2007, Krupinski & Beitel, 2009, Lowery & Sive, 2005). By contrast, upregulated genes in *smo*^{s294} mutants are involved in cell migration processes. While some of them are associated with the regulation of JAK-STAT cascade, which is known to trigger cell migration in epithelial cells of the intestine (Le et al., 2016), another group of upregulated genes is linked to focal adhesions (i.e. vitronectin, fibronectin receptor or regulatory myosin chains) and thus, to the modulation of cell migration as well.

In summary, RNA-seq analysis confirmed that intestinal epithelial cells of *smo*^{s294} and wild-type fish display distinctive gene expression profiles. Differentially expressed genes in *smo*^{s294} suggest that cell architecture proteins are critical for epithelial cells to achieve lumen resolution during gut development in zebrafish. However, according to Gene Ontology terms analysis, while downregulated genes are mainly associated with luminal expansion, upregulated genes are linked to cell migratory and adhesion processes and its regulation. Further characterization is needed to verify this screening and candidate genes that may have a key role during lumen coalescence in gut development.

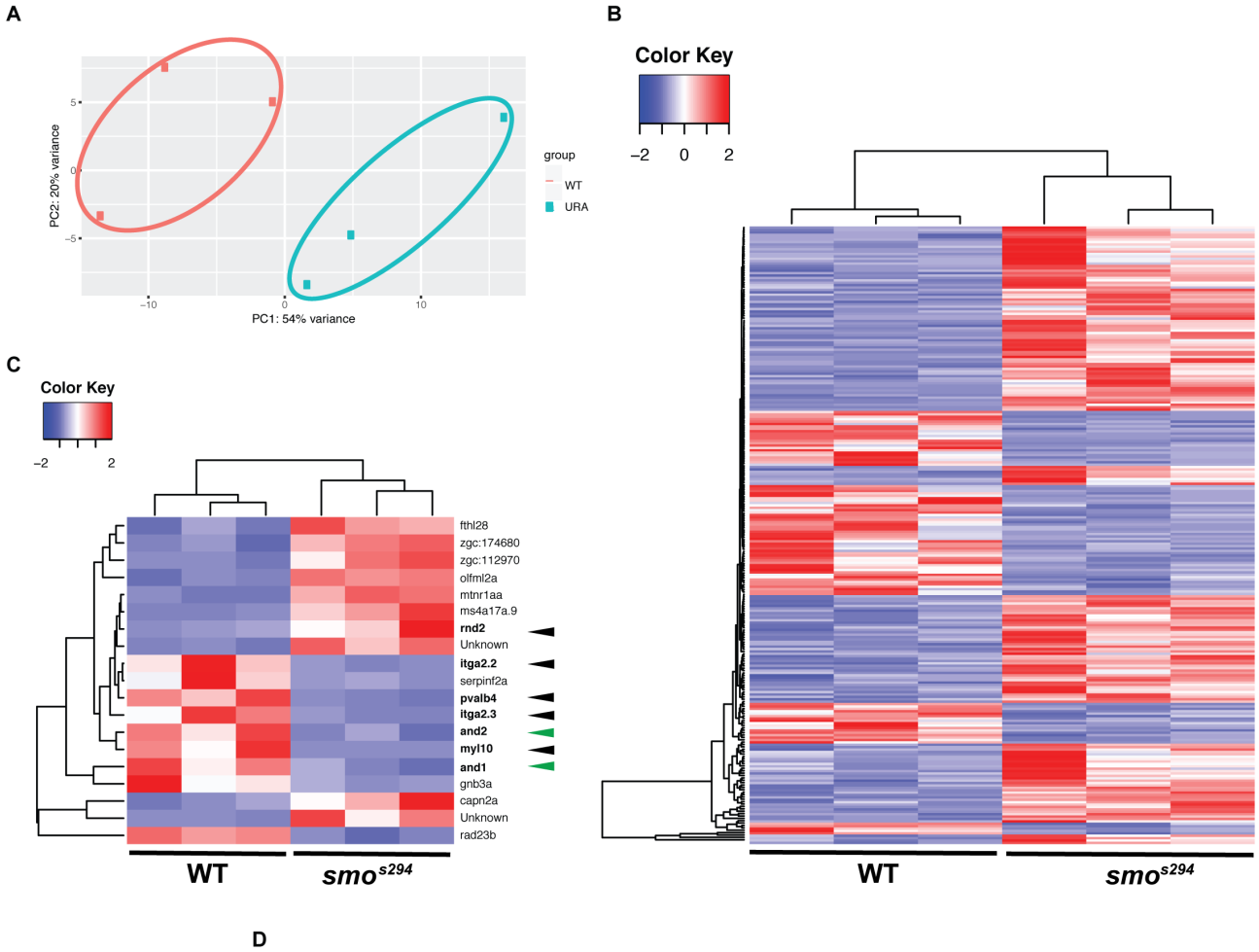

D

	Differentially expressed	Underexpressed	Overexpressed
Gene Ontology	Cell-cell signaling Cytoskeleton Cell division Chromosome positioning Cell adhesion Cell migration Cell growth Muscle contraction	Muscle contraction Ion and proton transport Inner ear morphogenesis Fin development	Cell migration Cell growth Cell-cell signaling Cell adhesion
KEGG Pathway	Glutathion metabolism p53 signaling pathway Focal adhesion	Glutathion metabolism p53 signaling pathway Muscle contraction	Arachidonic acid metabolism Focal adhesion Neuroactive ligand-receptor interaction

Figure R7. The zebrafish intestine shows specific transcriptional programs involved in lumen resolution during development. A) Principal components analysis shows that samples can be clustered in two groups, according to the variances, depending on the fish genotypes. **B)** Heatmap of DEGs and hierarchical clustering show that *smo*^{s294} and wild type intestinal epithelial cells display distinctive clusters of upregulated and downregulated genes. Red, increased expression; blue, reduced expression. **C)** Heatmap of both top ten underexpressed and top ten overexpressed genes in *smo*^{s294} fish. Red, increased expression; blue, reduced expression. Black arrowheads point to genes related to cytoskeleton dynamics, green arrowheads point to genes related to fin development and regeneration. **D)** Table showing top GO terms and KEGG pathways for each group of genes.

2.3. TGF-β inhibition impairs lumen resolution in developing zebrafish gut

As previously mentioned, the intestinal epithelium signals via Hh ligands to the surrounding mesenchymal cells. As a consequence, Hh signaling activation in mesenchymal cells triggers a mechanical or molecular response from the mesenchymal towards the epithelial layer that ensures proper tubulogenesis. To find out through which signaling pathways this communication from mesenchymal to epithelial cells is taking place, we targeted main candidate pathways that could be involved in the process of gut formation, in order to identify a phenotype that recapitulates the defects observed in the guts of *smo*^{s294} mutants. We separately inhibited FGF, BMP, Wnt and TGF-β pathways from 30 hpf on, when epithelial cells start the process of intestinal tubulogenesis (Ng et al., 2005), until 96 hpf, when every fish presents a single open lumen across the intestine (Alvers et al., 2014). Interestingly, the inhibition of transforming growth factor β (TGF-β), which had been previously linked to tubulogenesis (Denker et al., 2015; Viñals & Pouysségur, 2001), using the small molecule EW-7197 (a strong ATP-competitive inhibitor of type I TGF-β receptors) caused a phenotype of impaired lumen resolution at final stages of intestinal development (Figure R8B-B'). This phenotype, in which lumens remain close but unable to fuse, was similar to the one observed in *smo*^{294} mutants. We also identified a positive correlation between the concentration of the inhibitor and the number of fish presenting the phenotype (Figure R8C).

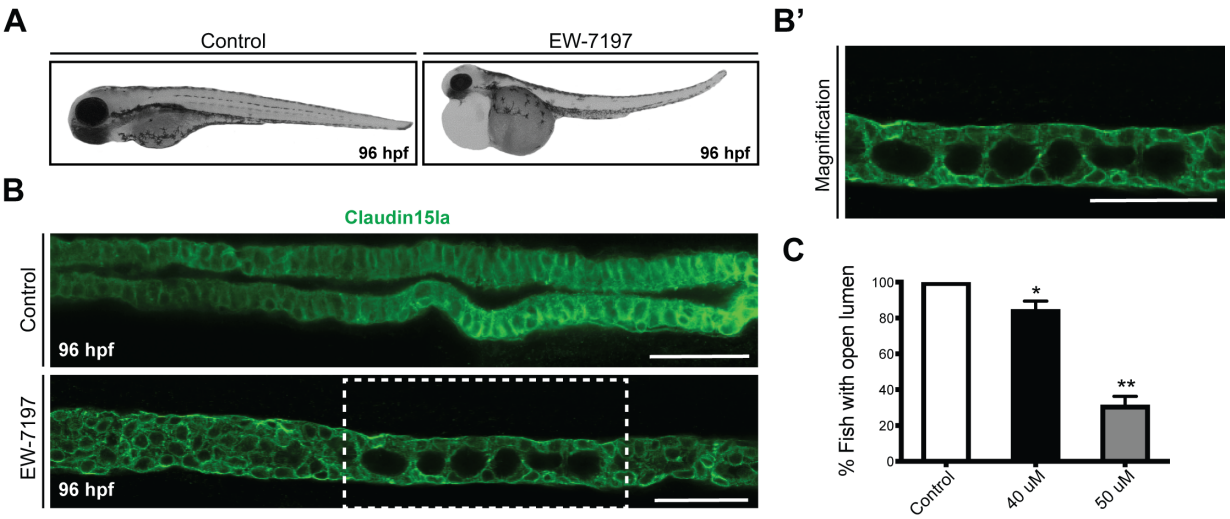

Figure R8. TGF-β inhibitor EW-7197 impairs lumen resolution during gut development in zebrafish. A) Phenotype observed in fish treated with non-lethal concentrations of EW-7197 from 30hpf to 96hpf compared to control fish. **B-B')** Confocal section of a Z-stack of *TgBAC(cldn15la-GFP)* fish at 96hpf of both control and fish treated with EW-7197 from 30hpf. Dashed line indicates magnified area shown in B'. Claudin15la (green). Scale bars, 30µm. **C)** Quantification of treated fish presenting multiple lumens in developing guts at 96hpf with different concentrations of EW-7197. Values are mean ± SD; n=3 independent experiments; *, P<0.05; **, P<0.01 (Student's *t*-test). Control fish were treated with DMSO.

2.4. EW-7197 alters mesenchymal cell migration around the intestinal epithelium

Previous studies have shown that TGF-β inhibition by other chemical inhibitors or the use of morpholinos impairs mesenchymal cells migration from the lateral plate mesoderm (LPM) to encircle the intestine before undergoing differentiation (Gays et al., 2017). Taken this into account, we investigated the impact that the inhibitor EW-7197 could have on mesenchymal cell migration during zebrafish development (Figure R9). We verified that mesenchymal cell migration was highly affected upon TGF-β inhibition, with stronger effects at higher levels of concentration (60μM), which impairs both ventral and dorsal migration from the LPM around epithelial cells or results in a thinner layer of mesenchymal cells. In addition, other remarkable defects upon TGF-β inhibition were the organization of epithelial cells in stratified layers instead of in monolayers, and the appearance of disorganized apical membranes (Figure R9).

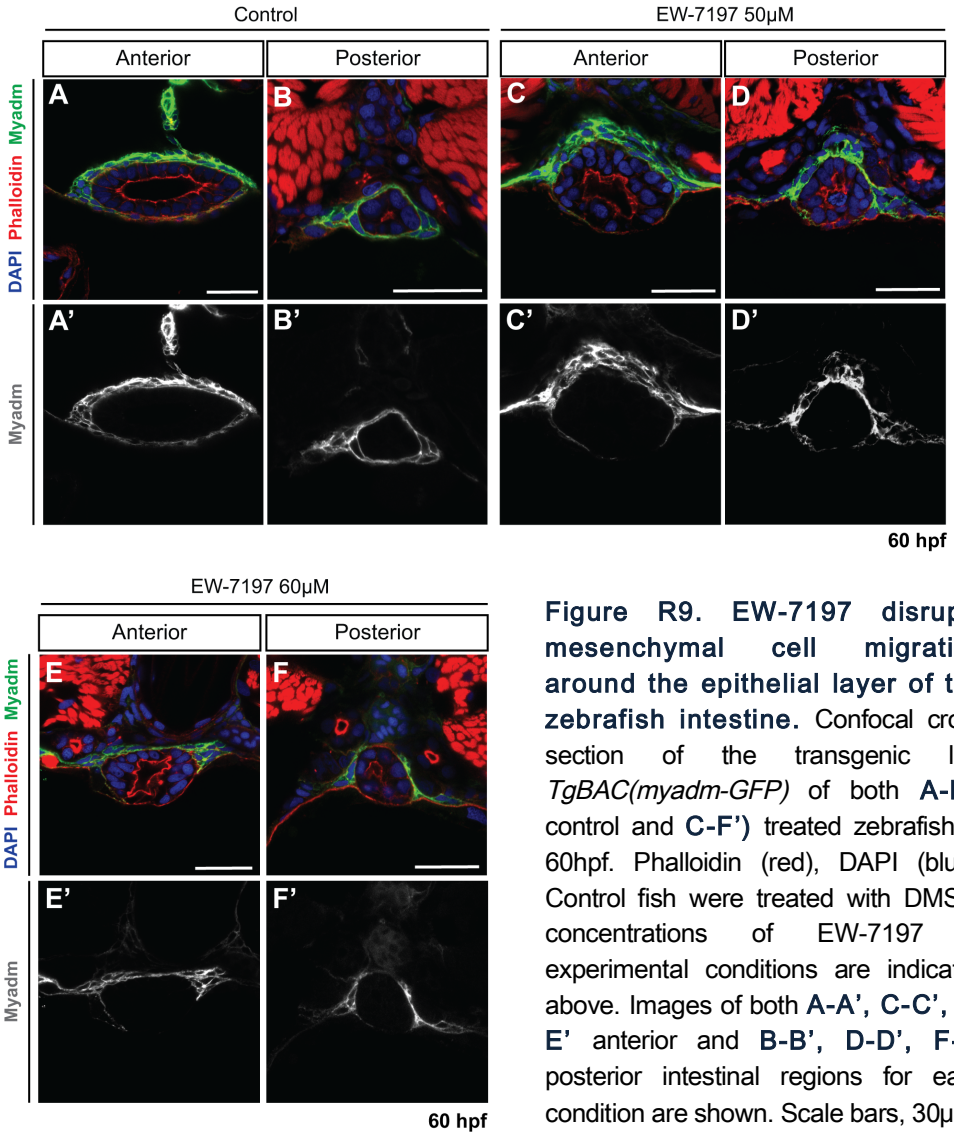

Figure R9. EW-7197 disrupts mesenchymal cell migration around the epithelial layer of the zebrafish intestine. Confocal cross section of the transgenic line *TgBAC(myadm-GFP)* of both **A-B')** control and **C-F')** treated zebrafish at 60hpf. Phalloidin (red), DAPI (blue). Control fish were treated with DMSO, concentrations of EW-7197 in experimental conditions are indicated above. Images of both **A-A', C-C', E-E'** anterior and **B-B', D-D', F-F'** posterior intestinal regions for each condition are shown. Scale bars, 30μm.

These effects open the possibility that the lumen resolution defects observed in developing zebrafish intestines at later stages (96hpf) when using EW-7197 (Figure R8) may be a consequence of (1) the lack of mechanical support and/or molecular signaling from mesenchymal to epithelial cells, (2) the result of the TGF-β pathway inhibition in epithelial cells or (3) both of them. In addition, our RNA-seq data reveals high expression of TGF-β type I and type II receptors in epithelial cells, which might be associated with the intestinal luminal defects, supporting the hypotheses (2) and (3) described above. Therefore, future work will need to address whether the intestinal phenotype is caused either by the effect of the TGF-β inhibitor on mesenchymal cell migration, a signaling defect on epithelial cells through TGF-β type I receptors, or a combination of both.

Interestingly, *smo*^{s294} mutant fish lack intestinal smooth muscle cells (iSMC), which derive from the mesenchymal precursors (Alvers et al., 2014), since Hh signaling is crucial in the differentiation process. Consequently, we could contemplate an alternative scenario in which TGF-β pathway does not act downstream Hh signaling but both Hh and TGF-β inhibition may separately lead to the same effect (the impairment of single lumen formation in the intestine) as a consequence of the lack of interaction between epithelial cells and iSMCs.

2.5. The removal of TGF-β inhibitor leads to the rescue of the multiluminal phenotype

Next, we tested whether the effects of the TGF-β inhibitor (EW-7197) are reversible or on the contrary, it targets key processes with permanent consequences. To address this question, we time-lapsed an area of the intestines presenting unfused lumens for 5 hours in 4dpf fish that had been treated with 50μM EW-7197 since initial stages of gut development (30 hpf).

We used the transgenic line *TgBAC(cldn15la-GFP)* to address whether the IECs could remodel the junctions and fuse the lumens upon withdrawing of the TGF-β inhibitor. We observed that the effects of EW-7197 in junction remodeling were mostly reversible, since epithelial cells were able to rearrange their junctions in a short time following EW-7197 removal (Figure R10).

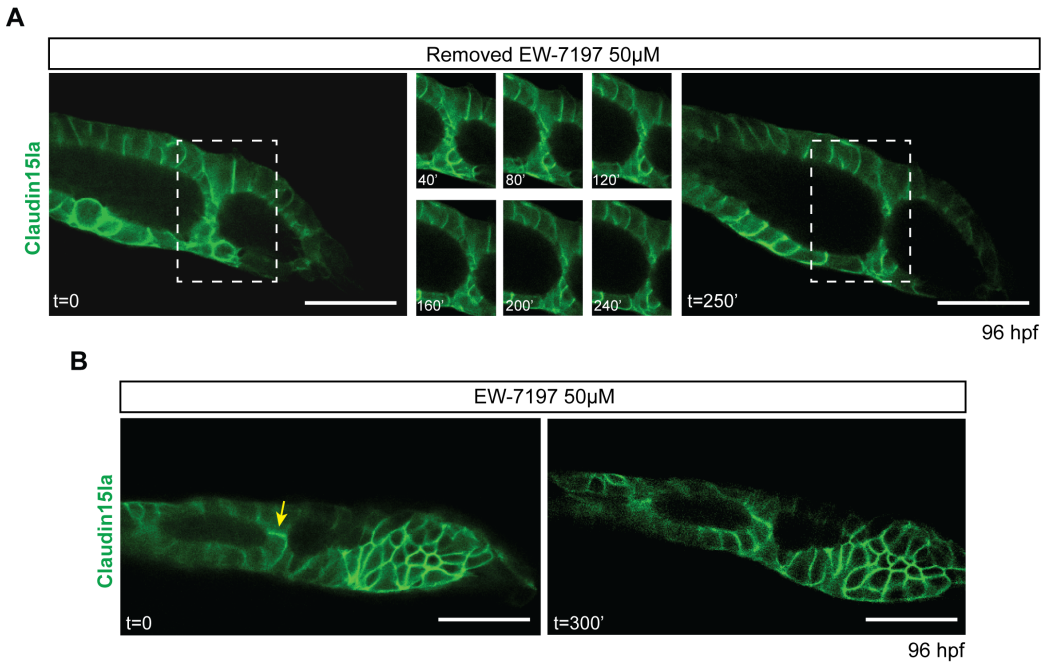

Figure R10. Intestinal epithelial cells can achieve lumen fusion if the TGF-β inhibitor EW-7197 is withdrawn from the media. A) *In vivo* confocal images taken from a *TgBAC(cldn15la-GFP)* fish once EW-7197 has been eliminated from the water. Dashed line indicates the area separating two unfused lumens. **B)** First and last *in vivo* images of *TgBAC(cldn15la-GFP)* fish with EW-7197 still present in the water. Yellow arrow points to the junction separating two unfused lumens that remain unfused during the experiment. Claudin15la (green). Scale bars, 30μm.

2.6. Canonical TGF-β signaling is not activated in the zebrafish intestinal epithelium at lumen resolution stages

To test the hypothesis that the TGF-β inhibitor is not only impairing mesenchymal cell migration from the LPM, but blocking TGF-β pathway in the epithelial compartment, we next investigated whether the canonical TGF-β pathway is activated in the epithelial layer at luminal resolution stages (54hpf). To examine canonical TGF-β activation, we stained to detect phosphorylated Smad2/3 (pSmad2/3), which appears in cell nuclei when the canonical pathway is activated. Interestingly, we observed a strong signal of pSmad2/3 in pronephric epithelial cells at those stages, while the intensity of pSmad2/3 in the nuclei of IECs was very reduced (Figure R11). Nevertheless, this result does not allow us to completely dismiss the hypothesis that the phenotype we observe is due to an inactivation of TGF-β pathway in the epithelium, since the canonical pathway could be active in earlier stages or TGF-β may be activating non-canonical pathways in epithelial cells.

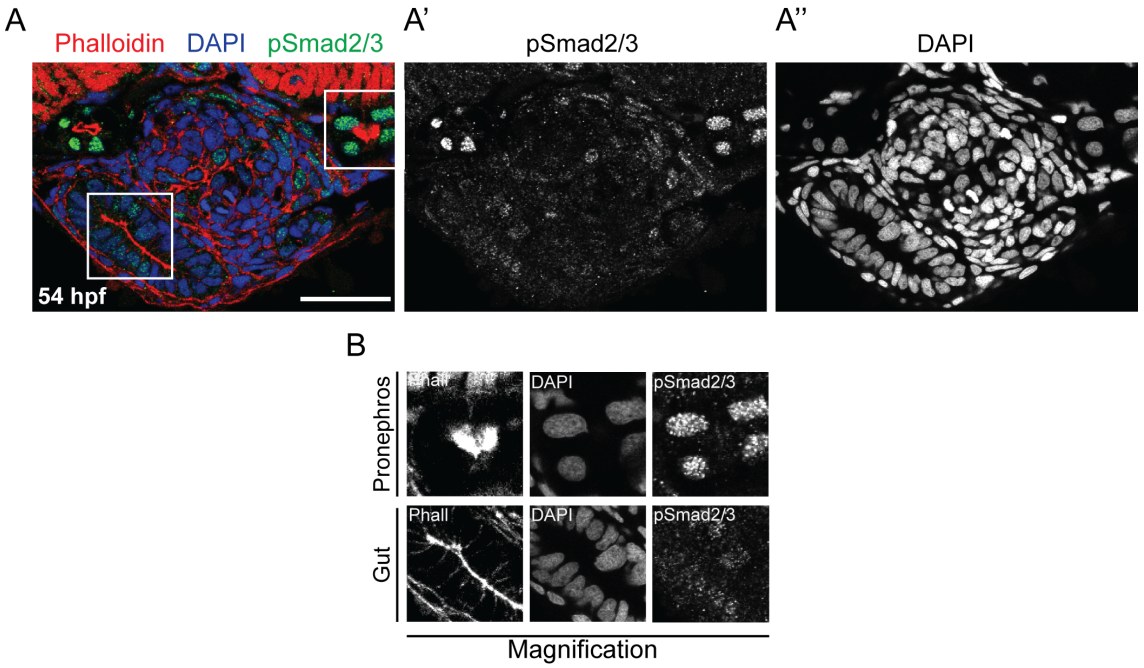

Figure R11. Canonical activation of TGF-β pathway in the intestinal epithelial layer when lumen fusion is taking place is reduced compared to that of pronephric epithelial cells. A-A'') Confocal cross section of wild type fish at 54hpf. Squares indicate magnified sections in **B)** P, pronephros; g, gut. Phalloidin (red), DAPI (blue), pSmad2/3 (green). Scale bars, 30µm.

To sum up, the chemical inhibition of TGF-β type I receptors causes a phenotype in zebrafish gut development in which lumens formed in the epithelial tube remain unfused, similarly to what can be observed when Hh signaling is blocked in *smo*^{s294} mutants. In both cases, upon TGF-β and Hh inhibition, mesenchymal cells that surround the intestine are being affected, showing impaired migration or reduced number/lack of differentiation, respectively. Therefore, further analyses need to be performed to elucidate whether both phenotypes are related and share mechanisms, and the specific reasons behind them.

3. Characterization of TGF-β inhibition in organotypic 3D cultures

3.1. Inhibition of TGF-β type I receptors in MDCK spheroids causes a multiple lumen defect

To clarify whether the effects of TGF-β inhibition could be intrinsic to epithelial cells, we evaluated the consequences of EW-7197 treatment in a reductionist epithelial cell model. We used *in vitro* 3D organotypic cultures of MDCK cells, which consist of canine epithelial kidney cells from

the distal tubule and collecting duct. We first checked the expression levels of the main components of the canonical TGF-β pathway through RT-qPCR. We observed that almost every gene is expressed at similar levels than the housekeeping gene (HPRT) and that those levels remain stable during epithelial morphogenesis, with no significant differences between 2D and 3D (Figure R12). Regarding TGF-β type I receptors, Alk4 is expressed at low levels as shown by its high Ct mean, while Alk5 is expressed at relatively high levels, similar to those of the housekeeping gene (Figure R11). The lack of induction of the expression of these genes in 3D cultures do not necessarily mean that TGF-β pathway is not required specifically for proper 3D morphogenesis in MDCK, as long as there is an activation of the pathway not detectable by mRNA levels.

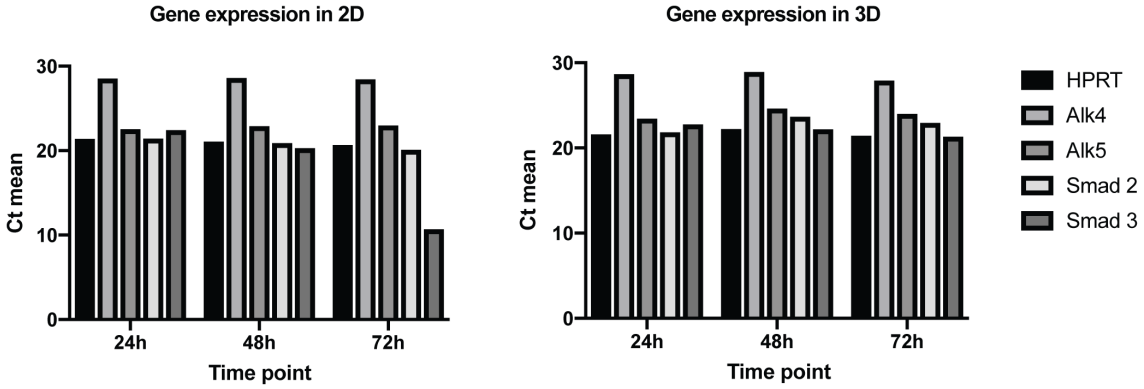

Figure R12. TGF-β canonical signaling components are expressed in both 2D and 3D MDCK cell cultures. Analysis by RT-qPCR of main proteins involved in TGF-β pathway in both 2D and 3D culture conditions and at different time points.

Then, we proceeded to test the effects of the TGF-β type I receptors inhibitor EW-7197 in both 2D and 3D MDCK epithelial morphogenesis. We first analyzed the effects in 2D since these results may also contribute to the understanding of the responses in MDCK 3D morphogenesis. We noticed that the effects on 2D cells vary depending on the concentration. When cells are treated 24h after seeding, once they have already adhered to the plate, a defect in lamellipodia and filopodia formation (Figure R13A, yellow arrows), although not quantified, seems to arise in treated cells, which have difficulties to spread and cover gaps between them and display a strong actin accumulation at the cell cortex (Figure R13B-C, white arrows). Cell division was quantified for each condition and no differences were reported (Figure R13D).

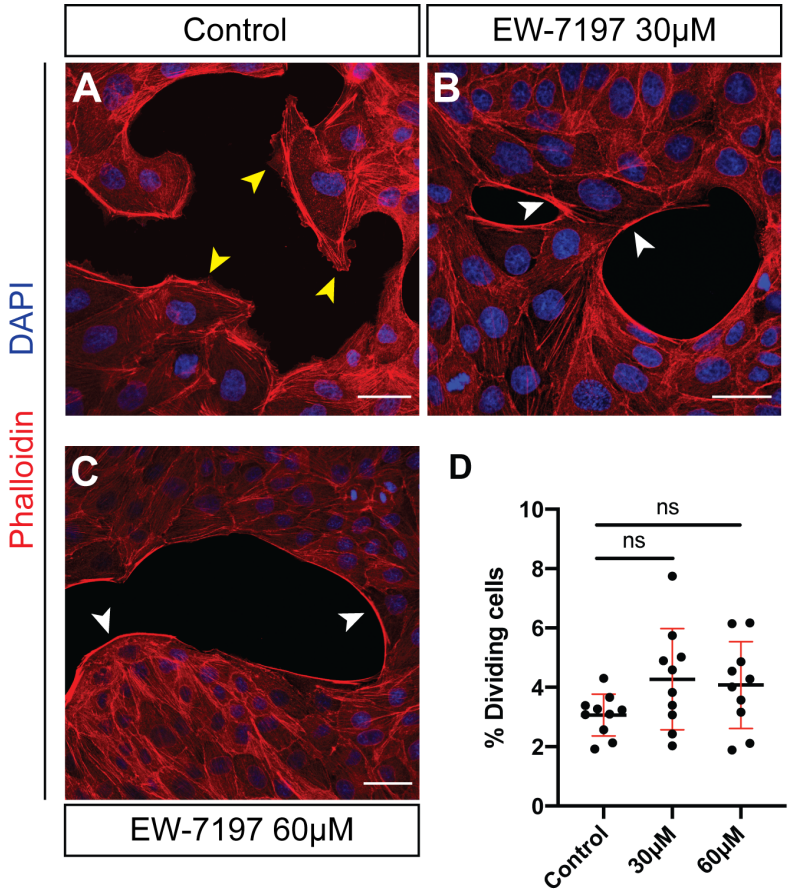

Figure R13. Inhibition of TGF-β type I receptors in 2D impairs cell adhesion and migratory processes. A-C) Confocal images of MDCK cells growing in a 2D monolayer treated with DMSO as a control or different concentrations of EW-7197. Picture (A) was taken from the cell culture edges, while (B) and (C) were taken from the center of the cell plate. Yellow arrowheads point to lamellipodia, white arrowheads point to cortical actin accumulation with no presence of lamellipodia. Phalloidin (red), DAPI (blue). Scale bars, 30μm. **D)** Quantification shows the percentage of dividing cells for each condition. Values are mean ± SD from n=3 independent experiments; ***, P<0.001; ns, not significant (Student's *t*-test).

By contrast, we observed that activation of TGF-β type I receptors is required for proper 3D-MDCK spheroid morphogenesis (Figure R14). MDCK cells were treated with different concentrations of EW-7197 from t=0h and the percentage of single lumen spheroids was quantified for each condition. Whereas most control spheroids display an open single lumen at 94h, cells treated with EW-7197 show significant differences in the number of multiluminal spheroids. In this context, the consequences of TGF-β inhibition closely resemble to the phenotype obtained in zebrafish developing intestines, with multiple lumens remaining unfused at stages in which spheroids should present an open single lumen. In addition, an increase in the concentration of the drug had an impact in the number of spheroids that display this defect, similarly to the results

obtained during zebrafish gut morphogenesis. This data suggests that both *in vivo* and *in vitro* epithelial models may share a common mechanism that depends on TGF-β type I receptors activation in the epithelial compartment in order to generate an open cavity as a consequence of lumen resolution (Figure R14).

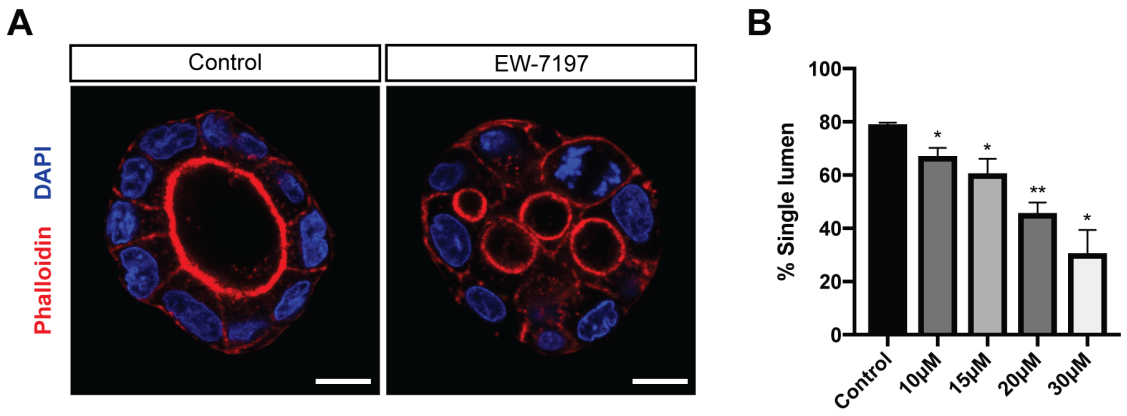

Figure R14. Single lumen formation of MDCK spheroids is impaired in the presence of EW-7197. A) Confocal images of control and EW-7197-treated spheroids. Drug concentration, 20μM. Phalloidin (red), DAPI (blue). Scale bars, 30μm. **B)** Quantification shows the percentage of spheroids with single lumen at 96h when treated with increasing concentrations of EW-7197. Treatment from t=0h. Values are mean ± SD from 3 independent experiments (n>100 spheroids/experiment); *, P<0.05; **, P<0.01 (Student's *t*-test).

3.2. MDCK multiluminal spheroids treated with TGF-β inhibitor EW-7197 show a defect in spindle orientation

A careful analysis of the phenotypes that can be observed in spheroids allows us to hypothesize the molecular mechanisms and pathways associated with these defects (Rodríguez-Fraticelli & Martín-Belmonte, 2013). As we did not detect alterations in markers for ECM laminin deposition, apical domain establishment (Gp135, PKCλ), tight junction assembly (ZO-1), apical vesicle trafficking (Rab11) and Golgi positioning (GM130), which presented a normal subcellular localization in polarized cells (Figure R15), we discarded major defects affecting polarity acquisition and intracellular trafficking in spheroids treated with the TGF-β inhibitor.

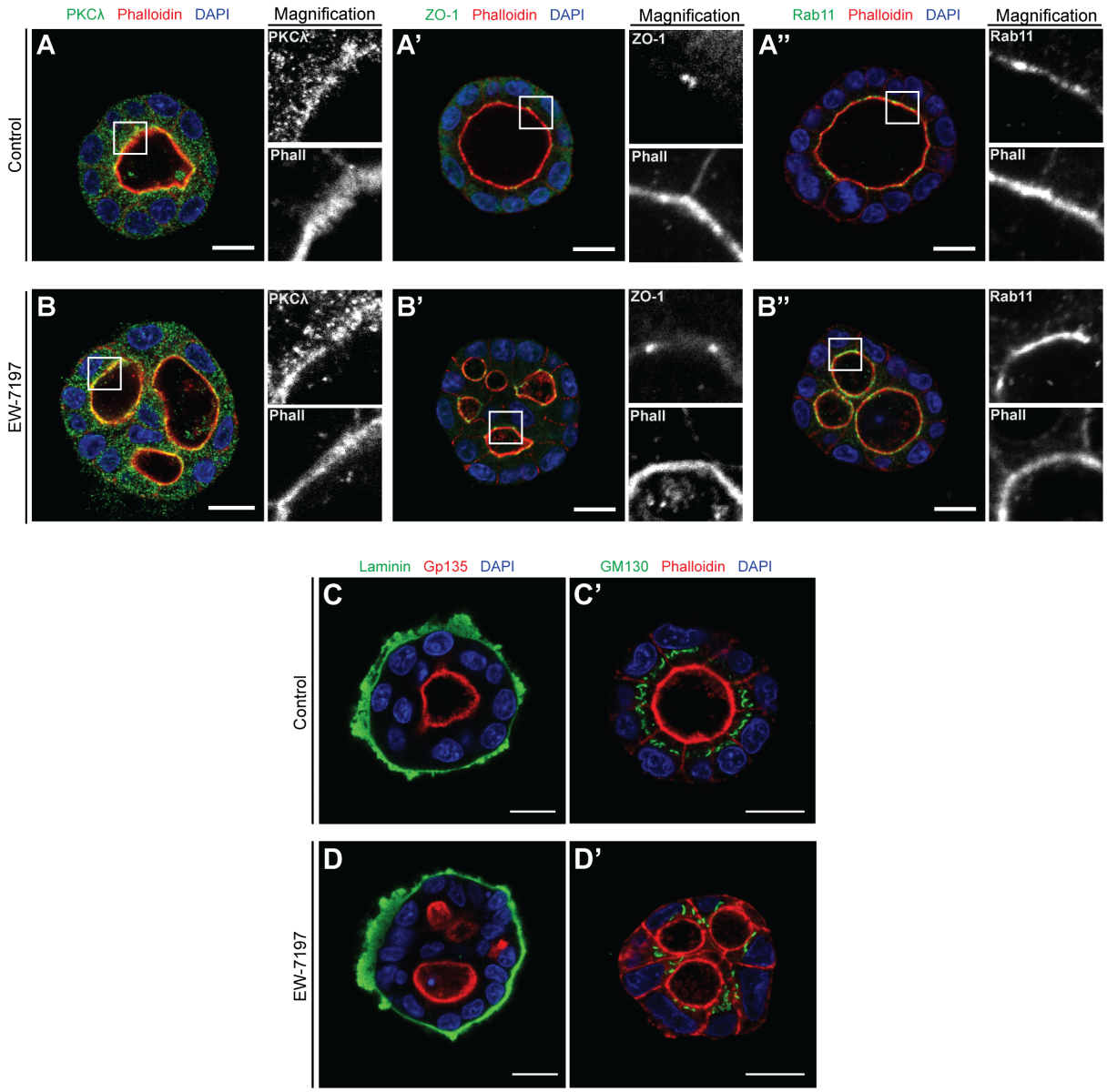

Figure R15. Localization of a variety of proteins related to polarity acquisition and apical membrane formation reveals no differences in treated spheroids. A-D'') Confocal images of control and EW-7197-treated spheroids. PKCλ, ZO-1, Rab11, Laminin GM130 (depending on the panel) (green), Phalloidin and gp135 (depending on the panel) (red), DAPI (blue). All treatments performed from t=0h; drug concentration, 20μM. Scale bars, 15um.

Nonetheless, previous data from our group and others have identified that if spheroids display multiple lumens, and there is not noticeable internal accumulation of apical markers, it is usually due to defects in the processes controlling the orientation of cell spindles during mitotic cell division (Bañón-Rodríguez et al., 2014; Hao et al., 2011; Qin et al., 2010) (Figure R16A). Moreover, the localization of the initial lumen is regulated by spindle orientation, as the machinery that

originates the apical membrane is recruited to the midbody while cytokinesis takes place during asymmetric abscission (Jaffe et al., 2008; Luján et al., 2016; Rodríguez-Fraticelli et al., 2010).

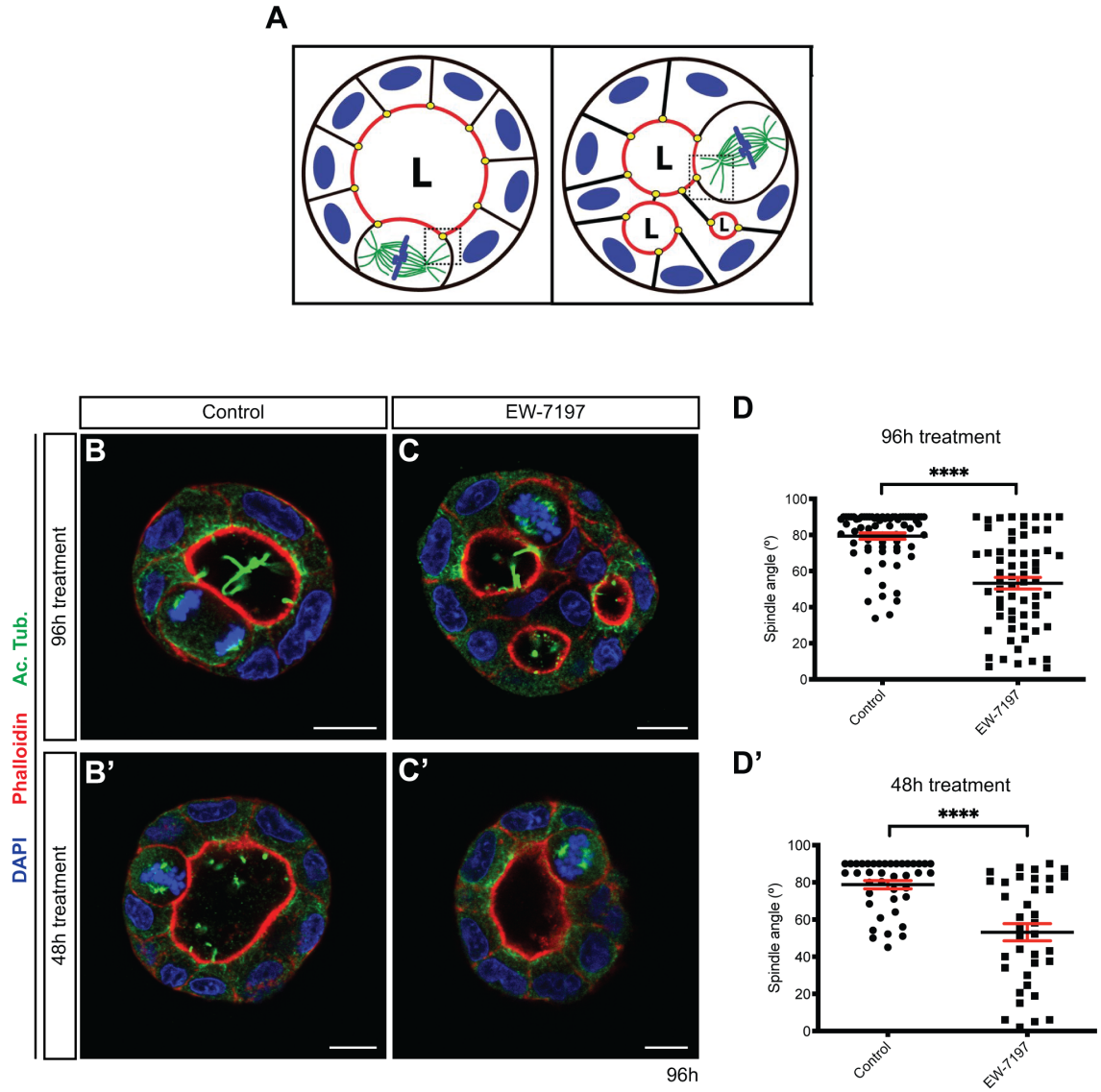

Figure R16. Inhibiting TGF-β type I receptors activity results in spindle orientation randomization. A) Simplified scheme summarizing the effects of spindle orientation during spheroid morphogenesis. Adapted from Bañón-Rodríguez et al., 2014. **B-C')** Confocal images of control and treated MDCK cells forming spheroids at 96h. **B, C)** Treatments done for 96h. **B', C')** Treatments done for the last 48h prior to fixation. Acetylated tubulin (green), Phalloidin (red), DAPI (blue). Scale bars, 10µm. **D-D')** Quantifications show spindle angles in regards to the apicobasal axis either for 96h-treated cyst or 48h-treated spheroids. Values are mean ± SEM from three independent experiments (n>15 spindles/experiment); ****, P<0.0001) (Student's t-test).

Spindle orientation is finely controlled in cells that require specific spatial organization. In epithelial cells, spindles orient perpendicularly to the apicobasal axis of the cell to maintain apical

polarity and facilitate single lumen formation (Figure R16A). We measured the angles of the spindle poles in regards to the apical membrane of dividing cells in both control and experimental conditions. Angles should be close to 90º in control conditions to ensure single lumen formation. However, TGF-β type I receptors inhibition results in the randomization of mitotic spindle orientation (Figure R16B-D). To verify the result, we also treated MDCK spheroids for only 48h prior fixation, which caused spindles to randomize without having a strong effect in single lumen formation (Figure R16B'-D').

3.3. EW-7197 removal allows rescue of the multiluminal phenotype in 3D-MDCK cysts

Next, we investigated whether the effects of the TGF-β inhibitor were reversible during epithelial luminogenesis. For this experiment, we removed the inhibitor EW-7197 at different time points before fixing the cells and quantifying for each condition both the percentage of MDCK spheroids presenting single lumen and the orientation of the spindle in dividing cells (Figure R17).

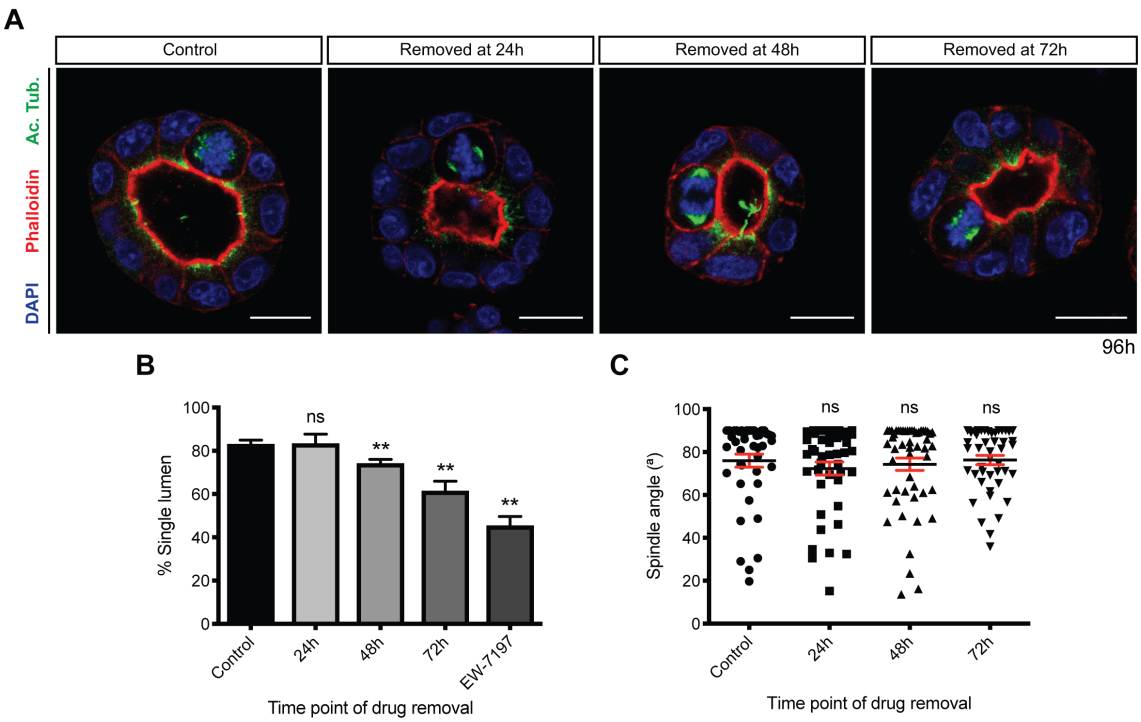

Figure R17. The effects of the TGF-β inhibitor EW-7197 are reversible during epithelial lumen morphogenesis. A) Confocal images of control and EW-7197 treated spheroids fixed at 96h. Acetylated tubulin (green), phalloidin (red), DAPI (blue). Scale bars,15µm. **B)** Quantification shows the percentage of spheroids presenting single lumen for each condition. Values are mean ± SD from n=3 independent experiments (n>100 spheroids/experiment); **, P<0.01; ns, not significant. **C)** Quantification shows spindle angles for each condition. Values are mean ± SD from n=3 independent experiments (n>30 spindles/experiment); ns, not significant.

As we observed in fish guts, the removal of EW-7197 from the cell media results in the recovery from the phenotype, both in terms of multiple lumen formation and appropriate spindle orientation (Figure R17). These results suggest that both spindle orientation and the emergence of multiple lumens are associated, although correlation does not always mean causation. Furthermore, these results further associate the phenotype we observe in epithelial 3D-MDCK spheroids with the phenotype we detected during the development of the intestinal tube in zebrafish, which is also rescued when eliminating the inhibitor from the fish water.

3.4. NuMA localization seems to be affected when cells are treated with the TGF-β inhibitor EW-7197

As we detected a spindle mispositioning in mitotic cells, we decided to investigate the localization of some of the machinery directly involved in this process. Three conserved proteins, called NuMA, LGN and Gαi in vertebrates, form the main cortical complex that controls spindle positioning during cell division by applying a pulling force on astral microtubules through dynein/dynactin activity (di Pietro et al., 2016) (Figure R-18B).

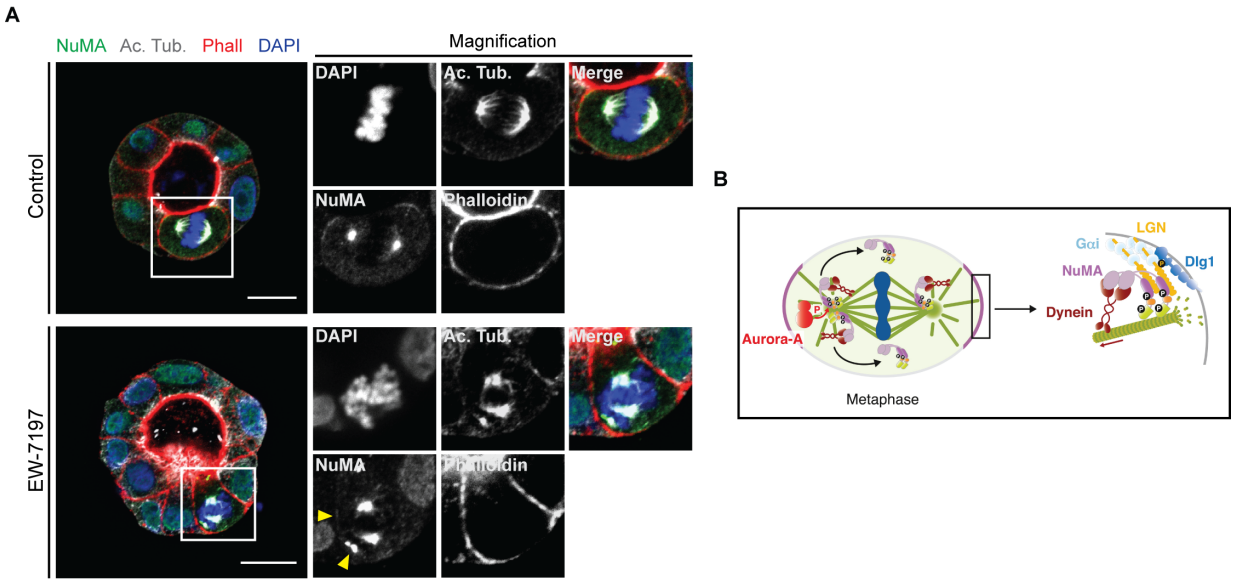

Figure R18. NuMA localization is affected upon TGF-β type I receptors inhibition. A) Confocal images of control and EW-7197-treated spheroids at 96h. Squares indicate magnified areas. Yellow arrowheads point to NuMA aberrant positioning. NuMA (green), acetylated tubulin (gray), Phalloidin (red), DAPI (blue). Scale bars, 15μm. **B)** Simplified scheme of principal components taking part in spindle positioning. Adapted from Gallini et al., 2016.

The mislocalization of the proteins that constitute this machinery often results in altered spindle orientation (Gallini et al., 2016; Hao et al., 2011; Rodríguez-Fraticelli et al., 2010; Zheng et al., 2010). We observed that NuMA, which is normally found at spindle poles and the lateral cortex in line with the pulling direction of the spindles, was aberrantly found forming aggregates and at the lateral membrane, (showing a perpendicular localization to the spindle direction) when EW-7197 is added to the culture (Figure R-18A). However, this interesting but preliminary result requires further analysis regarding the activity and distribution of other key proteins controlling spindle orientation, such as LGN, Cdc42 or aPKC (Hao et al., 2010; Jaffe et al., 2008).

3.5. SMAD2 and SMAD3 are required for epithelial morphogenesis of 3D-MDCK spheroids

To analyze the hypothetical implication of the canonical TGF-β pathway in lumen formation and resolution, we designed specific siRNAs for canine *SMAD2* and *SMAD3*. We tested their knock-down (KD) efficiency by western-blot or RT-qPCR after a double knock-down sequentially using both nucleofection and lipofection techniques (Figure R19A-C). We transfected MDCK cells with each siRNA (siSmad2 and siSmad3) or both at the same time, performed 3D culture and fixed them after 48h to avoid loss of siRNAs effect, since we observed that *SMAD2* and *SMAD3* mRNAs were rapidly recovered after silencing. Then, we measured both the percentage of MDCK spheroids with single lumen and the orientation of the spindle in dividing cells (Figure R19D-F).

We observed that KD of *SMAD2* and *SMAD3* mRNAs had a significant impact in lumen morphogenesis in MDCK spheroids (with a similar percentage of spheroids with single lumen when compared to the drug treatment fixed at 48h) and the spindle orientation in mitotic cells. The simultaneous silencing of both *SMAD2* and *SMAD3* mRNAs had severe consequences in MDCK spheroid morphogenesis, which were unable to properly develop. In addition to the multiluminal phenotype other effects could be perceived, such as in lumen formation, which is strongly impaired in a high number of spheroids, especially in *SMAD2* KD conditions (Figure R20A).

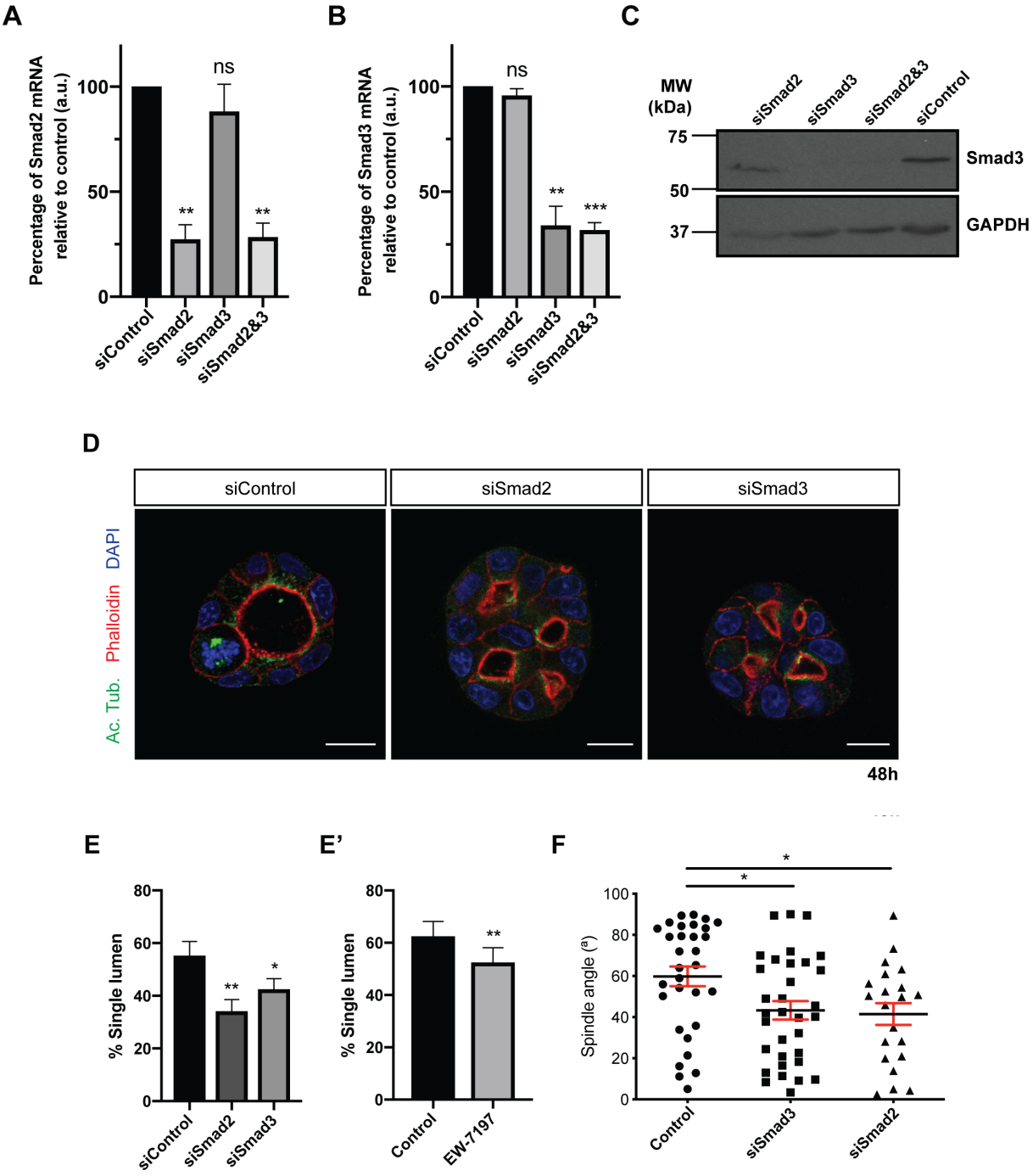

Figure R19. *SMAD2* and *SMAD3* silencing affect single lumen formation and spindle orientation. A-B) Quantification shows the percentage of *SMAD2* or *SMAD3* mRNA relative to control when using siRNAs against *SMAD2*, *SMAD3*, or both. Values are mean ± SD from n=3 independent experiments; **, P<0.01; ***, P<0.01, ns, not significant. (Student's *t*-test). **C)** Western blot against SMAD3 in all experimental conditions using GAPDH as a control. MW, molecular weight. **D)** Confocal images of MDCK spheroids at 48h knocked down for either *SMAD2* or *SMAD3*. Acetylated tubulin (green), Phalloidin (red), DAPI (blue). Scale bars, 15µm. **E-E')** Quantification shows the percentage of spheroids with single lumen at 48h, either by knocking down *SMAD2* or *SMAD3* (E) or by using EW-7197 (E'). Values are mean ± SD from 3 independent experiments (n>100 spheroids/experiment); *, P<0.05; **, P<0.01. (Student's *t*-test). **F)** Quantification shows spindle angles of dividing cells of cyst at 48h after KD with *SMAD2* or *SMAD3*. Values are mean ± SEM from n=3 independent experiments; *, P<0.05. (Student's *t*-test).

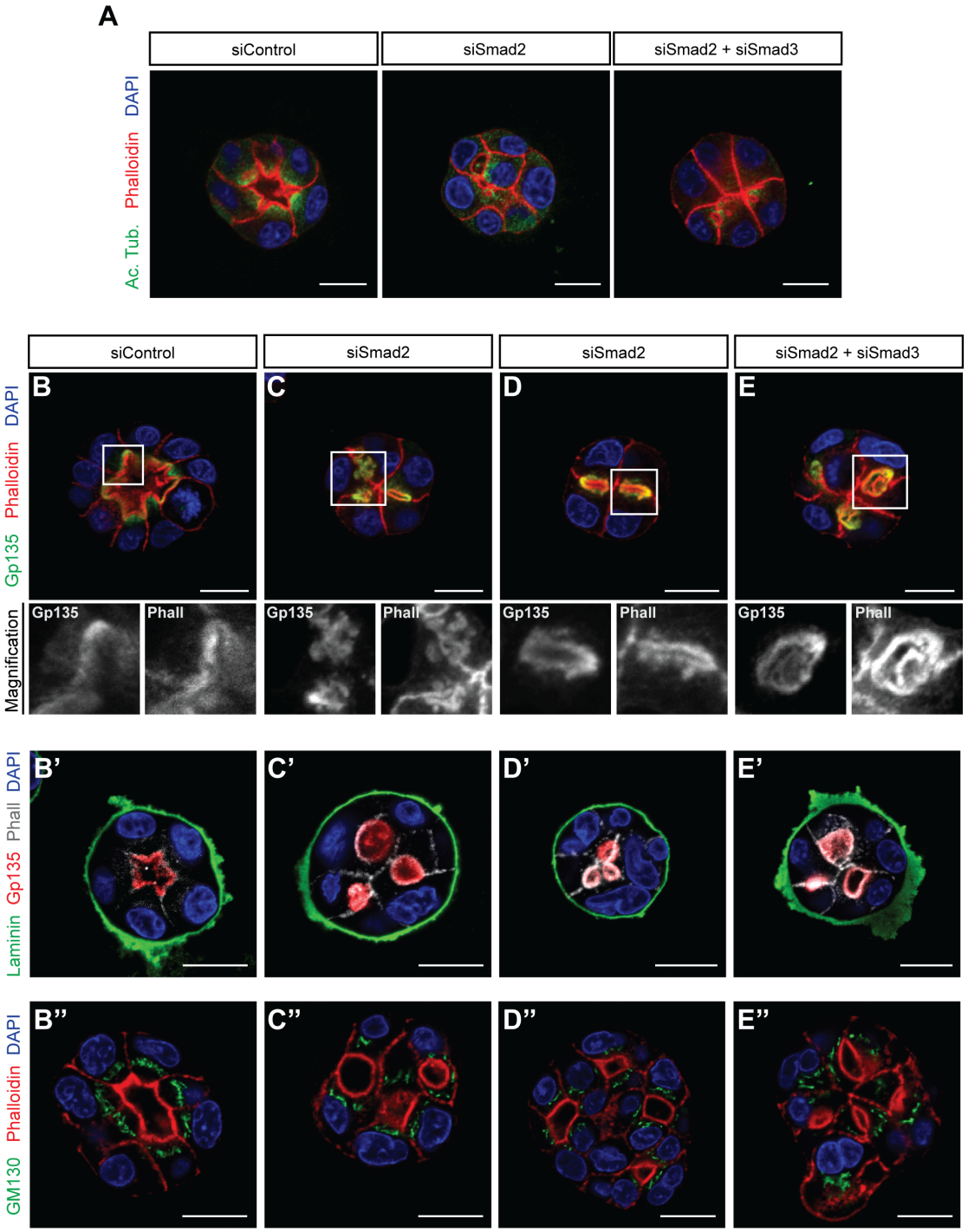

Figure R20. MDCK spheroids silenced for *SMAD2*, *SMAD3* or both *SMAD2* and *SMAD3* show defects in lumen opening but not in polarity acquisition or apical membrane identity. **A)** Confocal images of 48h spheroids showing a strong defect in lumen opening after KD of *SMAD2* or *SMAD2* and *SMAD3*. Acetylated tubulin (green), Phalloidin (red), DAPI (blue). Scale bars, 15µm. **B-E)** Confocal images of control and KD spheroids for *SMAD2*, *SMAD3* or both, showing normal localization of apical Gp135. Gp135 (green), Phalloidin (red), DAPI (blue). Scale bars, 15µm. **B'-E')** Confocal images of control and KD spheroids for *SMAD2*, *SMAD3* or both, showing normal deposition of laminin. Laminin (green), Phalloidin (red), DAPI (blue). Scale bars, 15µm. **B''-E'')** Confocal images of control and KD spheroids for *SMAD2*, *SMAD3* or both, showing normal positioning of Golgi apparatus. GM130 (green), Phalloidin (red), DAPI (blue). Scale bars, 15µm.

Furthermore, when only *SMAD3* is silenced, a characteristic phenotype is repeatedly observed, consisting of 4-cell stage spheroids with two apical membrane initiation sites (AMIS). This could be caused by a range of different reasons, like defects in spindle orientation, in midbody positioning and loss of asymmetric abscission during cell division, or impairment in the machinery involved in lumen resolution through junction remodeling or apical membrane enlargement (Figure R20D). In case the acquisition of apicobasal polarity could have been affected upon *SMAD2* and/or *SMAD3* silencing, we characterized apical markers such as podocalyxin/Gp135 (Figure R20B-E), ECM laminin deposition (Figure R20B'-E'), and Golgi positioning (GM130) (Figure R20B''-E''), which is normally closed to the apical membrane of polarized cells to facilitate vesicle transport, and we found no observable defects.

3.6. *SMAD3* KD does not block cell motility

TGF-β activation has a key and conserved role in cell motility and migration (Ferrarelli, 2019; Wendt et al., 2009; Xu et al., 2009). Interestingly, previous work has demonstrated that MDCK cells are constantly in movement during spheroid morphogenesis, which facilitates single lumen formation (Kim et al., 2015). Therefore, we considered the possibility that these two processes could be linked and that TGF-β inhibition may be impairing spheroid cell motility and hence hindering lumen resolution. We decided to test this hypothesis performing overnight *in vivo* experiments of MDCK spheroids silenced for siControl or just siSmad3 (since the majority of spheroids silenced for *SMAD2* or simultaneously for *SMAD2* and *SMAD3* are unable to correctly open lumens). To follow cell movements during the experiment, we mixed mCherry-positive MDCK cells with normal MDCK cells, all silenced with siSmad3 or siControl. We observed that *SMAD3* KD did not inhibit general cell motility (Figure R21). Interestingly, we detected the formation of group of cells that seem to be extruded from the spheroid (Figure R21B, yellow arrowheads), which suggests some defects in the adherence and/or motility of these cells. However, further analysis is needed to better address the role of cell motility and adhesion in epithelial morphogenesis.

In conclusion, TGF-β signaling is necessary for MDCK spheroid morphogenesis. Whereas both the use of the chemical TGF-β type I receptors inhibitor EW-7197 and the silencing of key components of the canonical TGF-β pathway *(SMAD2* and *SMAD3)* provoke a decrease in the number of spheroids with single lumen and a defect in spindle orientation, the morphological phenotype slightly differs between them. The mechanisms by which the machinery that orients the

spindle in dividing cells is being altered and whether additional SMAD-independent pathways play a role in epithelial 3D morphogenesis are issues that need to be addressed in future works.

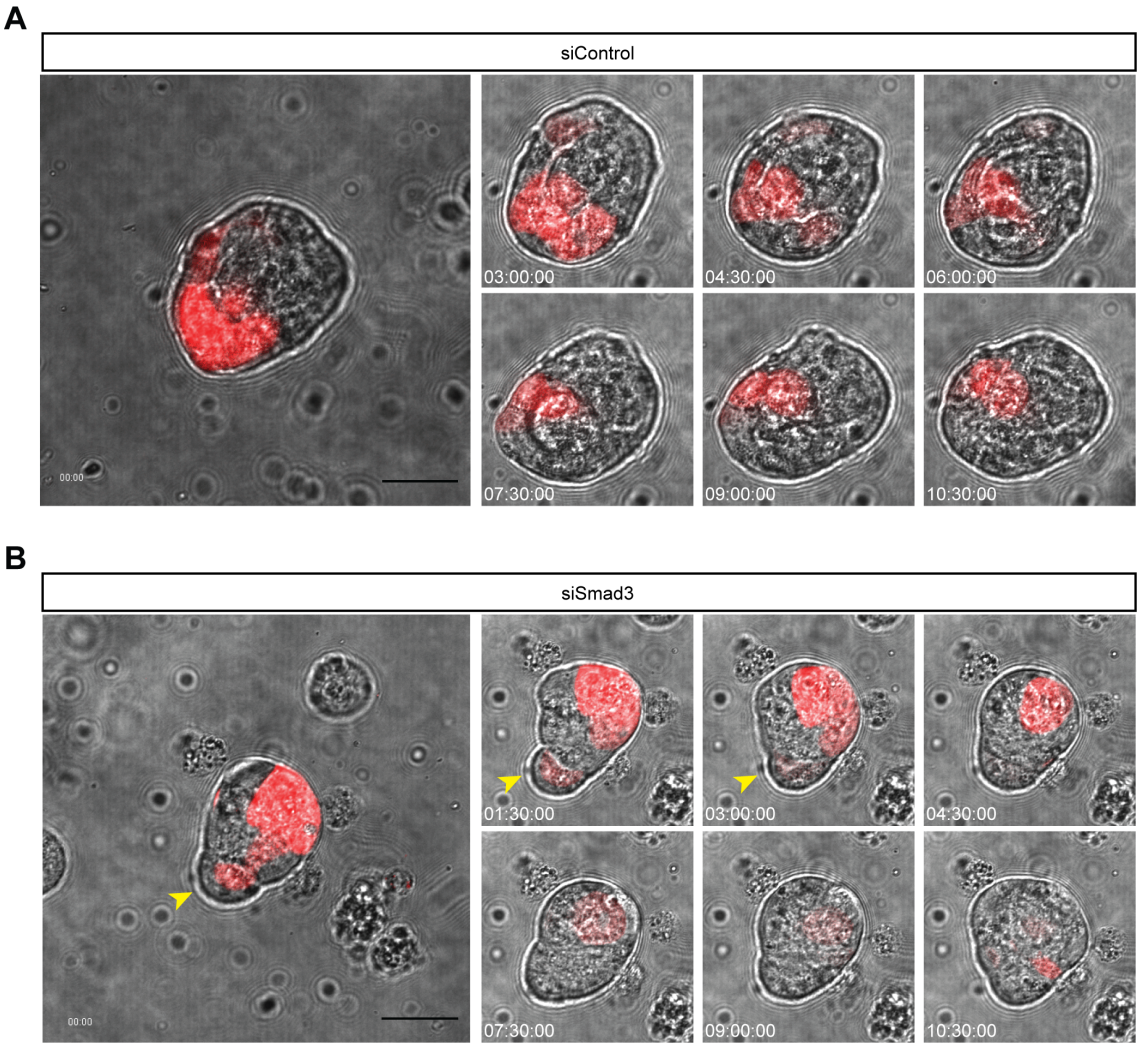

Figure R20. MDCK cells silenced for *SMAD3* do not display important defects in motility during spheroid morphogenesis. A) Confocal images of MDCK spheroids after silencing with siControl at different time points during spheroid morphogenesis. mCherry (red). Scale bars, 10µm. **B)** Confocal images of MDCK spheroids after silencing with siSmad3 at different time points during cyst morphogenesis. Yellow arrowheads point to gropus of cells presenting extrusion-like behavior. mCherry (red). Scale bars, 10µm. Time point indicated in HH:MM:SS.

DISCUSSION

1. *Sfrp3* role as Wnt ligand diffusor

SFRPs are considered the largest family of secreted Wnt inhibitory proteins, but little is known about the role of SFRP3 in Wnt pathway modulation. Previous studies showed that SFRP3 could bind Wnt1 and Wnt8 and inhibit the canonical Wnt pathway in cultured cells and *Xenopus*, respectively (Lin et al., 1997; Wang et al., 1997). The Wingless (Wh) pathway in *Drosphila* is one of the best-characterized signaling pathways and its characterization has helped to understand conserved mechanisms in the vertebrate Wnt pathway (Swarup & Verheyen, 2012). In this present work we proved that, at least in *Drosophila*, SFRP3 does not function as Wg inhibitor but as an extracellular diffusor of the Wg morphogen. We showed how the ectopic expression of *Sfrp3* in the posterior compartment of *Drosophila* wing imaginal discs alters the expression pattern of *wg*, which appears expanded at the DV boundary. As a consequence, *Sfrp3* expression also affects the expression of the Wg pathway targets *sens* and *dll*, whose expressions were reduced or broaden, respectively, when compared to the control compartment of the wing imaginal discs. In addition, adult wings in which *Sfrp3* was expressed in the whole wing pouch under the Nubbin driver presented a decreased number of sensory organs as a result of the altered expression of *sens*. Other studies support these results, as previous work showed that *Sfrp3* promoted the diffusion of Wnt8 and Wnt11 in *Xenopus* embryo (Mii & Taira, 2009). Hence, our results suggest that SFRP3 might act as an extracellular diffusor of Wnt ligands in other contexts as well, such as the mammary gland. In this case, SFRP3 would act as a modulator of Wnt pathway by binding to Wnt2, secreted by stromal cells to the intercellular space, and expanding Wnt2 territory of action. In knockout mice for *Sfrp3*, Wnt2 would accumulate at the boundary between stromal and epithelial cells and cause a defective mammary epithelial morphogenesis (Bernascone et al., 2019). However, further analyses are required to better understand how the communication between stromal and epithelial cells is being carried out.

2. Main signaling pathways in zebrafish intestinal development

2.1. The Hedgehog pathway

Zebrafish embryos presenting a mutation in *smo*, the Hh pathway transducer, are unable to undergo lumen fusion during the process of gut development (Alvers et al., 2014). However, Hh

pathway does not act in epithelial cells but in the surrounding mesenchymal layer, which must be interacting through mechanical or morphogen signaling with the epithelium to achieve proper lumen resolution in the intestine. The mechanisms that are being regulated in epithelial cells upon these interactions with surrounding mesenchyme are unknown. In this work, we performed a transcriptomic analysis to identify candidate genes in epithelial cells that may have a role in the process of lumen resolution by comparing the gene expression profiles of IECs of control fish to that of *smo*^{s294} mutants. We found that differentially expressed genes were mainly associated with cytoskeletal architecture, cell-cell signaling, cell adhesion and cell migration processes. It is remarkable that among the top ten downregulated genes, we mostly observed genes that are part of the actomyosin cytoskeleton, such as Myosin regulatory light chain 10 *(myl10)*, or contribute to the regulation of the cytoskeletal activity, such as Parvalbumin 4 *(pvalb4)*, Integrin alpha 2.2 (*itga2.2)* and Integrin alpha 2.3 (*itga2.3)*. Interestingly, *myl10* had been identified as a Hh pathway target gene in a previous study, in which *myl10* expression was shown to be extremely reduced in *gli1; gli2a* double mutant zebrafish embryos (Wang et al., 2013). On the other hand, parvalbumin proteins are high affinity calcium ion-binding proteins structurally and functionally similar to calmodulin and troponin C and thus, believed to be involved in cell contraction/relaxation processes. Integrins are transmembrane receptors that mediate cell adhesion to the ECM and act as signal transductors to regulate cell processes, such as cell cycle or cytoskeletal rearrangements. Therefore, our results suggest that Hh pathway is necessary to activate mechanisms associated with cell architecture changes in epithelial cells that facilitate the process of lumen resolution. Furthermore, *smo*^{s294} mutants also show an accumulation of enlarged Rab11a compartments in IECs, which resembles to the phenotype caused by Rab11fip1 overexpression (Alvers et al., 2014). We did not find any Rab11 interactor to be differentially expressed in our transcriptomic analysis, although the actomyosin network components and regulators whose expression we found to be altered in the *smo*^{s294} mutants could also be connected to the disturbed endosomal trafficking. For instance, Rab11-FIP2 interacts with Myosin Vb to regulate recycling processes (Hales et al., 2002; Lapierre et al., 2001), and the disruption of this interaction results in a multiluminal phenotype in MDCK spheroids (Lapierre et al., 2012). Other research articles have also linked the dynamic regulation of the actomyosin network to junction remodeling and cell shape changes during epithelial tissues morphogenesis (Curran et al., 2017; Heisenberg & Bellaïche, 2013; Martin et al., 2009; Munjal and Lecuit, 2014; Rauzi et al., 2010) and specifically to tubulogenesis (Barry et al., 2016; Booth et al., 2014; Denker et al., 2015), which further supports the hypothesis of the critical

role that these cell shape changes under the control of Hh pathway might have in the lumen resolution during zebrafish gut development.

Furthermore, among the ten most downregulated genes in *smo*^{s294} mutants, we also found two genes, *actinodin1* (*and1*) and *actinodin2* (*and2*), directly associated with fin development and regeneration, a function that is not apparently related to intestinal development. Actinodins are structural proteins that form actinotrichia, which are rigid fibrils of the teleost fins (König et al., 2018) that act as a scaffold for the migration of mesenchymal cells (Wood and Thorogood, 1984). It has been described that actinotrichia formation is blocked by chemical Hedgehog inhibition, which also impairs fin regeneration (Armstrong et al., 2017; Quint et al., 2002). Our data suggest that actinodins may have additional roles, apart from their implication in fin development and regeneration, potentially related to the guiding of mesenchymal cell migration around the intestinal epithelia during gut development.

Remarkably, looking at down- and upregulated separately, we detect different enrichments in specific GO terms. Downregulated genes are associated with ion/proton transport and inner ear morphogenesis, which are processes tightly linked, as fluid accumulation depending on ion transporters is responsible for generating the force needed for inner ear development and function (Hoijman et al., 2015; Mosaliganti et al., 2018). Hydrostatic pressure, which is modulated by molecule and ion transport and junction permeability (Fishbarg, 2010; Günzel & Yu, 2013), has been shown to be critical for the development of different organs that present lumens, including the embryonic brain (Lowery & Sive, 2005), the Kupffer's vesicle (Dasgupta et al., 2018; Navis et al., 2013) or the intestine (Bagnat et al., 2007). Hence, it is possible that *smo*^{s294} mutants also present a disruption in some epithelial mechanisms controlling luminal expansion through fluid accumulation necessary for the intestinal lumens to grow and fuse.

Besides, in experiments using the transgenic line *Tg(ptch2::kaede),* we have shown that the expression of Kaede under *ptch2* promoter is maintained after the lumen resolution stages of gut development, being detectable at least until 96hpf. This result suggests that Hh is not only involved in lumen resolution but also in other processes related to the zebrafish intestinal development or physiological function. For instance, Hedgehog signaling is required for villus patterning processes (Kosinski et al., 2010; Madison et al., 2005), intestinal smooth muscle differentiation and homeostasis (Ramalho-Santos et al., 2000; Zacharias et al., 2011), intestinal secretory cell maturation and autophagy (Gagné-Sansfaçon et al., 2014), and intestinal epithelium homeostasis (Buller et al., 2012, van den Brink, 2007). Moreover, Hh signaling disruption is related

to different gastrointestinal diseases, such as cancer (Katoh & Katoh, 2005) or inflammatory syndromes (Nielsen et al., 2004; van Dop & van den Brink, 2010; Zacharias et al., 2010). Most of these studies are focused on mammal intestinal development, and thus, whether the different roles of Hh signaling are conserved in zebrafish should be further investigated. Indeed, zebrafish gut would serve to further analyze the molecular mechanisms of intestinal diseases, providing a very interesting model to elucidate possible treatments.

2.2. The TGF-β pathway

In this work, we also aim to identify the molecular pathways by which mesenchymal cells signal toward the IECs to ensure the cellular rearrangements required for tube morphogenesis. Among the candidate pathways, we found that the inhibition of TGF-β signaling using the chemical TGF-β type I receptor inhibitor EW-7197 leads to the disruption of lumen resolution in the zebrafish intestine, similarly to the phenotype observed in *smo*^{s294} mutants. Besides, we showed that this effect is reversible in a short period of time when EW-7197 is eliminated from the fish water, which indicates that the mechanisms required for lumen resolution are rapidly restored. In addition, we also demonstrated that EW-7197 is also blocking ventral and dorsal mesenchymal cell migration from the LPM around the epithelial layer of the intestine, an effect that has been previously observed when blocking TGF-β pathway using different strategies (Gays et al., 2017). Therefore, we can contemplate different scenarios that might explain the defects in lumen coalescence observed upon TGF-β inhibition during gut development:

1) Complete surrounding of the epithelium layer by mesenchymal cells is essential for lumen resolution due to one or both of these causes:

   i. Mesenchymal cells offer mechanical support needed for proper epithelial tube morphogenesis.
   ii. Mesenchymal cells signaling through morphogens to neighboring epithelial cells after mesenchymal migration is crucial for lumen resolution.

2) TGF-β pathway is activated in epithelial cells by autocrine/paracrine signaling and controls a downstream reaction that facilitates lumen coalescence.

Changes in the physical properties of the substrate to which cells attach *in vitro* influence cell shape, polarity and morphogenesis (Elosegui-Artola et al., 2016; Gupta et al., 2019; Papusheva & Heisenberg, 2010; Prager-Khoutorsky et al., 2011). Furthermore, the physical microenvironment has an important role in tumor progression and metastasis, as stiffer environments offer suitable characteristics for cell invasion in several cancer models (Levental et al., 2009; Reid et al., 2017; Samuel et al., 2011). Mesenchymal cells that give raise to smooth muscle cells surround a variety of tubular organs, including the gut, blood vessels, or the lungs. Smooth muscle cells are stiffer than epithelial or endothelial cells and offer a physical constraint when the epithelial or endothelial layers are proliferating. In mammary small intestine, smooth muscle cell sequential differentiation and compressive stresses have been shown to be critical for villi formation (Shyer et al., 2013). The support that smooth muscle cells offer is also necessary for ureter and blood vessel development, in which the tube diameter enlarges or develops aneurysms if the smooth muscle is knocked out (Hellstrom et al., 1999; Yan et al., 2014). Consequently, the lack of mesenchymal support in the developing zebrafish intestine as a result of the inhibition of mesenchymal cell migration by the blockade of TGF-β signaling could result in defects in lumen resolution, leading to impaired epithelial tube morphogenesis. To test this hypothesis, first we would need to check whether mesenchymal migratory properties are restored after EW-7197 removal from the fish water, and if lumen resolution takes place at the spots where mesenchymal cells completely surround epithelial cells. However, according to our RNA-seq data, epithelial cells also express type I and type II TGF-β receptors, and prior works have demonstrated that IECs can also secrete TGF-β ligands that act in these cells through SMAD-dependent and SMAD-independent pathways (Yakovich et al., 2010; Yamada et al., 2013). Hence, further analyses will establish whether the phenotype that can be observe in the epithelial tube upon TGF-β inhibition is a consequence of (1) the blocking of the communication mediated by ligands secreted by mesenchymal or epithelial cells and received by the epithelial layer transmembrane receptors or (2) disrupted physical interaction between the epithelial and mesenchymal layers. An alternative scenario would consist of both physical contacts and ligand-secreted communication being key synergistic players in intestinal morphogenesis. Thus, further research is necessary to elucidate the role of each kind of cell interaction in the context of intestinal zebrafish development.

Regarding the possibility that epithelial cells are activating TGF-β pathway, we did not found a strong accumulation of phosphorylated Smad2/3 in epithelial cells nuclei at lumen resolution stages. Nevertheless, we cannot discard the hypothesis of canonical signaling being active in epithelial cells at earlier stages of gut development, or other non-canonical TGF-β signaling having a role in lumen coalescence. For instance, SMAD3 has been shown to be activated in IECs in mammalian GI tract, in which both SMAD-dependent and non-dependent mechanisms cooperate to promote Focal adhesion kinase (FAK) synthesis to regulate cell motility and focal adhesions formation and disassembly (Walsh et al., 2008). In addition, it has been recently described that TGF-β signaling induces SMAD1 and SMAD5 phosphorylation by a mechanism dependent on two type I receptors, TGFBR1 (ALK5) and ACVR1 (ALK4), and that this SMAD1/5 activation is required for TGF-β-induced EMT (Ramachandran et al., 2018). Furthermore, SMAD1/5 phosphorylation via TGF-β had been previously reported in several types of cell lines, including endothelial cells, epithelial cells and fibroblasts (Daly et al., 2008; Goumans et al., 2002; Goumans et al., 2003; Wrighton et al., 2009). Consequently, SMAD1/5 phosphorylation and localization in intestinal epithelial and mesenchymal cells should be studied to determine their possible implication in the process we investigate.

However, considering the links between TGF-β pathway and the cytoskeleton, we can also hypothesize that the mechanism by which TGF-β regulates lumen resolution might be through the regulation of proteins involved in the actomyosin network activity. Previous work describes the regulation of *Ciona intestinalis* notochord tubulogenesis by a TGF-β—ROCK axis that controls actomyosin contractility (Denker et al., 2015). ROCK activity had been previously shown to have a role in *in vitro* MDCK model as its inhibitor, Y27632, enhances lumen initiation and opening (Ferrari et al., 2008) and the activity of p114RhoGEF, upstream of RHOA and ROCK, is required for cell motility and lumen formation in tubules (Kim et al., 2015). During lumen resolution in the zebrafish gut intestine, cells undergo shape changes and junctions remodeling that facilitate the fusion of adjacent lumens. It is possible that these cell shape changes are driven by actomyosin contractility and regulated by RHOA-ROCK signaling upon TGF-β activity.

In conclusion, TGF-β might be participating in gut lumen resolution by activation of both canonical or non-canonical pathways in epithelial cells, and future investigations would serve to determine through which signaling cascades TGF-β is regulating this developmental process.

2.3. The link between Hh and TGF-β

We initially hypothesized that TGF-β pathway could function downstream Hh pathway as a potential interactive link between mesenchymal and epithelial cells. Indeed, we found a phenotype that fit this initial hypothesis, but deeper analyses showed that the observable defects were different in both *smo*^{s294} mutants and EW-7197—treated fish. They both presented defects in smooth muscle development and unresolved lumens in the gut tube at stages in which control fish displayed a completely open single lumen. However, unfused lumens in fish treated with the TGF-β inhibitor are in most cases closer between them than those observed in *smo*^{s294} mutants, which suggests a problem in the machinery involved in the final stages of lumen resolution when TGF-β is blocked. In addition, while in *smo*^{s294} mutants the mesenchymal layer displays a decreased number of cells that do not differentiate (Alvers et al., 2014), the inhibition of the TGF-β type I receptors leads to impaired mesenchymal cell migration and therefore a lack of mesenchymal layer surrounding certain areas of the epithelial tube. Hence, we contemplate several hypotheses:

1) The defects in the process of epithelial lumen resolution in the guts of both *smo*^{s294} and EW-7197—treated fish are similar but derive from different causes. Guts of *smo*^{s294} mutants are completely surrounded by mesenchymal cells that offer physical constraint for the epithelial tissue to undergo morphogenesis, in contrast to what we observed in fish treated with the TGF-β inhibitor. Therefore, the reason behind the unfused lumens in fish treated with the TGF-β inhibitor would be mostly associated with the lack of physical constraint.

2) The phenotypes are coincident because there is a crosstalk between Hh and TGF-β signaling pathways. We performed a preliminary RNA-seq analysis in which we compared Myadm-GFP—positive cells at lumen resolution stages of cyclopamine-treated and control fish that were isolated by FACS sorting. Cyclopamine is a chemical inhibitor of Smo that mimics the effect observed in *smo*^{s294} mutants. We looked for differentially expressed TGF-β ligand genes, but we found no differences in the expression levels of these genes, and thus concluding that TGF-β ligands expression in the mesenchymal layer was not under the control of Hh pathway. We also carried out the same analysis in our RNA-seq data of IECs comparing *smo*^{s294} mutants and control fish, with similar results. Therefore, we can conclude

that TGF-β ligand expression is not under the control of Hh pathway in neither epithelial nor mesenchymal cells of the developing zebrafish gut. However, several studies have shown a modulation of Hh pathway by TGF-β signaling. For instance, TGF-β induces the expression of Gli transcription factors independently of Hh signaling, in a mechanism that relies on SMAD3 (Dennler et al., 2007; Dennler et al., 2009), and that this link also seems to operate in the development of bladder cancer (Mechlin et al., 2010). Long-standing studies have also demonstrated that the post-transcriptional regulation of Ihh is controlled by TGF-β (Murakami et al., 1997) and other investigations have linked the decrease of TGF-β signaling to the inhibition of Hh pathway in bone marrow fibrosis (Chaundhry et al., 2017). Hence, future research will be needed to address the possibility that Hh pathway is being modulated by TGF-β signaling in mesenchymal or epithelial cells in the context of gut development in zebrafish.

3. TGF-β role in epithelial cell cultures

3.1. TGF-β in 2D MDCK cell culture

In the present work, we observed that 2D MDCK epithelial cell cultures show difficulties to undergo cell spreading and generate lamellipodia and filopodia upon TGF-β inhibition. Epithelial cells change from a migratory state to the establishment of a polarized simple epithelium, through a process triggered by the initiation of cell-cell contacts followed by the generation of an apico-basal axis of polarity (Nelson, 2009). However, after polarization, cells can still move within the tissue without breaking its integrity, which was believed to occur either by collective cell migration (Friedl & Gilmour, 2009; Rorth, 2009) or by acquisition of a temporary, or partial, epithelial-to-mesenchymal transition (EMT) state (Thiery et al., 2009). In this kind of epithelial cell behavior, we can find leader cells at front edges of the epithelial sheets that show increased migratory morphological features (lamellipodia and filopodia) with changes in apico-basal polarity and cell-cell junctions (still present in cell areas in contact with following cells, but absent from the free edge). Lamellipodia and filopodia are dynamic actin-rich protrusion structures required for cell movement and migration (Jacquemet et al., 2015; Rottner et al., 2017; Small et al., 2002). The assembly of these protrusions is dependent on the activity of many proteins that regulate cytoskeletal reorganization, such as Rho GTPases (Hall, 1998; Nobes & Hall, 1995; Ridley, 2015), polarity complexes (Mayor & Etienne-

Manneville, 2016; Nishimura & Kaibuchi, 2007) and downstream proteins like Arp2/3 (Vinzenz et al., 2012; Wu et al., 2012) or formins (Iden & Collard, 2008; Kage et al., 2017). Our results support previous data that links TGF-β activity with both the initiation of EMT (Ferrarelli, 2019; Wendt et al., 2009; Xu et al., 2009), and the modulation of Rho GTPases activity and actin rearrangements (Edlund et al., 2002; Ungefroren et al., 2018; Vardouli et al., 2008). However, further analyses including quantification of lamellipodia formation and cell spreading assays will serve to validate our results.

3.2. TGF-β in 3D MDCK spheroid morphogenesis

We also found that the inhibition of TGF-β in 3D MDCK cultures results in an increase in the number of spheroids with multiple lumens. As the addition of the TGF-β inhibitor at 48h after cell seeding did not lead to multiluminal spheroids, we believe the treatment is not causing sudden lumen opening but regulating other aspects of spheroid morphogenesis, such as cell motility, cell division and lumen resolution. We observed that spindle orientation was randomized when the TGF-β inhibitor was added to the cell media, and that the defects were reversible when the inhibitor was removed. In addition, NuMA, a key protein of the spindle orientation machinery, was found to be mislocalized upon TGF-β inhibition. NuMA is part of the complex that directly controls spindle positioning, which also includes LGN and Gαi (Kotak & Gönczy, 2013). RhoGTPases like RHOA and CDC42 play a central role in the regulation of not only the cytoskeleton but also microtubules in many cell processes, including cell division and cytokinesis (Chircop, 2014; Etienne-Manneville & Hall, 2002; Ridley, 2006). Several studies have demonstrated the role of RhoGTPases in NuMA/LGN localization and spindle orientation (Gotta et al., 2001; Lázaro-Diéguez et al., 2013; Mitsushima et al., 2009; Qin et al., 2010; Rodríguez-Fraticelli et al., 2010), and TGF-β regulation of RhoGTPases activity (Black & Trackman, 2008; Edlund et al., 2002; Mythreye & Blobe, 2009; Shao et al., 2013; Ungefroren et al., 2018; Vardouli et al., 2008). We hypothesize that TGF-β regulates RhoGTPases (Cdc42 and/or Rho proteins) activity, which in turn modulate NuMA/LGN localization and spindle orientation in MDCK spheroids.

When silencing canonical TGF-β pathway components *SMAD2* and *SMAD3*, we also found defects in single lumen formation and spindle orientation, but the spheroid morphological phenotypes slightly differ from those of the spheroids grown with EW-7197. The actin cytoskeleton and lumen opening were strongly affected when silencing *SMAD2* or both *SMAD2* and *SMAD3*,

while *SMAD3*-silenced spheroids displayed alterations in the actin network structure as well, a high number of four-cell spheroids with two AMIS was found in these samples. It is likely that the appearance of multiple unfused lumens in spheroids when TGF-β is inhibited is related to the randomization of spindle orientation, as it has been described that the positioning of the initial apical space is controlled by spindle orientation (Jaffe et al., 2008; Luján et al., 2016; Rodríguez-Fraticelli et al., 2010). Further *in vivo* imaging of spheroid morphogenesis upon TGF-β inhibition with EW-7197 or *SMAD2/3* silencing would be needed to establish whether cell divisions are properly taking place. In addition, although we did not observe strong defects in cell motility during spheroid morphogenesis upon Smad3 silencing, we believe cells might be having peculiar extruding-like behaviors that need to be further investigated.

Consequently, TGF-β might be acting through Smad-dependent and non-dependent signaling to regulate RhoGTPases activity, affecting processes like spindle positioning through NuMA/LGN localization or actomyosin activity and structure that affects cell motility during spheroid morphogenesis. Further analyses would include the study of the localization and activity of RhoGTPases at different stages of spheroid morphogenesis, and also localization of other components regulating spindle positioning (dynactin, dynein, LGN…), and deeper examination of cell motility behaviors during spheroid formation.

4. The link between defects in zebrafish intestinal development and MDCK spheroid morphogenesis upon TGF-β inhibition

The phenotypes observed in both zebrafish embryo intestine and 3D MDCK spheroids when TGF-β is inhibited share some similarities. Both of them display multiple unfused lumens at stages in which control conditions show an open single lumen. The actin network also seems to be affected in zebrafish guts and MDCK spheroids if TGF-β signaling is blocked, with apical membrane of the guts showing a disorganized appearance and the actin cytoskeleton of the spheroids presenting a diffused distribution. Therefore, although the intestine is a much more complex system than the MDCK spheroids culture, it is possible that both models share common mechanisms that lead to the phenotypes observed. Hence, future investigations would be needed to determine if for instance, the defect in spindle orientation is also affecting the epithelial cells of the zebrafish intestine, which could be responsible for the stratified epithelial layers observable upon TGF-β inhibition. Moreover, using more complex *in vitro* systems, such as micropatterns,

organoids, or a combination of both (Bosch-Fortea et al., 2019) could also shed light on the mechanisms controlled by TGF-β and the role of mesenchymal cells in epithelial organs morphogenesis.

CONCLUSIONS

1. SFRP3 functions as a diffusor of Wg in the *Drosophila* wing imaginal disc and modifying the pattern of expression of Wg target genes. We propose that this mechanism is also modulating mammary gland development, in which we believe that stromal-secreted SFRP3 is binding Wnt2 and expanding its territory of action.

2. We have characterized the transcriptomic profile of intestinal epithelial cells of developing zebrafish embryos carrying a mutation in the hedgehog co-receptor *smoothened* (*smo*) compared to control fish. This RNA-seq analysis suggests that the activation of hedgehog pathway in mesenchymal cells is necessary to initiate a specific response in epithelial cells of the developing gut.

3. The RNA-seq data obtained from intestinal epithelial cells of developing zebrafish reveals that Hedgehog pathway is indirectly regulating the expression of a group of genes possibly required for single lumen formation. These genes are mainly associated with cell migration, cytoskeletal changes, cell motility and cell-cell interaction. Our RNA-seq data also offers several candidate genes potentially essential for lumen coalescence, such as *myl10*, *and1*, *and2*, *pvalb4*, *itga2.2* and *itga2.3*.

4. The inhibition of TGF-β pathway during zebrafish embryo development results in a defect in single lumen formation due to the incapacity of epithelial cells to undergo lumen resolution. We found that dorsal and ventral mesenchymal cell migration required to surround the epithelial tube is partially or entirely blocked upon TGF-β inhibition. This result suggests that physical constraints could be necessary for epithelial cells to resolve the lumens.

5. In epithelial MDCK spheroids, TGF-β inhibition either by adding the inhibitory drug EW-7197 or by silencing canonical pathway components *SMAD2* and/or *SMAD3* causes the impairment of single lumen formation due to the randomization of spindle orientation. However, these results do not exclude the possibility that other canonical or non-canonical pathways downstream TGF-β could also regulate lumen formation and resolution in epithelial 3D MDCK cultures and in zebrafish gut development.

1. SFRP3 funciona como difusor de Wg en el disco imaginal de ala de *Drosophila* modificando el patrón de expresión de los genes diana de Wg. Proponemos que este mecanismo está a su vez modulando el desarrollo de la glándula mamaria, en el que creemos que SFRP3 secretada por el estroma se une a Wnt2 y expande su territorio de actuación.

2. Hemos caracterizado el perfil transcriptómico de las células epiteliales intestinales de peces cebra en desarrollo portadores de una mutación en el co-receptor de hedgehog *smoothened* (*smo*) comparado con los peces control. El análisis de RNA-seq sugiere que la activación de la ruta de hedgehog en las células mesenquimales es necesaria para iniciar una respuesta específica en las células epiteliales del intestino en desarrollo.

3. Los datos de RNAseq obtenidos de las células epiteliales intestinales de peces cebra en desarrollo revelan que la ruta de Hedgehog está indirectamente regulando la expresión de un grupo de genes posiblemente necesarios en el proceso de formación de un único lumen. Estos genes están principalmente asociados a migración celular, cambios en el citoesqueleto, motilidad celular e interacción célula-célula. Nuestros datos de RNA-seq también sugieren varios genes candidatos potencialmente esenciales para la coalescencia de lúmenes, como *myl10*, *and1*, *and2*, *pvalb4*, *itga2.2* e *itga2.3*.

4. La inhibición de la ruta TGF-β durante el desarrollo de los embriones de pez cebra causa un defecto en la formación de un único lumen debido a la incapacidad de las células epiteliales para llevar a cabo la resolución de los lúmenes. Observamos que la migración dorsal y ventral de las células mesenquimales para rodear al tubo epitelial es parcial o completamente bloqueada por la inhibición de TGF-β. Esto sugiere que las restricciones físicas podrían ser necesarias para que las células epiteliales resuelvan los lúmenes.

5. En esferoides de células MDCK epiteliales, la inhibición de TGF-β tanto añadiendo la droga EW-7197 como silenciando los componentes de la ruta canónica *SMAD2* y/o *SMAD3* causa una alteración en la formación de un único lumen debido a la aleatorización de la orientación del huso. No obstante, estos resultados no excluyen la posibilidad de que otras rutas canónicas o no canónicas aguas abajo de TGF-β podrían también regular la formación y resolución de lúmenes en cultivos de MDCK 3D y en el desarrollo del intestino de pez cebra.

BIBLIOGRAPHY

Aanstad, P., Santos, N., Corbit, K. C., Scherz, P. J., Trinh, A. Salvenmoser, W., Huisken, J., Reiter, J. F. & Stainier, D. Y. R. (2009). The extracelular domain of Smoothened regulates ciliary localization and is required for high-level Hh signaling. *Current Biology, 19*, 1034-1039.

Afgan, E., Baker, D., van den Beek, M., Blankenberg, D., Bouvier, D., Cech, M., Chilton, J., Clements, D., Coraor, N., Eberhard, C., et al. (2016). The Galaxy platform for accesible, reproducible and collaborative biomedical analyses: 2016 update. *Nucleic Acid Reserch 44*, W3-W10.

Aldaz, S. & Escudero, L. M. (2010). Imaginal discs. *Current Biology 20*, R429-431.

Alexandre, C., Baena-Lopez, A., & Vincent, J.-P. (2013). Patterning and growth control by membrane-tethered Wingless. *Nature*, *505*, 180.

Alvers, A. L., Ryan, S., Scherz, P. J., Huisken, J., & Bagnat, M. (2014). Single continuous lumen formation in the zebrafish gut is mediated by smoothened-dependent tissue remodeling. *Development*, *141*(5), 1110–1119.

Anders, S., Pyl, P. T., Huber, W. (2015). HTSeq—a Python framework to work with high-throughput sequencing data. *Bioinformatics 31*, 166-169.

Andrew, D. J. & Ewald, A. J. (2010). Morphogenesis of epitelial tubes: Insights into tuve formation, elongation and elaboration. *Developmental Biology, 341*(1), 34-55.

Apelqvist, Å., Ahlgren, U., & Edlund, H. (1997). Sonic hedgehog directs specialised mesoderm differentiation in the intestine and pancreas. *Current Biology*, *7*(10), 801–804.

Archambeault, D. R., Tomaszewski, J., Joseph, A., Hinton, B. T. & Yao, H. H. C. (2009). Epithelial-mesenchymal crosstalk in Wolffian duct and fetal testis cord development. *Genesis 47*, 40-48.

Arias, A. M. (2001). Epithelial mesenchymal interactions in cancer and development. *Cell 105*, 425-431.

Armstrong, B. E., Henner, A., Stewart, S., Stankunas, K. (2017). Shh promotes direct interactions between epidermal cells and osteoblast progenitors to shape regenerated zebrafish bone. *Development, 144,* 1165-1176.

Bagnat, M., Cheung, I. D., Mostov, K. E., & Stainier, D. Y. R. (2007). Genetic control of single lumen formation in the zebrafish gut. *Nature Cell Biology*, *9*, 954.

Bagnat, M., Navis, A., Herbstreith, S., Brand-Arzamendi, K., Curado, S., Gabriel, S., Mostov, K. E., Huisken, J., & Stainier, D. Y. (2010). Cse1l is a negative regulator of CFTR-dependent fluid secretion. *Current Biology 20*, 1840-1845.

Balla, T. (2013). Phosphoinositides: tiny lipids with giant impact on cell regulation. *Physiological Reviews 93*(3), 1019-1137.

Bañón-Rodríguez, I., Gálvez-Santisteban, M., Vergarajauregui, S., Bosch, M., Borreguero-Pascual, A., Martín-Belmonte, F. (2014). EFGR controls IQGAP basolateral membrane localization and mitotic spindle orientation during epithelial morphogenesis. *EMBO Journal 33*(2), 129-145.

Barry, D. M., Koo, Y., Norden, P. R., Wylie, L. A., Xu, K., Wichaidit, C., Azizoglu, D. B., Zheng, Y., Cobb, M. H., Davis, G. E., Cleaver, O. (2016). Rasip1-Mediated Rho GTPase Signaling Regulates Blood Vessel Tubulogenesis via Nonmuscle Myosin II. *Circulation research*, *119*(7), 810–826.

Bayless, K. J. & Davis, G. E. (2002). The Cdc42 and Rac1 GTPases are required for capillary lumen formation in three-dimensional extracelular matrices. *Journal of Cell Science 115*, 1123-1136.

Bergstrahl, D. T., Dawney, N. S., St. Johnston, D. (2017). Spindle orientation: a question of complex positioning. *Development 144*, 1137-1145.

Bernascone, I., González, T., Barea, M. D., Carabaña, C., Hachimi, M., Bosch-Fortea, M., Santamaria, S., Martín, R., Tarnick, J., García-Sanz, J. A. & Martín-Belmonte, F. (2019). Sfrp3 modulates stromal-epithelial crosstalk during mammary gland development by regulating Wnt levels. *Nature Communications 10*(1), 2481.

Bernascone, I. & Martín-Belmonte, F. (2013). Crossroads of Wnt and Hippo in epithelial tissues. *Trends in Cell Biology 23*, 380-389.

Bilder, D. & Perrimon, N. (2000). Localization od apical epitelial determinants by the basolateral PDZ protein Scribble. *Nature 403*, 676-680.

Black Jr., S. A. & Trackman, P. C. (2008). Transforming Growth Factor- β1 (TGFβ1) stimulates connective tissue growth factor (CCN2/CTGF) expression in human gingival fibroblasts through a RhoA-indeendent, Rac1/Cdc42.dependent mechanism. *Journal of Biological Chemistry 283*, 10835-10847.

Booth, A. J. R., Blanchard, G. B., Adams, R. J., & Röper, K. (2014). A Dynamic microtubule cytoskeleton directs medial actomyosin function during tube formation. *Developmental Cell*, *29*(5), 562–576.

Bornens, M. (2008). Organelle positioning and cell polarity. *Nature Reviews Molecular and Cell Biology 9*, 874-886.

Bosch-Fortea, M., Rodríguez-Fraticelli, A. E., Herranz, G., Barea, M. D., Hachimi, M., Young, J., Ladoux, B., & Martín-Belmonte, F. (2019). Micropattern-Based Platform as a Physiologically Relevant Model to study epithelial morphogenesis and nephrotoxicity. *Biomaterials 218*, 119339.

Bosveld, F., Markova, O., Guirao, B., Martin, C., Wang, Z., Pierre, A., Balakireva, M., Gaugue, I., Ainslie, A., Christophorou, N. et al. (2016). Epithelial tricellular junctions act as interphase cell shape sensors to orient mitosis. *Nature 530*, 495-498.

Bovolenta, P., Esteve, P., Ruiz, J. M., Cisneros, E., & Lopez-Rios, J. (2008). Beyond Wnt inhibition: new functions of secreted Frizzled-related proteins in development and disease. *Journal of Cell Science*, *121*(6), 737–746.

Brand, A. H. & Perrimon, N. (1993). Targeted gene expression as a means of altering cell fates and generating dominant phenotypes. *Development 118*, 401-415.

Brennan, D., Chen, X., Cheng, L., Mahoney, M., & Riobo, N. A. (2012). Noncanonical Hedgehog signaling. *Vitamines and Hormones 88*, 55-72.

Briscoe, J. & Thérond, P. P. (2013). The mechanisms of Hedgehog signalling and its roles in development and disease. *Nature Reviews Molecular and Cell Biology 14*, 418-431.

Bryant, D. M., Datta, A., Rodríguez-Fraticelli, A. E., Peränen, J., Martín-Belmonte, F., & Mostov, K. E. (2010). A molecular network for *de novo* generation of the apical surface and lumen. *Nature Cell Biology 12*, 1035-1045.

Buller, N. V., Rosekrans, S. L., Westerlund, J. & van den Brink, G. R. (2012). Hedgehog signaling and maintenance of homeostasis in the intestinal epithelium. *Physiology 27*, 148-155.

Calleja, M., Moreno, E., Pelaz, S. & Morata, G. (1996). Visualization of gene expression in living adult Drosophila. *Science 274*, 252-255.

Cau, J., & Hall, A. (2005). Cdc42 controls the polarity of the actin and microtubule cytoskeletons through two distinct signal transduction pathways. *Journal of Cell Science 118*, 2579-2587.

Chaundry, P., Singh, M., Siddiqi, I., O'Connell, C. L., Zhao, Z. J., & Merchant, A. (2017). Modulating Hedgehog signaling reduces MAPK, TGF-beta, and marrow fibrosis in a transgenic mouse model of JAK2V617F associated myeloproliferative disease. *Blood 130*, 4216.

Chen, X., & Macara, I. G. (2005). Par-3 controls tight junction assembly through the Rac Exchange factor Tiam1. *Nature Cell Biology 7*, 262-269.

Chen, C. M., & Struhl, G. (1999). Wingless transduction by the Frizzled and Frizzled2 proteins of Drosophila. *Development*, *126*(23), 5441–5452.

Chircop, M. (2014). Rho GTPases as regulators of mitosis and cytokinesis in mammalian cells. *Small GTPases 5*, e29770.

Colas, J. F. & Schoenwolf, G. C. (2001). Towards a celular and molecular understanding of neurulation. *Developmental Dynamics 221*(2), 117-145.

Couso, J. P., Bishop, S. A., & Martinez Arias, A. (1994). The wingless signalling pathway and the patterning of the wing margin in Drosophila. *Development*, *120*(3), 621–636.

Couto, A., Mack, N. A., Favia, L., & Georgiou, M. (2017). An apicobasal gradient of Rac activity determines protrusion form and position. *Nature Communications 8*, article 15385.

Crespo, C. L., Vernieri, C., Keller, P. J., Garre, M., Bender, J. R., Wittbrodt, J., & Pardi, R. (2014). The PAR complex controls the spatiotemporal dynamics of F-actin and the MTOC in directionally migrating leukocytes. *Journal of Cell Science 127*, 4381-4395.

Curran, S., Strandkvist, C., Bathmann, J., de Gennes, M., Kabla, A., Salbreux, G., & Baum, B. (2017). Myosin II Controls Junction Fluctuations to Guide Epithelial Tissue Ordering. *Developmental Cell*, *43*(4), 480-492.e6.

Dahan, I., Petrov, D., Cohen-Kfir, E., & Ravid, S. (2014). The tumor supresor Lgl1 forms discrete complexes with NMII-A and Par6alpha-aPKCzeta that are affected by Lgl1 phosphorylation. *Journal of Cell Science 127*, 295-304.

Daly, A. C., Randall, R. A., & Hill, C. S. (2008). Transforming growth factor β-induced Smad1/5 phosphorylation in epithelial cells is mediated by novel receptor complexes and is essential for anchorage-independent growth. *Molecular and Cellular Biology 28*, 6889-6902.

Dasgupta, A., Merkel, M., Clark, M. J., Jacob, A. E., Dawson, J. E., Manning, M. L. & Amack, J. D. (2018). Cell volumen changes contribute to epitelial morphogenesis in zebrafish Kupffer's vesicle. *eLife 7*, e30963.

Davis, G. E. & Bayless, K. J. (2003). An integrin and Rho GTPase-dependent pinocytic vacuole mechanism controls capillary lumen formation in collagen and fibrin matrices. *Microcirculation 10*, 27-44.

Denker, E., Sehring, I. M., Dong, B., Audisso, J., Mathiesen, B., & Jiang, D. (2015). Regulation by a TGF -ROCK-actomyosin axis secures a non-linear lumen expansion that is essential for tubulogenesis. *Development*, *142*(9), 1639–1650.

Dennler, S., Andre, J., Alexaki, I., Li, A., Magnaldo, T., ten Dijke, P., Wang, X. J., Verrecchia, F. & Mauviel, A. (2007). Induction of Sonic hedgehog mediators by transforming growth factor-beta: Smad3-dependent activation og Gli2 and Gli1 expression in vitro and in vivo. *Cancer Research 67*, 6981-6986.

Dennler, S., Andre, J., Verrecchia, F. & Mauviel, A., (2009). Cloning of the human GLI2 promoter: transcriptional activation by transforming growth factor-beta via SMAD3/beta-catenin cooperation. *Journal of Biological Chemistry 284*, 31523-31531.

Desclozeaux, M., Venturato, J., Wylie, F. G., Kay, J. G., Joseph, S. R., Le, H. T., & Stow, J. L. (2008). Active Rab11 and functional recycling endosome are required for E-cadherin trafficking and lumen formation during epitelial morphogenesis. *American Journal of Cell Physiology 295*, 545-556.

di Pietro, F., Echard, A., & Morin, X. (2016). Regulation of mitotic spindle orientation:an integrated view. *EMBO Reports 17*, 1106-1130.

Dow, L. E., Kauffman, J. S., Caddy, J., Zarbalis, K., Peterson, A. S., Jane, S. M., Russell, S. M., & Humbert, P. O. (2007). The tumour-supressor Scriblle dictates cell polarity during directed

epitelial migration: regulation of Rho GTPase recruitment to the leading edge. *Oncogene 26*, 2272-2282.

Drubin, D. G. & Nelson, W. J. (1996). Origins of cell polarity. *Cell 84*, 335-344.

Eaton, S., & Martín-Belmonte, F. (2014). Cargo sorting in the endocytic pathway: a key regulator of cell polarity and tissue dynamics. *Cold Spring Harbor Perspectives in Biology 6*, a016899.

Edlund, S., Landström, M., Heldin, C. H., Aspenström, P. (2002). Transforming growth factor-beta-induced mobilization of actin cytoskeleton requires signaling by small GTPases Cdc42 and RhoA. *Molecular Biology of the Cell 13*(3), 902-914.

Eiraku, M., Takata, N., Ishibashi, H., Kawada, M., Sakakura, E., Okuda, S., Sekiguchi, K., Adachi, T., & Sasai, Y. (2011). Self-organizing optic-cup morphogenesis in three-dimensional culture. *Nature 472*, 51-56.

Elosegui-Artola, A., Oria, R., Chen, Y., Kosmalska, A., Pérez-González, C., Catro, N., Zhu, C., Trepat, X. & Roca-Cusachs, P. (2016). Mechanical regulation of a molecular clutch defines force transmission and transduction in response to matrix rigidity. *Nature Cell Biology 18*(5), 540-548.

Esteve, P., Sandonis, A., Ibanez, C., Shimono, A., Guerrero, I., & Bovolenta, P. (2011). Secreted frizzled-related proteins are required for Wnt/ -catenin signalling activation in the vertebrate optic cup. *Development*, *138*(19), 4179–4184.

Esteve, P., Sandonis, A., Cardozo, M., Malapeira, J., Ibañez, C., Crespo, I., Marcos, S., Gonzalez-Garcia, S., Toribio, M. L., Arribas, J., Shimono, A., Guerrero, I., & Bovolenta, P. (2011). SFRPs act as negative modulators of ADAM10 to regulate retinal neurogenesis. *Nature Neuroscience*, *14*(5), 562–570.

Etienne-Manneville, S., & Hall, A. (2002). Integrin-mediated activation of Cdc42 controls cell polarity in migrating astrocytes through PKCzeta. *Cell 106*, 489-498.

Fanning, A. S., Jameson, B. J., Jesaitis, L. A., Anderson, J. M. (1998). The tight junction protein ZO-1 establishes a link between the transmembrane protein occludin and the actin cytoskeleton. *Journal of Biological Chemistry 273*, 29745-29753.

Feldman, J. L., & Priess, J. R. (2012). A role for the centrosome and PAR-3 in the hand-off of MTOC function during epitelial polarization. *Current Biology 22*, 575-582.

Ferrarelli, L. K. (2019). Revisiting TGF-β and EMT. *Science, 363*(6430), 941-943.

Ferrari, A., Veligodskiy, A., Berge, U., Lucas, M. S. & Kroschewski, R. (2008). ROCK-mediated contractility, tight junctions and channels contribute to the conversión of a preapical patch into apical surface during isochoric lumen initiation. *Journal of Cell Science 121*, 3649-3663.

Fischbarg, J. (2010). Fluid transport across leaky epithelia: central role of the tight junction and supporting role of aquoporins. *Physiological Reviews 90*, 1271-1290.

Fletcher, D. A. & Mullins, R. D. (2010). Cell mechanics and the cytoskeleton. *Nature 463*, 485-492.

Folsch, H. (2008). Regulation of membrane trafficking in polarized epitelial cells. *Current Opinion in Cell Biology 20*, 208-213.

Friedl, P. & Gilmour, D. (2009). Collective cell migration in morphogenesis, regeneration and cancer. *Nature Reviews Molecular and Cell Biology, 10*, 445-457.

Gagné-Sansfaçon, J., Allaire, J. M., Jones, C., Boudreau, F. & Perreault, N. (2014). Loss of Sonic hedgehog leads to alterations in intestinal secretory cell maturation and autophagy. *PLoS ONE 9*(6), e98751.

Gallini, S., Carminati, M., De Mattia, F., Pirovano, L., Martinin, E., Oldani, A., Asteriti, I. A., Guarguaglini, G., & Mapelli, M. (2016). NuMA phosphorylation by Aurora-A orchestrates spindle orientation. *Current Biology 26*(4), 458-469.

Gálvez-Santisteban, M., Rodríguez-Fraticelli, A. E., Bryant, D., Vergarajauregui, S., Yasuda, T., Bañón-Rodríguez, I., Bernascone, I., Datta, A., Spivak, N., Young, K., et al. (2012). Synaptotagmin-like proteins control the formation of a single apical membrane domain in epitelial cells. *Nature Cell Biology 14*, 838-849.

Garrod, D., & Chidgey, M. (2008). Desmosome structure, composition and function. *Biochimica et Biophysica Acta 1778*(3), 572-587.

Gassama-Diagne, A., Yu, W., ter Beest, M., Martín-Belmonte, F., Kierbel, A., Engel, J., & Mostov, K. (2006). Phosphatidylinositol-3,4,5-triphosphate regulates the formation of the basolateral plasma membrane in epithelial cells. *Nature Cell Biology 8*(9), 963-970.

Gays, D., Hess, C., Camporeale, A., Ala, U., Provero, P., Mosimann, C., & Santoro, M. M. (2017). An exclusive cellular and molecular network governs intestinal smooth muscle cell differentiation in vertebrates. *Development*, *144*(3), 464–478.

Georgiou, M., & Baum, B. (2010). Polarity proteins and Rho GTPases cooperate to spatially organise epitelial actin-based protrusions. (2010). *Journal of Cell Science 123*, 1089-1098.

Georgiou, M., Marinari, E., Burden, J., & Baum, B. (2008). Cdc42, Par6, and aPKC regulate Arp2/3-mediated endocitosis to control local adherens junction stability. *Current Biology 18*, 1631-1638.

Gomes, E. R., Jani, S., Gundersen, G. G. (2005). Nuclear movement regulated by Cdc42, MRCK, myosin, and actin flow establishes MTOC polarization in migrating cells. *Cell 121*, 451-463.

Gotta, M., Abraham, M. C., & Ahringer, J. (2001). CDC-42 controls early cell polarity and spindle orientation in *C. elegans*. *Current Biology 11*, 482-488.

Goumans, M. J., Valdimarsdottir, G., Itoh, S., Lebrin, F., Larsson, J., Mummery, C., Karlsson, S., & ten Dijke, P. (2003). Activin receptor-like kinase (ALK)1 is an antagonistic mediator of lateral TGFβ/ALK5 signaling. *Molecular Cell 12*, 817-828

Goumans, M. J., Valdimarsdottir, G., Itoh, S., Rosendahl, A., Sideras, O., ten Dijke, P. (2002). Balancing the activation state of the endothelium via two distinct TGFβ type I receptors. *The EMBO Journal 21*, 1743-1753.

Günzel, D. & Yu, A. S. L. (2013). Claudins and the modulation of tight junction permeability. *Physiological Reviews 93*, 525-569.

Gupta, M., Doss, B. L., Kocgozlu, L., Pan, M., Mège, R.-M., Callan-Jones, A., Voituriez, R. & Ladoux, B. (2019). Cell shape and substrate stiffness drive actin-based cell polarity. *Physical Review E 99*, 012412.

Hales, C. M., Vaerman, J. P., & Goldenring, J. R. (2002). Rab11 family interacting protein 2 associates with myosin Vb and regulates plasma membrane recycling. *The Journal of Biological Chemistry 277*, 50415-50421.

Hall, A. (1998). Rho GTPases and the actin cytoskeleton. *Science 279*, 509.

Hao, Y., Du, Q., Chen, X., Zheng, Z., Balsbaugh, J. L., Maitra, S. Shabanowitz, J., Hunt, D. F. & Macara, I.G. (2010). Par3 controls epitelial spindle orientation by aPKC-mediated phosphorylation of apical pins. *Current Biology 20*, 1809-1818.

Hao, Y., Quansheng, D., Chen, X., Zheng, Z., Balsbaugh, J. L., Maitra, S., Shabanowitz, J., Hunt, D. F. & Macara, I. G. (2011). Par3 controls spindle pole orientation in epitelial cells by aPKC-mediated phosphorylation of pins at the apical cortex. *Current Biology 20*(20), 1809-1818.

Hartl, T. A., & Scott, M. P. (2014). Wing tips: the wing disc as a platform for studying Hedgehog signaling. *Methods 68*, 199-206.

Heisenberg, C. P. & Bellaïche, Y. (2013). Forces in tissue morphogenesis and patterning. *Cell 153*, 948-962.

Hellstrom, M., Kalen, M., Lindahl, P., Abramsson, A. & Betsholtz, C. (1999). Role of PDGF-B and PDGFR-beta in recruitment of vascular smooth muscle cells and pericytes during embryonic blood vessel formation in the mouse. *Development 126*, 3047-3055.

Herwig, L., Blum, Y., Krudewig, A., Ellertsdottir, E., Lenard, A., Belting, H. G., & Affolter, M. (2011). Distinct celular mechanisms of blood vessel fusión in the zebrafish embryo. *Current Biology 21*, 1942-1948.

Hogan, B. L. M., & Kolodziej, P. A. (2002). Organogenesis: molecular mechanisms of tubulogenesis. *Nature Reviews Genetics 3*, 513-523.

Hoijman, E., Rubbini, D., Colombelli, J. & Alsina, B. (2015). Mitotic cell rounding and epitelial thinning regulate lumen growth and shape. *Nature Communications 6*, 7355.

Howard, B. A. & Lu, P. (2014). Stromal regulation of embryonic and postanal mammary epitelial development and differentiation. *Seminars in Cell and Developmental Biology 25-26*, 43-51.

Huang, W., Sherman, B. T., & Lempicki, R. A. (2009). Bioinformatics enrichment tolos: paths toward the comprehensive functional analysis of large gene lists. *Nucleic Acids Research 37*, 1-13.

Huang, W., Sherman, B. T. & Lempicki, R. A. (2009). Systematic and integratve analysis of large gene lists using DAVID bioinformatics resources. *Nature Protocols 4*, 44-57.

Huang, P., Xiong, F., Megason, S. G. and Schier, A. F. (2012). Attenuation of Notch and Hedgehog signaling is required for fate specification in the spinal cord. *PLoS Genetics. 8*, e1002762.

Hynes, N. E. & Watson, C. J. (2010). Mammary gland growth factors: roles in normal development and in cancer. *Cold Spring Harbor Perspectives in Biology 2*, a003186.

Iden, S., & Collard, J. G. (2008). Crosstalk between small GTPases and polarity proteins in cell polarization. *Nature Reviews Molecular Cell Biology 9*, 846-859.

Ingham, P. W., & Placzek, M. (2006). Orchestrating ontogenesis: variations on a theme by sonic hedgehog. *Nature Reviews Genetics 7*, 841-850.

Iruela-Arispe, M. L. & Beitel, G. J. (2013). Tubulogenesis. *Development 140*(14), 2851-2855.

Ivanov, A. I., McCall, I. C., Parkos, C. A., Nusrat, A. (2004). Role for actin filament turnover and a myosin II motor in cytoskeleton-driven disassembly of the epithelial apical junctional complex. *Molecular Biology of the Cell 15*, 2639-2651.

Jacquemet, G., Hamidi, H., & Ivaska, J. (2015). Filopodia in cell adhesion, 3D migration and cancer cell invasion. *Current Opinion in Cell Biology 36*, 23-31.

Jarde, T. & Dale, T. (2012). Wnt signalling in murine postnatal mammary gland development. *Acta Physiologica 204*, 118-127.

Jaffe, A. B., Kaji, N., Durgan, J., & Hall, A. (2008). Cdc42 controls spindle orientation to position the apical surface during epithelial morphogenesis. *Journal of Cell Biology 183*, 625-633.

Joberty, G., Petersen, C., Gao, L., Macara, I. G. (2000). The cell-polarity protein Par6 links Par3 and atypical protein kinase C to Cdc42. *Nature Cell Biology 2*, 531-539.

Jung, J.-J., Inamdar, S. M., Tiwari, A., Ye, D., Lin, F., & Choudhury, A. (2013). Syntaxin 16 regulates lumen formation during epithelial morphogenesis. *PLoS ONE 8*, e61857.

Kage, F., Winterhoff, M., Dimchev, V., Mueller, J., Thalheim, T., Freise, A., Brühmann, S., Kollasser, J., Block, J., Dimchev, et al. (2017). FMNL formins boost lamellipodia force generation. *Nature Communications 8*, 14832.

Katoh, Y. & Katoh, M. (2005). Hedgehog signaling pathway and gastric cancer. *Cancer Biology and Therapy 4,* 1050-1054.

Kim, D., Langmead, B., Salzberg, S. L. (2015). HISAT: a fast spliced aligner with low memory requirements. *Nature Methods 12*, 357-360.

Kim, M., Shewan, A. M., Ewald, A. J., Werb, Z., & Mostov, K. E. (2015). p114RhoGEF governs cell motility and lumen formation during tubulogenesis through a ROCK-myosin-II pathway. *Journal of Cell Science 128*(23), 4317-4327.

Knust, E., & Bossinger, O. (2002). Composition and formation of intracellular junctions in epithelial cells. *Science 298*, 1955-1959.

Kolterud, A., Grosse, A. S., Zacharias, W. J., Walton, K. D., Kretovich, K. E., Madison, B. B., Waghray, M., Ferris, J. E., Hu, C., Merchant, J. L., et al. (2009). Paracrine hedgehog signaling in stomach and intestine: new roles for hedgehog in gastrointestinal patterning. *Gastroenterology, 137*(2), 618-628.

Komiya, Y. & Habas, R. (2008). Wnt signal transduction pathways. *Organogenesis 4*(2), 68-75.

König, D., Page, L., Chassot, B., Jazwinska, A. (2018). Dynamics of actinotrichia regeneration in the adult zebrafish fin. *Developmental Biology, 433*(2), 416-432.

Kosinski, C., Stange, D. E., Xu, C., Chan, A. S., Ho, C., Yuen, S: T., Mifflin, R. C., Powell, D. W., Clevers, H., Leung, S. Y. & Chen, X. (2010). Indian hedgehog regulates intestinal stem cell fate through epithelial-mesenchymal interactions during development. *Gastroenterology 139*, 893-903.

Kotak, S. & Gönczy, P. (2013). Mechanisms of spindle positioning: cortical force generators in the limelight. *Current Opinion in Cell Biology 25*(6), 741-748.

Kovacs, E. M., Verma, S., Ali, R. G., Ratheesh, A., Hamilton, N. A., Akhmanova, A., & Yap, A. S. (2011). N-WASP regulates the epithelial junctional actin cytoskeleton through a non-canonical post-nucleation pathway. *Nature Cell Biology 13*, 934-943.

Krueger, D., Quinkler, T., Mortensen, S. A., Sachse, C. & De Renzis, S. (2019). Cross-linker—mediated regulation of actin network organization controls tissue morphogenesis. *Journal of Cell Biology*, jbc.201811127.

Krupinski, T. & Beitel, G. J. (2009). Unexpected roles of the Na-K-ATPase and other ion transporters in cell junctions and tubulogenesis. *Physiology, 24*, 192-201.

Lapierre, L. A., Avant, K. M., Caldwell, C. M., Oztan, A., Apodaca, G., Knowles, B. C., Roland, J. T., Ducharme, N. A., & Goldenring, J. R. (2012). Phosphoryltion of Rab11-FIP2 regulates polarity in MDCK cells. *Molecular Biology of the Cell 23*, 2302-2318.

Lázaro-Diéguez, F., Cohen, D., Fernández, D., Hodgson, L., van IJzendoorn, S. C. D., & Müsch, A. (2013). Par1b links lumen polarity with LGN-NuMA ositioning for distinct epithelial cell division phenotypes. The Journal of Cell Biology 203(2), 251-264.

Lapierre, L. A., Kumar, R., Hales, C. M., Navarre, J., Bhartur, S. G., Burnette, J. O., Provance, D. W., Mercer, J. A, Bahler, M. & Goldenring, J. R. (2001). Myosin Vb is associated with plasma membrane recycling systems. *Molecular Biology of the Cell 12*, 1843-1857.

Le, J., Zhang, D. Y., Zhao, Y., Qiu, W., Wang, P. & Sun, Y. (2016). ITF promotes migration of intestinal epithelial cells through crosstalk between ERK and JAK/STAT3 pathways. *Scientific Reports 6*, 33014.

Lecuit, T., & Lenne, P. F. (2007). Cell surface mechanics and the control of cell shape, tissue patterns and morphogenesis. *Nature Reviews Molecular and Cell Biology 8*, 633-644.

Lemmers, C., Michel, D., Lane-Guermonprez, L., Delgrossi, M. H., Medina, E., Arsanto, J. P., Le Bivic, A. (2004). CRB3 binds directly to Par6 and regulates the morphogenesis of the tight junctions in mammalian epithelial cells. *Molecular Biology of the Cell 15*, 1324-1333.

Levental, K. R., Yu, H., Kass, L., Lakins, J. N., Egeblad, M., Erler, J. T., Fong, S. F., Csiszar, K., Giaccia, A., Weninger, W., et al. (2009). Matrix crosslinking forces tumor progression by enhancing integrin signaling. *Cell 139*, 891-906.

Leyns, L., Bouwmeester, T., Kim, S. H., Piccolo, S. & De Robertis, E. M. (1997). Frzb-1 is a secreted antagonist of Wnt signaling expressed in the Spemann organizer. *Cell 88*, 747-756.

Li, M. O. & Flavell, R. A. (2008). TGFβ: a master of all T cell trades. *Cell 134*, 392-404.

Lin, K, Wang, S., Julius, M. A., Kitajewski, J., Moos, M. Jr. & Luyten, F. P. (1997). The cysteine-rich frizzled domain of Frzb-1 is required and sufficient for modulation of Wnt signaling. *Proceedings of the National Academy of Sciences of the United States of America 94*(21), 11196-11200.

Llense, F., & Etienne-Manneville, S. (2015). Front-to-rear polarity in migrating cells. In: Ebnet, K. (eds) Cell Polarity 1. Springer, Cham.

Logan, C. Y. & Nusse, R. (2004). The Wnt signaling pathway in development and disease. *Annual Review of Cell and Developmental Biology 20*, 781-810.

Love, M. I., Huber, W., & Anders, S. (2014). Moderated estimation of fold change and dispersion for RNA-seq data with DESeq2. *Genome Biology 15*, 550.

Lowery, L. A. & Sive, H. (2005). Initial formation of zebrafish brain ventricles occurs independently of circulation and requires the nagie oko and snakehead/atp1a1a.1 gene product. *Development, 132*, 2057-2067.

Luján, P., Varsano, G., Rubio, T., Hennrich, M. L., Sachsenheimer, T., Gálvez-Santisteban, M., Martín-Belmonte, F., Claude-Gavin, A., Brügger, B. & Köhn. (2016). PRL-3 disrupts epithelial

architecture by altering the post-mitotic midbody position. *Journal of Cell Science 129*, 4130-4142.

Macara, I. G. (2004). Parsing the polarity code. *Nature Reviews Molecular Cell Biology 5*, 220-231.

Madison, B. B., Braunstein, K., Kuizon, E., Portman, K., Qiao, X. T. & Gumucio, D. L. (2005). Epithelial hedgehog signals pattern the intestinal crypt-villus axis. *Development 132*(2), 279-289.

Madrid, R., Aranda, J. F., Rodríguez-Fraticelli, A. E., Ventimiglia, L., Andrés-Delgado, L., Shehata, M., Fanayan, S., Shahheydari, H., Gomez, S., Jimenez, A., et al. (2010). The formin INF2 regulates basolateral-to-apical transcytosis and lumen formation in association with Cdc42 and MAL2. *Developmental Cell 18*, 814-827.

Mammoto, T., & Ingber, D. E. (2010). Mechanical control of tissue and organ development. *Development*, *137*(9), 1407–1420.

Mao, J., Kim, B. M., Rajurkar, M., Shivdasani, R. A., & McMahon, A. P. (2010). Hedgehog signaling controls mesenchymal growth in the developing mammalian digestive tract. *Development*, *137*(10), 1721–1729.

Margolis, B. & Borg, J. P. (2005). Apicobasal polarity complexes. *Journal of Cell Science 118*, 5157-5159.

Martin, A. C., Kaschube, M. & Wieschaus, E. F. (2009). Pulsed contractions of an actin-myosin network drive apical constriction. *Nature 457*, 495-499.

Martín-Belmonte, F., Gassama, A., Datta, A., Yu, W., Rescher, U., Gerke, V., & Mostov, K. (2007). PTEN-mediated apical segregation of phosphoinositides controls epithelial morphogenesis through Cdc42. *Cell 128*, 383-397.

Martín-Belmonte, F., & Mostov, K. (2007). Phosphoinositides control epithelial development. *Cell Cycle 6*, 1957-1961.

Martín-Belmonte, F. & Mostov, K. (2008). Regulation of cell polarity during epithelial morphogenesis. *Current Opinion in Cell Biology 20*, 227-234.

Martín-Belmonte, F., Pérez-Moreno, M. (2012). Epithelial cell polarity, stem cells and cancer. *Nature Reviews Cancer 12*(1), 23-38.

Massagué, J. (2008). TGFβ in cancer. *Cell 134*, 215-230.

Massagué, J. (2012). TGFβ signalling in context. *Nature Reviews Molecular Cell Biology 13*, 616-630.

Matusek, T., Wendler, F., Polès, S., Pizette, S., D'Angelo, G., Fürthauer, M. & Thérond, P. P. (2014). The ESCRT machinery regulates the secretion and long-range activity of Hedgehog. *Nature 516*, 99-103.

Mayor, R. & Etienne-Manneville, S. (2016). The front and rear of collective cell migration. *Nature Reviews Molecular and Cell Biology 17*, 97-109.

Mayor, R. & Theveneau, E. (2013). The role of the non-canonical Wnt-planar cell polarity pathway in neural crest migration. *Biochemical Journal 457*(1), 19-26.

McMahon, A. P., Ingham, P. W. & Tabin, C. J. (2003). Developmental roles and clinical significance of hedgehog signaling. *Current Topics in Developmental Biology 53,* 1-114.

Mechlin, C. W., Tanner, M. J., Chen, M., Buttyan, R., Levin, R. M. & Mian, B. M. (2010). Gli2 expression and human bladder transitional carcinoma cell invasiveness. *Journal of Urology 184*, 344-351.

Meder, D., Sevchenko, A., Simons, K. & Füllekrug, J. (2005). Gp135/podocalyxin and NHERF-2 participate in the formation of a preapical domain during polarization of MDCK cells. *Journal of Cell Biology 168*, 303-313.

Mellman, I. & Nelson, W. J. (2008). Coordinated protein sorting, targeting and distribution in polarized cells. Nature Reviews Molecular Cell Biology 9, 833-845.

Metzger, R. J. & Krasnow, M. A. (1999). Genetic control of branching morphogenesis. *Science 284*, 1635-1639.

Mii, Y. & Taira, M. (2009). Secreted Frizzled-related proteins enhance the diffusion of Wnt ligands and expand their signaling range. *Development 136*(24), 4083-4088.

Mitsushima, M., Toyoshima, F., & Nishida, E. (2009). Dual role of Cdc42 in spindle orientation control of adherent cells. *Molecular and Cellular Biology 29*(10), 2816-2827.

Montesano, R., Schaller, G., & Orci, L. (1991). Induction of epithelial tubular morphogenesis in vitro by fibroblast-derived soluble factors. *Cell 66*, 697-711.

Mosaliganti, K. R., Swinburne, I. A., Chan, C. U., Obholzer, N. D., Green, A. A., Tanksale, S., Mahadevan, L. & Megason, S. G. (2018). Size control of the inner ear via hydraulic feedback. *BioRxiv*, 349381.

Mullen, A. C., Orlando, D. A., Newman, J. J., Lovén, J., Kumar, R. M., Bilodeau, S., Reddy, J., Guenther, M. G., DeKoter, R. P. & Young, R. A. (2011). Master transcription factors determine cell-type-specific responses to TGFβ signaling. *Cell 147*, 565-576.

Mu, Y., Gudey, S. K. & Landstrom, M. Non-Smad signaling pathways. *Cell and Tissue Research 347*, 11-20.

Munjal, A., & Lecuit, T. (2014). Actomyosin networks and tissue morphogenesis. *Development*, *141*(9), 1789–1793.

Murakami, S., Nifuji, A., & Noda, M. (1997). Expression of Indian hedgehog in osteoblasts and its posttranscriptional regulation by transforming growth-factor-beta. *Endocrinology 138*, 1972-1978.

Mythreye, K. & Blobe, G. C. (2009). The type III TGFβ receptor regulates epithelial and cancer cell migration through β-arrestin2-mediated activation of Cdc42. *Proceedings of the National Academy of Sciences of the United States of America 106*(20), 8221-8226.

Nakamura, Y., de Paiva Alves, E., Veenstra, G. J. C. & Hoppler, S. (2016). Tissue- and stage-specific Wnt target gene expression is controlled subsequent to β-catenin recruitment to cis-regulatory modules. *Development 143*, 1914-1925.

Nakaya, Y. & Sheng, G. (2013). EMT in developmental morphogenesis. *Cancer Letters 341*, 9-15.

Navarro, C., Nola, S., Audebert, S., Santoni, M. J., Arsanto, J. P., Ginestier, C., Marchetto, S., Jacquemier, J., Isnardon, D., Le Bivic, A., et al. (2005). Junctional recruitment of mammalian Scribble relies on E-cadherin engagement. *Oncogene 24*, 4330-4339.

Navis, A., Marjoram, L. & Bagnat, M. (2013). Cftr controls lumen expansión and function of Kupffer's vesicle in zebrafish. *Development 140*, 1703-1712.

Nelson, W. J. (2003). Adaptation of core mechanisms to generate cell polarity. *Nature 422*, 766-774.

Nelson, W. J. (2009). Remodeling epitelial cell organization: transitions between front-rear and apical-basal polarity. *Cold Spring Harbor Perspectives in Biology, 1*(1), a000513.

Neumann, C. J., & Cohen, S. M. (1997). Long-range action of Wingless organizes the dorsal-ventral axis of the *Drosophila* wing. *Development, 124*(4), 871–880.

Ng, A. N. Y., De Jong-Curtain, T. A., Mawdsley, D. J., White, S. J., Shin, J., Appel, B., Si Dong, P. D., Stainier, D. Y. R., Heath, J. K. (2005). Formation of the digestive system in zebrafish: III. Intestinal epithelium morphogenesis. *Developmental Biology*, *286*(1), 114–135.

Nguyen-Ngoc, K. V., Shamir, E. R., Huebner, R.J., Beck, J. N., Cheung, K. J., & Ewald, A. J. (2015). 3D culture assays of murine mammary branching morphogenesis and epitelial invasión. *Methods in Molecular Biology 1189*, 135-162.

Nielsen, J. S., & McNagny, K. M. (2008). Novel functions of the CD34 family. *Journal of Cell Science 121*, 3683-3692.

Nielsen, C. M., Williams, J., van den Brink, G. R., Lauwers, G. Y. & Roberts, D. J. (2004). Hh pathway expression in human gut tissues and in inflammatory gut diseases. *Laboratory Investigation 84*, 1631-1642.

Nishimura, T. & Kaibuchi, K. (2007). Numb controls integrin endocytosis for directional cell migration with aPKC and PAR-3. *Developmental Cell, 13*(1), 15-28.

Nobes, C. D. & Hall, A. (1995). Rho, Rac, and Cdc42 GTPass regulate the assembly of multimolecular focal complexes associated with actin stress fibers, lamellipodia, and filopodia. *Cell 81*, 53-62.

Nolo, R., Abbott, L. A., & Bellen, H. J. (2000). Senseless, a Zn finger transcription factor, is necessary and sufficient for sensory organ development in *Drosophila*. *Cell*, *102*, 349–362.

Nüsslein-Volhard, C. & Wieschaus, E. (1980). Mutations affecting segment number and polarity in Drosophila. *Nature 287*, 795-801.

O'Brien, L. E., Jou, T. S., Pollack, A. L., Zhang, Q., Hansen, S. H., Yurchenco, P. & Mostov, K. E. (2001). Rac1 orientates epithelial apical polarity through effects on basolateral laminin assembly. *Nature Cell Biology 3*, 831-838.

Otani, T., Ichii, T., Aono, S. & Takeichi, M. (2006). Cdc42 GEF Tuba regulates the junctional configuration of simple epithelial cells. *Journal of Cell Biology 175*, 135-146.

Ozdamar, B., Bose, R., Barrios-Rodiles, M., Wang, H. R., Zhang, Y., & Wrana, J. L. (2005). Regulation of the polarity protein Par6 by TGFβ receptors controls epithelial cell plasticity. *Science 307*, 1603-1609.

Pak, E., & Segal, R. A. (2016). Hedgehog signal transduction: key players, oncogenic drivers and cancer therapy. *Developmental Cell 38*(4), 333-344.

Papusheva, E. & Heisenberg, C. P. (2010). Spatial organization of adhesion: force-dependent regulation and function in tissue morphogenesis. *EMBO Journal 29*(16), 2753-2768.

Pașca, S. P. (2019). Assembling human brain organoids. *Science 363*, 126-127.

Pfaffl, M. W. (2001). A new mathematical model for relative quantification in real-time RT-PCR. *Nucleic Acids Research 29(*9), e45.

Pollack, A. L., Runyan, R. B. & Mostov, K. E. (1998). Morphogenetic mechanisms of epithelial tubulogenesis: MDCK cell polarity is transiently rearranged without loss of cell-cell contact during scatter factor/hepatocyte growth factor-induced tubulogenesis. *Developmental Biology 204*(1), 64-79.

Prager-Khoutorsky, M., Lichtenstein, A., Krishnan, R., Rajendran, K., Mayo, A., Kam, Z., Geiger, B. & Bershadsky, A. D. (2011). Fibroblast polarization is a matrix-rigidity-dependent process controlled by focal adhesion mechanosensing. *Nature Cell Biology 13*(12), 1457-1465.

Qin, Y., Meisen, W. H., Hao, Y. & Macara, I. G. (2010). Tuba, a Cdc42 GEF, is required for polarized spindle orientation during epithelial cyst formation. *Journal of Cell Biology 189*(4), 661-669.

Quint, E., Smith, A., Avaron, F., Laforest, L., Miles, J., Gaffield, W., Akimenko, M. A. (2002). Bone patterning is altered in the regenerating zebrafish caudal fin after ectopic expression of sonic hedgehog and bmp2b or exposure to cyclopamine. *Proceedings of the National Academy of Sciences of the United States, 99,* 8713-8718.

Ramachandran, A., Vizán, P., Das, D., Chakravarty, P., Vogt, J., Rogers, K. W., Müller, P., Hinck, A. P., Sapkota, G. P. & Hill, C. S. (2018). TGF-β uses a novel mode of receptor activation to phosphorylate SMAD1/5 and induce epithelial-to-mesenchymal transition. *Elife*, e31756.

Ramalho-Santos, M., Melton, D. A., & McMahon, A. P. (2000). Hedgehog signals regulate multiple aspects of gastrointestinal development. *Development*, *127*(12), 2763–2772.

Rauzi, M., Lenne, P.-F., & Lecuit, T. (2010). Planar polarized actomyosin contractile flows control epithelial junction remodelling. *Nature*, *468*, 1110.

Ravid, S. (2014). The tumor supresor Lgl1 regulates front-rear polarity of migrating cells. *Cell Adhesion & Migration 8*, 378-383.

Reid, S. E., Kay, E. J., Neilson, L. J., Henze, A. T., Serneels, J., McGhee, E. J., Shayade, S., Nixon, C., Mackey, J. B. G., Santi, A., et al. (2017). Tumor matrix stiffness promotes metastatic cancer cell interaction with the endothelium. *EMBO Journal 36*(16), 2373-2389.

Ribatti, D. & Santoiemma, M. (2014). Epithelial-mesenchymal interactins: a fundamental Developmental Biology mechanism. *International Journal of Developmental Biology 58*, 303-306.

Ridley, A. J. (2015). Rho GTPase signalling in cell migration. *Current Opinion in Cell Biology 36*, 103-112.

Roberts, D. J., Johnson, R. L., Burke, A. C., Nelson, C. E., Morgan, B. A., & Tabin, C. (1995). Sonic hedgehog is an endodermal signal inducing Bmp-4 and Hox genes during induction and regionalization of the chick hindgut. *Development*, *121*(10), 3163–3174.

Rodríguez-Boulan, E., & Macara, I. G. (2014). Organization and execution of the epithelial polarity program. *Nature Reviews Molecular and Cell Biology 6*, 233-247.

Rodríguez-Fraticelli, A. E., Auzan, M., Alonso, M. A., Bornens, M., & Martín-Belmonte, F. (2012). Cell confinement controls centrosome positioning and lumen initiation during epithelial morphogenesis. *Journal of Cell Biology 198*, 1011-1023.

Rodríguez-Fraticelli, A. E. & Martín-Belmonte, F. (2013). Methods for analysis of apical lumen trafficking using micropatterned 3D systems. In Franck Perez and David J. Stephens, editors: *Methods in Cell Biology,* Vol. 118, Burlington: Academic Press, pp. 105-123.

Rodríguez-Fraticelli, A. E., Vergarajauregui, S., Eastburn, D. J., Datta, A., Alonso, M. A., Mostov, K. E., & Martín-Belmonte, F. (2010). The Cdc42 GEF Intersectin 2 controls mitotic spindle orientation to for the lumen during epithelial morphogenesis. *The Journal of Cell Biology 189*, 725-738.

Roland, J. T., Bryant, D. M., Datta, A., Itzen, A., Mostov, K. E., & Goldenring, J. R. (2011). Rab GTPase-Myo5B complexes control membrane recycling and epithelial polarization. *Proceedings of the National Academy of Sciences of the United States 108*, 2789-2794.

Rorth, P. (2009). Collective cell migration. *Annual Review of Cell and Developmental Biology, 25*, 407-429.

Ross, J. L., Ali, M. Y., Warshaw, D. M. (2008). Cargo transport: molecular motors navigate a complex cytoskeleton. *Current Opinion in Cell Biology 20*, 41-47.

Rottner, K., Faix, J., Bogdan, S., Linder, S., & Kerkhoff, E. (2017). Actin assembly mechanisms at a glance. *Journal of Cell Science 130*, 3427-3435.

Sakisaka, T., Ikeda, W., Ogita, H., Fujita, N., & Takai, Y. (2007). The roles of nectins in cell adhesions: Cooperation with other cell adhesion molecules and growth factor receptors. *Current Opinion in Cell Biology 19*, 593-602.

Samuel, M. S., López, J. I., McGhee, E. J., Croft, D. R., Strachan, D., Timpson, P., Munro, J., Schroeder, E., Zhou, J., Brunton, V. G., et al. (2011). Actomyosin-mediated cellular tension drives increased tissue stiffness and beta-catenin activation to induce epidermal hyperplasia and tumor growth. *Cancer Cell 19*, 776-791.

Sato, T., Vries, R. G., Snippert, H. J., van de Wetering, M., Barker, N., Stange, D. E., van Es, J. H., Abo, A., Kujala, P., Peters, P. J., et al. (2009). Single Lgr5 stem cells build crypt-villus structures in vitro without a mesenchymal niche. *Nature 459*, 262-265.

Seiler, C., Davuluri, G., Abrams, J., Byfield, F. J., Janmey, P. A., & Pack, M. (2012). Smooth Muscle Tension Induces Invasive Remodeling of the Zebrafish Intestine. *PLoS Biology*, *10*(9).

Shannon, J. M., & Hyatt, B. A. (2004). Epithelial-Mesenchymal Interactions in the Developing Lung. *Annual Review of Physiology*, *66*(1), 625–645.

Shao, M. Y., Cheng, R., Wang, F. M., Yang, H., Cheng, L. & Hu, T. (2013). B-catenin and Rho GTPases as downstream targets of TGF-β1 during pulp repair. *Cell Biology International 35*(2), 105-109.

Sharma, R. P. & Chopra, V. L. (1976). Effect of the Wingless (wg1) mutation on wing and haltere development in Drosophila melanogaster. *Developmental Biology 48*, 461-465.

Shin, K., Straight, S., Margolis, B. (2005). PATJ regulates tight junction formation and polarity in mammalian epithelial cells. *Journal of Cell Biology 168*, 705-711.

Shyer, A. E., Tallinen, T., Nerurkar, N. L., Wei, Z., Gil, E. S., Kaplan, D. L., Tabin, C. J. & Mahadevan, L. (2013). Villification: how the gut gets its villi. *Science 342*, 212-218.

Schmoranzer, J., Fawcett, J. P., Segura, M., Tan, S., Vallee, R. B., Pawson T., & Gundersen, G. G. (2009). Par3 and dynein associate to regulate local microtubule dynamics and centrosome orientation during migration. *Current Biology 19*, 1065-1074.

Schneeberger, K., Roth, S., Nieuwenhuis, E. E. S., & Middendorp, S. (2018). Intestinal epithelial cell polarity defects in disease: lessons from microvillus inclusion disease. *Disease Models & Mechanisms 11*(2), dmm031088.

Schöck, F. & Perrimon, N. (2002). Molecular mechanisms of epithelial morphogenesis. *Annual Review of Cell and Developmental Biology 18*, 463-493.

Sit, S. T., & Manser, E. (2011). Rho GTPases and their role in organizing the actin cytoskeleton. *Journal of Cell Science 124*, 679-683.

Small, J. V., Stradal, T., Vignal, E. & Rottner, K. (2002). The lamellipodium: where motility begins. *Trends in Cell Biology 12*, 112-120.

Stein, M. P., Wandinger-Ness, A., & Roitbak, T. (2002). Altered trafficking and epithelial cell polarity in disease. *TRENDS in Cell Biology 12*(8), 374-381.

Sternlicht, M. D., Kouros-Mehr, H., Lu, P. & Werb, Z. (2006). Hormonal and local control of mammary branching morphogenesis. *Differentiation 74,* 365-381.

Sukegawa, A., Narita, T., Kameda, T., Saitoh, K., Nohno, T., Iba, H., Yasugi, S. & Fukuda, K. (2000). The concentric structure of the developing gut is regulated by Sonic hedgehog derived from endodermal epithelium. *Development 127*, 1971-1980.

Suzuki, A., Yamanaka, T., Hirose, T., Manabe, N., Mizuno, K., Shimizu, M., Akimoto, K., Izumi, Y., Ohnishi, T., Ohno, S. (2001). Atypical protein kinase C is involved in the evolutionarily conserved par protein complex and plays a critical role in establishing epithelia-specific junctional structures. *Journal of Cell Biology 152*, 1183-1196.

Swarup, A. & Verheyen, E. M. (2012). Wnt/Wingless signaling in *Drosophila*. *Cold Spring Harbor Perspectives in Biology 4*(6), a007930.

Takasato, M., & Little, M. H. (2016). A strategy for generating kidney organoids: Recapitulating the development in human pluripotent stem cells. *Developmental Biology 420*, 210-220.

Tanentzapf, G. & Tepass, U. (2003). Interactions between the crumbs, lethal giant larvae and bazooka pathways in epithelial polarization. *Nature Cell Biology 5*, 46-52.

Tanimoto, H., Itoh, S., ten Dijke, P., & Tabata, T. (2000). Hedgehog creates a gradient of DPP activity in Drosophila wing imaginal discs. *Molecular Cell 5*, 59-71.

Tepass, U. (2012). The apical polarity protein network in Drosophila epithelial cells: regulation of polarity, junctions, morphogenesis, cell growth, and survival. *Annual Reviews in Cell and Developmental Biology 28*, 655-685.

Théry, M. (2010). Micropatterning as a tool to decipher cell morphogenesis and functions. *Journal of Cell Science 123*(24), 4201-4213.

Thiery, J. P., Acloque, H., Huang, R. Y. J. & Nieto, M. A. (2009). Epithelial-mesenchymal transitions in development and disease*. Cell 139*, 871-890.

Ungefroren, H., Witte, D., Lehnert, H. (2018). The role of small GTPases of the Rho/Rac family in TGF-β-induced EMT and cell motility in cancer. *Developmental Dynamics 247*(3), 451-461.

Üren, A., Reichsman, F., Anest, V., Taylor, W. G., Muraiso, K., Bottaro, D. P., Cumberledge, S. & Rubin, J. S. (2000). Secreted frizzled-related protein-1 binds directly to wingless and is a biphasic modulator of Wnt signaling. *Journal of Biological Chemistry*, *275*(6), 4374–4382.

van den Brink, G. R. (2007). Hedgehog signaling in development and homeostasis of the gastrointestinal tract. *Physiological Reviews 87*, 1343-1375.

Van Dop, W. A. & van den Brink, G. R. (2010). Sonic hedgehog: a link between inflammation, gastric atrophy and acid supression. *Gastroenterology 138*, 426-429.

Vardouli, L., Vasilaki, E., Papadimitriou, E., Kardassis, D. & Stournaras, C. (2008). A novel mechanism of TGFbeta-induced actin reorganizaton mediated by Smad proteins and Rho GTPases. *The FEBS Journal 275*(16), 4074-4087.

Vinzenz, M., Nemethova, M., Schur, F., Mueller, J., Narita, A., Urban, E., Winkler, C., Schmeiser, C., Koestler, S. A., & Rottner, K. (2012). Actin branching in the initiation and maintenance of lamellipodia. *Journal of Cell Science* 125, 2775-2785.

Viñals, F. & Pouysségur, J. (2001). Transforming growth factor β1 (TGF-β1) promotes endotelial cell survival during in vitro angiogénesis via an autocrine mechanism implicating TGF-α signaling.

Volckaert, T. & De Langhe, S. P. (2015). Wnt and FGF mediated epitelial-mesenchymal crosstalk during lung development. *Developmental Dynamics 244*, 342-366.

Wallace, K. N., Dolan, A. C., Seiler, C., Smith, E. M., Yusuff, S., Chaille-Arnold, L., Judson, B., Sierk, R., Yengo, C., Sweeney, H. L., Pack, M. (2005). Mutation of smooth muscle myosin causes epithelial invasion and cystic expansion of the zebrafish intestine. *Developmental Cell*, *8*(5), 717–726.

Walsh, M., Ampasala, D. R., Rishi, A. K., & Basson, M. D. (2008). TGF-β1 modulates focal adhesión kinase expression in rat intestinal epitelial IEC-6 cells via stimulatory and inhibitory Smad binding elements. *Biochimica et Biophysica Acta 1789*(2), 88-98.

Walton, K. D., Kolterud, A., Czerwinski, M. J., Bell, M. J., Prakash, A., Kushwaha J., Grosse, A. S., Schnell S., & Gumucio, D. L. (2012). Hedgehog-responsive mesenchymal clusters direct patterning and emergence of intestinal villi. *Proceedings of the National Academy of Sciences of the United States 109*(39), 15817-15822.

Wang, J., Cao, J., Dickson, A. L. & Poss, K. D. (2015). Epicardial regeneration is guided by cardiac outflow tract and Hedgehog signalling. *Nature 522*, 226-230.

Wang, S., Jayaram, S. A., Hemphälä, J., Senti, K. A., Tsarouhas, V., Jin, H., & Samakovlis, C. (2006). Septate-junction-dependent luminal deposition of chitin deacetylases restricts tube elongation in the *Drosophila* trachea. *Current Biology 16*(2), 180-185.

Wang, S., Krinks, M., Lin, K., Luyten, F. P. & Moos, M. Jr. (1997). Frzb, a secreted protein expressed in the Spemann organizer, binds and inhibits Wnt-8. *Cell 88*(6), 757-766.

Wang, Q., & Margolis, B. (2007). Apical junctional complexes and cell polarity. *Kidney International 72*(12), 1448-1458.

Wang, X., Zhao, Z., Muller, J., Iyu, A., Khng, A. J., Guccione, E., Ruan, Y., Ingham, P. W. (2013). Targeted inactivation and indentification of targets of the Gli2a transcription factor in the zebrafish. *Biology Open 2*, 1203-1213.

Wehner, D. & Weidinger, G. (2015). Signaling networks organizing regenerative growth of the zebrafish fin. *Trends in Genetics 31*, 336-343.

Wendt, M. K., Allington, T. M., Schiemann, W. P. (2009). Mechanisms of epithelial-mesenchymal transition by TGF-β. *Future Oncology 5*(8), 1145-1168.

Westerfield, M. (2000). The Zebrafish Book. A guide for the laboratory use of zebrafish *(Danio rerio).* 4th Edition, University of Oregon Press, Eugene.

Wimmer, E. A. (2003). Applications of insect transgenesis. *Nature Reviews Genetics 4*, 225-232.

Winata, C. L., Korzh, S., Kondrychyn, I., Zheng, W., Korzh, V., & Gong, Z. (2009). Development of zebrafish swimbladder: The requirement of Hedgehog signaling in specification and organization of the three tissue layers. *Developmental Biology*, *331*(2), 222–236.

Wood, A., & Thorogood, P. (1984). An analysis of *in vivo* cell migration during teleost aphyosemion-scheeli fin morphogenesis. *Journal of Cell Science, 66,* 205-222.

Wrighton, K. H., Lin, X., Yu, P. B., & Feng, X. H. (2009). Transforming growth factor β can stimulate smad1 phosphorylation independently of bone morphogenic protein receptors. *Journal of Biological Chemistry 284*, 9755-9763.

Wu, C., Asokan S. B., Berginski, M. E., Haynes, E. M., Sharpless, N. E., Griffith, J. D., Gomez, S. M. & Bear, J. E. (2012). Arp2/3 is critical for lamellipodia and response to extracellular matrix cues but is dispensable for chemotaxis. *Cell 148*, 973-987.

Wu, W., Kitamura, S., Truong, D. M., Rieg, T., Vallon, V., Sakurai, H., Bush, K. T., Vera, D. R., Ross, R. S., & Nigam, S. K. (2009). Beta1-integri is required for kidney collecting duct morphogenesis and maintenance of renal function. *American Journal of Renal Physiology 297*, 210-217.

Xu, J., Lamouille, S., & Derynck, R. (2009). TGF-beta-induced epithelial to mesenchymal transition. *Cell Research 19*(2), 156-172.

Yakovich, A. J., Huang, Q., Du, J., Jiang, B., & Barnard, J. A. (2010). Vectorial TGFbeta signaling in polarized intestinal epithelial cells. *Journal of Cell Physiology 224*(2), 398-404.

Yamada, Y., Mashima, H., Sakai, T., Matsuhashi, T., Jin, M., & Ohnishi, H. (2013). Functional roles of TGF-β1 in intestinal epithelial cells through Smad-dependent and non-Smad pathways. *Digestive Diseases and Sciences 58*(5), 1207-1217.

Yamanaka, T., Horikoshi, Y., Sugiyama, Y., Ishiyama, C., Suzuki, A., Hirose, T., Iwamatsu, A., Shinohara, A., Ohno, S. (2003). Mammalian Lgl forms a protein complex with PAR-6 and aPKC independently of PAR-3 to regulate epithelial cell polarity. *Current Biology 13*, 734-743.

Yan, J., Zhang, L., Xu, J., Sultana, N., Hu, J., Cai, X., Li, J., Xu, P. X. & Cai, C. L. (2014). Smad4 regulates uteral smooth muscle differentiation during mouse embryogenesis. *PLoS ONE 9*, e104503.

Yap, A. S., Crampton, M. S., & Hardin, J. (2007). Making and breaking contacts: The cellular biology of cadherin regulation. *Current Opinion in Cell Biology 19*, 508-514.

Young, R. A. (2011). Control of the embryonic stem cell state. *Cell 144*, 940-945.

Yu, Q. C., Verheyen, E. M. & Zeng, Y. A. (2016). Mammary development and breast cancer: a Wnt perspective. *Cancers 8*, 65-91.

Zacharias, W. J., Li, X., Madison, B. B., Kretovich, K., Kao, J. Y. et al. (2010). Hedgehog is an anti-inflammatory epithelial signal for the intestinal lamina propria. *Gastroentrology 138*, 2368-2377.

Zacharias, W. J., Madison, B. B., Kretovich, K. E., Walton, K. D., Richards, N., Udager, A. M., Li, X. & Gumucio, D. L. (2011). Hedgehog signaling controls homeostasis of adult intestinal smooth muscle. *Developmental Biology 355*, 152-162.

Zecca, M., Basler, K., & Struhl, G. (1996). Direct and long-range action of a wingless morphogen gradient. *Cell*, *87*(5), 833–844.

Zhang, X., Mernaugh, G., Yang, D. H., Gewing, L., Srichai, M. B., Harris, R. C., Iturregui, J. M., Nelson, R. D., Kohan, D. E., Abrahamson, D., et al. (2009). Beta1-integrin is necessary for ureteric bud branching morphogenesis and maintenance of collecting duct structural integrity. *Development 136*, 3357-3366.

Zhang, M. & Schekman, R. (2013). Unconventional secretion, unconventional solutions. *Science 340*, 559-561.

Zheng, Z., Zhu, H., Wan, Q., Liu, J., Xiao, Z., Siderovski, D. P., & Du, Q. (2010). LGN regulates mitotic spindle orientation during epithelial morphogenesis. *Journal of Cell Biology 189*(2), 275-288.